





PHAS 2112

Astrophysical Processes:

Nebulae to Stars

(©Ian Howarth 2008–2010)

# Contents

<b>1</b>	<b>Radiation</b>	<b>1</b>
1.1	Specific Intensity, $I_\nu$	1
1.1.1	Mean Intensity, $J_\nu$	2
1.2	Physical Flux, $F_\nu$	3
1.3	Flux vs. Intensity	5
1.3.1	Flux from a star	6
1.4	Flux Moments	7
1.5	Other ‘Fluxes’, ‘Intensities’	8
1.6	Black-body radiation (reference/revision only)	8
1.6.1	Integrated flux	9
1.6.2	Approximate forms	9
1.6.3	Wien’s Law	11
1.7	Radiation Energy Density, $U_\nu$	11
1.8	Radiation Pressure	13
<b>2</b>	<b>The interaction of radiation with matter</b>	<b>15</b>
2.1	Emission: increasing intensity	15
2.2	Extinction: decreasing intensity	16
2.3	Opacity	16
2.3.1	Optical depth	17
2.3.2	Opacity sources	17

<b>3</b>	<b>Radiative transfer</b>	<b>21</b>
3.1	Radiative transfer along a ray . . . . .	21
3.1.1	Solution 1: $j_\nu = 0$ . . . . .	22
3.1.2	Solution 2: $j_\nu \neq 0$ . . . . .	22
3.2	Radiative Transfer in Stellar Atmospheres . . . . .	23
3.3	Energy transport in stellar interiors . . . . .	25
3.3.1	Radiative transfer . . . . .	25
3.3.2	Convection in stellar interiors . . . . .	27
3.3.3	Convective energy transport . . . . .	30
<b>4</b>	<b>Introduction: Gas and Dust in the ISM</b>	<b>31</b>
4.1	Gas . . . . .	31
4.2	Dust . . . . .	32
4.2.1	The normalized interstellar extinction curve . . . . .	33
4.2.2	The ratio of total to selective extinction. . . . .	34
4.3	Other ingredients . . . . .	35
<b>5</b>	<b>Ionization equilibrium in H II Regions</b>	<b>37</b>
5.1	Recombination . . . . .	37
5.2	Ionization . . . . .	38
5.3	Ionization equilibrium . . . . .	39
5.4	Nebular size and mass; the ‘Strömgren Sphere’ . . . . .	40
<b>6</b>	<b>The Radio-Frequency Continuum</b>	<b>43</b>
<b>7</b>	<b>Heating &amp; Cooling in the Interstellar Medium</b>	<b>47</b>
7.1	Heating . . . . .	47
7.1.1	Photoionization . . . . .	47

7.1.2	Photoejection . . . . .	48
7.2	Cooling processes . . . . .	50
7.2.1	Cooling of the neutral ISM . . . . .	51
7.2.2	Cooling of the ionized gas . . . . .	52
7.3	Equilibrium Temperatures . . . . .	54
7.3.1	The Diffuse Neutral ISM . . . . .	54
7.3.2	Ionized gas . . . . .	54
<b>8</b>	<b>Line Broadening</b>	<b>57</b>
8.1	Natural Line Broadening . . . . .	58
8.1.1	Peak value and width . . . . .	61
8.2	Thermal Line Broadening . . . . .	62
8.2.1	Peak value and width . . . . .	64
8.3	‘Turbulent’ Broadening . . . . .	65
8.4	Combined results . . . . .	66
<b>9</b>	<b>Interstellar absorption lines</b>	<b>67</b>
9.1	The transformation between observed and theoretical quantities . . . . .	69
9.1.1	Equivalent width . . . . .	69
9.2	Interstellar Curve of Growth . . . . .	73
9.2.1	Weak lines: optically thin limit . . . . .	73
9.2.2	General case without damping – flat part of the CoG. . . . .	73
9.2.3	Damping dominates – square root part of the CoG. . . . .	74
9.3	The Empirical Curve of Growth . . . . .	75
9.3.1	Results . . . . .	76
9.4	Summary . . . . .	80

<b>10 The Equations of Stellar structure</b>	<b>81</b>
10.1 Hydrostatic Equilibrium . . . . .	81
10.2 Mass Continuity . . . . .	82
10.3 Energy continuity . . . . .	84
10.4 Virial Theorem . . . . .	84
10.4.1 Implications . . . . .	86
10.4.2 Red Giants . . . . .	87
10.5 Mean Molecular Weight . . . . .	88
10.6 Pressure and temperature in the cores of stars . . . . .	89
10.6.1 Solar values . . . . .	89
10.6.2 Central pressure (1) . . . . .	89
10.6.3 Central temperature . . . . .	90
10.6.4 Mean temperature . . . . .	91
10.7 Mass–Luminosity Relationship . . . . .	92
10.8 The role of radiation pressure . . . . .	93
10.9 The Eddington limit . . . . .	93
10.10 Introduction . . . . .	95
10.11 Homologous models . . . . .	96
10.11.1 Results . . . . .	99
10.12 Polytropes and the Lane-Emden Equation . . . . .	100
<b>11 LTE</b>	<b>103</b>
11.1 Local Thermodynamic Equilibrium . . . . .	103
11.2 The Saha Equation . . . . .	104
11.3 Partition functions . . . . .	106
11.3.1 An illustration: hydrogen . . . . .	107

<b>12 Stellar Timescales</b>	<b>109</b>
12.1 Dynamical timescale . . . . .	109
12.1.1 ‘Hydrostatic equilibrium’ approach . . . . .	109
12.1.2 ‘Virial’ approach . . . . .	110
12.2 Kelvin-Helmholtz and Thermal Timescales . . . . .	111
12.3 Nuclear timescale . . . . .	112
12.4 Diffusion timescale for radiative transport . . . . .	113
<b>13 Nuclear reactions in stars</b>	<b>115</b>
13.1 Introduction . . . . .	115
13.2 Tunnelling . . . . .	116
13.3 The mass defect and nuclear binding energy . . . . .	121
13.4 Hydrogen burning – I: the proton–proton (PP) chain . . . . .	122
13.4.1 PP–I . . . . .	122
13.4.2 PP–II, PP–III . . . . .	124
13.5 Hydrogen burning – II: the CNO cycle . . . . .	125
13.5.1 CNO-II . . . . .	126
13.6 Helium burning . . . . .	128
13.6.1 $3\alpha$ burning . . . . .	128
13.6.2 Further helium-burning stages . . . . .	129
13.7 Advanced burning . . . . .	129
13.7.1 Carbon burning . . . . .	129
13.7.2 Neon burning . . . . .	130
13.7.3 Oxygen burning . . . . .	130
13.7.4 Silicon burning . . . . .	130
13.8 Pre-main-sequence burning . . . . .	131

13.9	Synthesis of heavy elements . . . . .	131
13.9.1	Neutron capture: $r$ and $s$ processes . . . . .	131
13.9.2	The $p$ process (for reference only) . . . . .	134
13.10	Summary . . . . .	134
<b>14</b>	<b>Supernovae</b>	<b>137</b>
14.1	Observational characteristics . . . . .	137
14.2	Types Ib, Ic, II . . . . .	139
14.2.1	The death of a massive star . . . . .	139
14.2.2	Light-curves . . . . .	141
14.3	Type Ia SNe . . . . .	142
14.3.1	Observational characteristics . . . . .	142
14.3.2	Interpretation . . . . .	142
14.4	Pair-instability supernovae (for reference only) . . . . .	143
<b>A</b>	<b>SI units</b>	<b>145</b>
A.1	Base units . . . . .	145
A.2	Derived units . . . . .	146
A.3	Prefixes . . . . .	149
A.4	Writing style . . . . .	150
<b>B</b>	<b>Constants</b>	<b>151</b>
B.1	Physical constants . . . . .	151
B.2	Astronomical constants . . . . .	151
B.2.1	Solar parameters . . . . .	151
<b>C</b>	<b>Abbreviations</b>	<b>153</b>

<b>D Atomic spectra</b>	<b>155</b>
D.1 Notation . . . . .	155
<b>E Structure</b>	<b>159</b>
E.1 Transitions . . . . .	160
E.1.1 Electric dipole transitions. . . . .	160
E.1.2 Magnetic dipole transitions. . . . .	161
E.1.3 Electric quadrupole transitions. . . . .	161
E.2 Transition probabilities. . . . .	161
<b>F Another go...</b>	<b>163</b>
F.1 Quantum Numbers of Atomic States . . . . .	163
F.2 Spectroscopic Notation . . . . .	163
F.3 More Spectroscopic Vocabulary . . . . .	164
F.4 Allowed and Forbidden Transitions . . . . .	165
F.5 Spectral Line Formation . . . . .	165
F.5.1 Spectral Line Formation-Line Absorption Coefficient . . . . .	165
F.6 Classical Picture of Radiation . . . . .	165
F.7 Atomic Absorption Coefficient . . . . .	165
F.8 The Classical Damping Constant . . . . .	166
F.9 Line Absorption with QM . . . . .	166



# PART I: INTRODUCTION

## Radiation and Matter

# Section 1

## Radiation

Almost all the astrophysical information we can derive about distant sources results from the radiation that reaches us from them. Our starting point is, therefore, a review of the principal ways of describing radiation. (In principle, this could include polarization properties, but we neglect that for simplicity).

The fundamental definitions of interest are of (specific) *intensity* and (physical) *flux*.

### 1.1 Specific Intensity, $I_\nu$

The specific intensity (or radiation intensity, or surface brightness) is defined as:

the rate of energy flowing at a given point,  
per unit area,  
per unit time,  
per unit frequency interval,  
per unit solid angle (in azimuth  $\phi$  and direction  $\theta$  to the normal; refer to the geometry sketched in Fig. 1.1)

or, expressed algebraically,

$$\begin{aligned} I_\nu(\theta, \phi) &= \frac{dE_\nu}{dS dt d\nu d\Omega} \\ &= \frac{dE_\nu}{dA \cos \theta dt d\nu d\Omega} \quad [\text{J m}^{-2} \text{s}^{-1} \text{Hz}^{-1} \text{sr}^{-1}]. \end{aligned} \tag{1.1}$$

We've given a 'per unit frequency definition', but we can always switch to 'per unit wavelength' by noting that, for some frequency-dependent physical quantity 'X', we can write

$$X_\nu d\nu = X_\lambda d\lambda$$

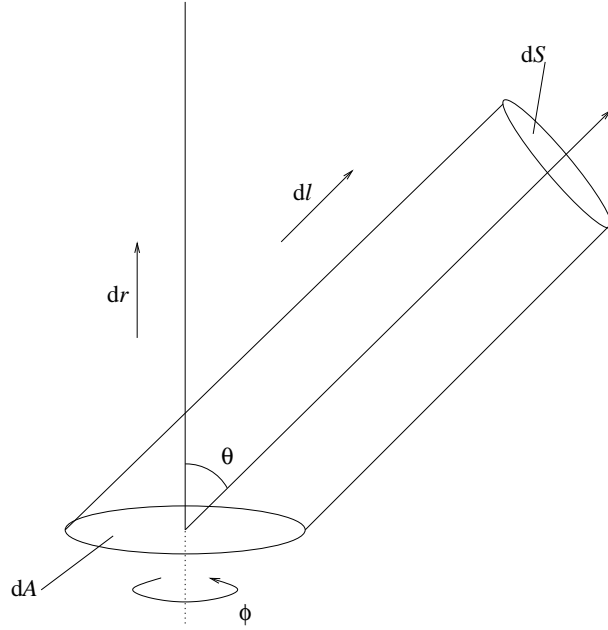


Figure 1.1: Geometry used to define radiation quantities. The element of area  $dA$  might, for example, be on the surface of a star.

or

$$X_\lambda = X_\nu \left| \frac{d\nu}{d\lambda} \right|$$

(which has the same dimensionality on each side of the equation). Mathematically,  $d\nu/d\lambda = -c/\lambda^2$ , but physically this just reflects the fact that increasing frequency means decreasing wavelength (clearly, we require a positive physical quantity on either side of the equation), so specific intensity per unit *wavelength* is related to  $I_\nu$  by

$$I_\lambda = I_\nu \left| \frac{d\nu}{d\lambda} \right| = I_\nu \frac{c}{\lambda^2} \quad [\text{J m}^{-2} \text{ s}^{-1} \text{ m}^{-1} \text{ sr}^{-1}]$$

where the  $\theta, \phi$  dependences are implicit (as will generally be the case; the sharp-eyed will note also that we appear to have ‘lost’ a minus sign in evaluating  $d\nu/d\lambda$ , but this just is because frequency increases as wavelength decreases). Equation (1.1) defines the *monochromatic* specific intensity (‘monochromatic’ will usually also be implicit); we can define a *total* intensity by integrating over frequency:

$$I = \int_0^\infty I_\nu d\nu \quad [\text{J m}^{-2} \text{ s}^{-1} \text{ sr}^{-1}].$$

### 1.1.1 Mean Intensity, $J_\nu$

The mean intensity is, as the name suggests, the average of  $I_\nu$  over solid angle; it is of use when evaluating the rates of physical processes that are photon dominated but independent of the

angular distribution of the radiation (e.g., photoionization and photoexcitation rates).

$$\begin{aligned}
 J_\nu &= \frac{\int_\Omega I_\nu d\Omega}{\int d\Omega} = \frac{1}{4\pi} \int_\Omega I_\nu d\Omega \\
 &= \frac{1}{4\pi} \int_0^{2\pi} \int_0^\pi I_\nu \sin\theta d\theta d\phi \quad [\text{J m}^{-2} \text{ s}^{-1} \text{ Hz}^{-1} \text{ sr}^{-1}]
 \end{aligned}
 \tag{1.2}$$

since

$$\int_\Omega d\Omega = \int_0^{2\pi} \int_0^\pi \sin\theta d\theta d\phi.
 \tag{1.3}$$

Introducing the standard astronomical nomenclature  $\mu = \cos\theta$  (whence  $d\mu = -\sin\theta d\theta$ ), we have

$$\int d\Omega = \left( - \int_0^{2\pi} \int_{+1}^{-1} d\mu d\phi \right) = \int_0^{2\pi} \int_{-1}^{+1} d\mu d\phi
 \tag{1.4}$$

and eqtn. (1.2) becomes

$$J_\nu = \frac{1}{4\pi} \int_0^{2\pi} \int_{-1}^{+1} I_\nu(\mu, \phi) d\mu d\phi
 \tag{1.5}$$

(where for clarity we show the  $\mu, \phi$  dependences of  $I_\nu$  explicitly).

If the radiation field is independent of  $\phi$  but not  $\theta$  (as in the case of a stellar atmosphere without starspots, for example) then this simplifies to

$$J_\nu = \frac{1}{2} \int_{-1}^{+1} I_\nu(\mu) d\mu.
 \tag{1.6}$$

From this it is evident that if  $I_\nu$  is *completely* isotropic (i.e., no  $\theta[\equiv \mu]$  dependence, as well as no  $\phi$  dependence), then  $J_\nu = I_\nu$ . (This should be intuitively obvious – if the intensity is the same in all directions, then the mean intensity must equal the intensity [in any direction].)

## 1.2 Physical Flux, $F_\nu$

The physical flux (or radiation flux density, or radiation flux, or just ‘flux’) is the net rate of energy flowing across unit area (e.g., at a detector), *from all directions*, per unit time, per unit frequency interval:

$$F_\nu = \frac{\int_\Omega dE_\nu}{dA dt d\nu} \quad [\text{J m}^{-2} \text{ s}^{-1} \text{ Hz}^{-1}]$$

It is the absence of directionality that crucially distinguishes *flux* from *intensity*, but the two are clearly related. Using eqtn. (1.1) we see that

$$F_\nu = \int_{\Omega} I_\nu \cos \theta \, d\Omega \quad (1.7)$$

$$= \int_0^{2\pi} \int_0^\pi I_\nu \cos \theta \sin \theta \, d\theta \, d\phi \quad [\text{J m}^{-2} \text{ Hz}^{-1}] \quad (1.8)$$

$$= \int_0^{2\pi} \int_{-1}^{+1} I_\nu(\mu, \phi) \mu \, d\mu \, d\phi$$

or, if there is no  $\phi$  dependence,

$$F_\nu = 2\pi \int_{-1}^{+1} I_\nu(\mu) \mu \, d\mu. \quad (1.9)$$

Because we're simply measuring the energy flowing across an area, there's no explicit directionality involved – other than if the energy impinges on the area from ‘above’ or ‘below’.<sup>1</sup> It's therefore often convenient to divide the contributions to the flux into the ‘upward’ (emitted, or ‘outward’) radiation ( $F_\nu^+$ ;  $0 \leq \theta \leq \pi/2$ , Fig 1.1) and the ‘downward’ (incident, or ‘inward’) radiation ( $F_\nu^-$ ;  $\pi/2 \leq \theta \leq \pi$ ), with the net upward flux being  $F_\nu = F_\nu^+ - F_\nu^-$ :

$$\begin{aligned} F_\nu &= \int_0^{2\pi} \int_0^{\pi/2} I_\nu \cos \theta \sin \theta \, d\theta \, d\phi && + \int_0^{2\pi} \int_{\pi/2}^\pi I_\nu \cos \theta \sin \theta \, d\theta \, d\phi \\ &\equiv F_\nu^+ && - F_\nu^- \end{aligned}$$

As an important example, the surface flux emitted by a star is just  $F_\nu^+$  (assuming there is no incident external radiation field);

$$F_\nu = F_\nu^+ = \int_0^{2\pi} \int_0^{\pi/2} I_\nu \cos \theta \sin \theta \, d\theta \, d\phi$$

or, if there is no  $\phi$  dependence,

$$\begin{aligned} &= 2\pi \int_0^{\pi/2} I_\nu \cos \theta \sin \theta \, d\theta. \\ &= 2\pi \int_0^{+1} I_\nu(\mu) \mu \, d\mu. \end{aligned} \quad (1.10)$$

---

<sup>1</sup>In principle, flux is a vector quantity, but the directionality is almost always implicit in astrophysical situations; e.g., from the centre of a star outwards, or from a source to an observer.

If, furthermore,  $I_\nu$  has no  $\theta$  dependence *over the range*  $0-\pi/2$  then

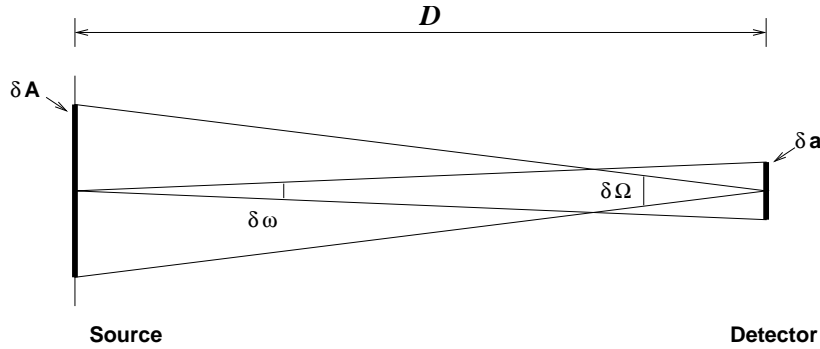
$$F_\nu = \pi I_\nu \quad (1.11)$$

(since  $\int_0^{\pi/2} \cos \theta \sin \theta d\theta = 1/2$ ). If  $I_\nu$  is *completely* isotropic, then  $F_\nu^+ = F_\nu^-$ , and  $F_\nu = 0$ .

### 1.3 Flux vs. Intensity

A crucial difference between  $I_\nu$  and  $F_\nu$  should be noted: the *specific intensity is independent of distance from the source* (but requires the source to be resolved), while the *physical flux falls off as  $r^{-2}$* .

This can be understood by noting that specific intensity is defined in terms of ‘the rate of energy flow per unit area of surface... per unit solid angle’. The energy flow per unit area falls off as  $r^{-2}$ , but the area per unit solid angle increases as  $r^2$ , and so the two cancel.



Expressing this formally: suppose some area  $\delta A$  on a source at distance  $D$  subtends a solid angle  $\delta \Omega$  at a detector; while the detector, area  $\delta a$ , subtends a solid angle  $\delta \omega$  at the source. The energy emitted towards (and received by) the detector is

$$\begin{aligned} E &= I_\nu \delta A \delta \omega; \text{ but} \\ \delta A &= D^2 \delta \Omega \text{ and } \delta \omega = \delta a / D^2, \text{ so} \\ \frac{E}{\delta \Omega} &= I_\nu D^2 \frac{\delta a}{D^2}; \end{aligned}$$

that is, the energy received *per unit solid angle* (i.e., the intensity) is distance independent. Equivalently, we can say that the *surface brightness* of source is distance independent (in the absence of additional processes, such as interstellar extinction).

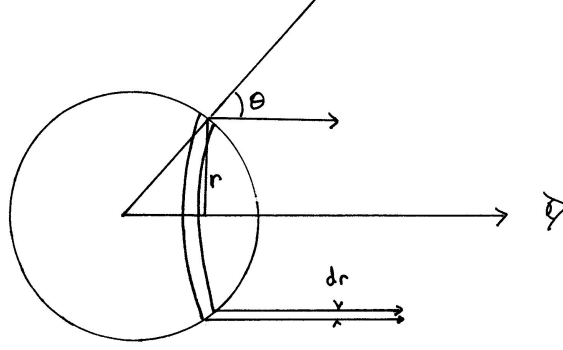
A source must be spatially resolved for us to be able to measure the intensity; otherwise, we can measure ‘only’ the flux – if the source is unresolved, we can’t identify different directions towards it. Any spatially extended source will, at some large enough distance  $D$ , produce an image source at the focal plane of a telescope that will be smaller than the detector (pixel) size. For such an unresolved source, the detected energy is

$$\begin{aligned} E &= I_\nu \delta a \delta \Omega \\ &= I_\nu \delta a \frac{\delta A}{D^2} \end{aligned}$$

and we recover the expected inverse-square law for the detected flux.

### 1.3.1 Flux from a star

To elaborate this, consider the flux from a star at distance  $D$ .



The observer sees the projected area of the annulus as

$$dA = 2\pi r dr$$

and since

$$r = R \sin \theta \quad (dr = R \cos \theta d\theta)$$

we have

$$\begin{aligned} dA &= 2\pi R \sin \theta R \cos \theta d\theta \\ &= 2\pi R^2 \sin \theta \cos \theta d\theta \\ &= 2\pi R^2 \mu d\mu \end{aligned}$$

where as usual  $\mu = \cos \theta$ . The annulus therefore subtends a solid angle

$$d\Omega = \frac{dA}{D^2} = 2\pi \left(\frac{R}{D}\right)^2 \mu d\mu.$$

The flux received from this solid angle is

$$df_\nu = I_\nu(\mu) d\Omega$$

so that the total observed flux is

$$f_\nu = 2\pi \left(\frac{R}{D}\right)^2 \int_0^1 I_\nu \mu d\mu$$

or, using eqtn. (1.10),

$$\begin{aligned} &= \left(\frac{R}{D}\right)^2 F_\nu \\ &= \theta_*^2 F_\nu \quad [\text{J m}^{-2} \text{ s}^{-1} \text{ Hz}^{-1}] \end{aligned}$$

where  $\theta_*$  is the solid angle subtended by the star (measured in radians).

## 1.4 Flux Moments

Flux moments are a traditional ‘radiation’ topic, of use in studying the transport of radiation in stellar atmospheres. The  $n^{\text{th}}$  moment of the radiation field is defined as

$$M_\nu \equiv \frac{1}{2} \int_{-1}^{+1} I_\nu(\mu) \mu^n \, d\mu. \quad (1.12)$$

We can see that we’ve already encountered the *zeroth-order moment*, which is the mean intensity:

$$J_\nu = \frac{1}{2} \int_{-1}^{+1} I_\nu(\mu) \, d\mu. \quad (1.6)$$

We have previously written the flux as

$$F_\nu = 2\pi \int_{-1}^{+1} I_\nu(\mu) \mu \, d\mu; \quad (1.9)$$

to cast this in the same form as eqtns. (1.12) and (1.6), we define the ‘Eddington flux’ as  $H_\nu = F_\nu/(4\pi)$ , i.e.,

$$H_\nu = \frac{1}{2} \int_{-1}^{+1} I_\nu(\mu) \mu \, d\mu. \quad (1.13)$$

We see that  $H_\nu$  is the *first-order moment* of the radiation field.

The second-order moment, the so-called ‘ $K$  integral’, is, from the definition of moments,

$$K_\nu = \frac{1}{2} \int_{-1}^{+1} I_\nu(\mu) \mu^2 \, d\mu \quad (1.14)$$

In the special case that  $I_\nu$  is isotropic we can take it out of the integration over  $\mu$ , and

$$\begin{aligned} K_\nu &= \frac{1}{2} \frac{\mu^3}{3} I_\nu \Big|_{-1}^{+1} \\ &= \frac{1}{3} I_\nu \quad \left[ \text{also} = \frac{1}{3} J_\nu \text{ for isotropy} \right] \end{aligned} \quad (1.15)$$

We will see in Section 1.8 that the  $K$  integral is straightforwardly related to radiation pressure.

Higher-order moments are rarely used. So, to recap (and using the notation first introduced by Eddington himself), for  $n = 0, 1, 2$ :

$n = 0$	Mean Intensity	$J_\nu = \frac{1}{2} \int_{-1}^{+1} I_\nu(\mu) \, d\mu$
$n = 1$	Eddington flux	$H_\nu = \frac{1}{2} \int_{-1}^{+1} I_\nu(\mu) \mu \, d\mu$
$n = 2$	$K$ integral	$K_\nu = \frac{1}{2} \int_{-1}^{+1} I_\nu(\mu) \mu^2 \, d\mu$

(all with units  $[\text{J m}^{-2} \text{s}^{-1} \text{Hz}^{-1} \text{sr}^{-1}]$ ).

We can also define the integral quantities

$$J = \int_0^\infty J_\nu \, d\nu$$

$$F = \int_0^\infty F_\nu \, d\nu$$

$$K = \int_0^\infty K_\nu \, d\nu$$

## 1.5 Other ‘Fluxes’, ‘Intensities’

Astronomers can be rather careless in their use of the terms ‘flux’ and ‘intensity’. The ‘fluxes’ and ‘intensities’ discussed so far can all be quantified in terms of physical (e.g., SI) units.

Often, however, astronomical signals are measured in more arbitrary ways (such ‘integrated signal at the detector’, or even ‘photographic density’); in such cases, it’s commonplace to refer to the ‘intensity’ in a spectrum, but this is just a loose shorthand, and doesn’t allude to the true specific intensity defined in this section.

There are other physically-based quantities that one should be aware of. For example, discussions of model stellar atmospheres may refer to the ‘*astrophysical flux*’; this is given by  $F_\nu/\pi$  (also called, rarely, the ‘radiative flux’), which is evidently similar to the Eddington flux,  $H_\nu = F_\nu/(4\pi)$ , which has itself also occasionally been referred to as the ‘Harvard flux’. Confusingly, some authors also call it just ‘the flux’, but it’s always written as  $H_\nu$  (never  $F_\nu$ ).

## 1.6 Black-body radiation (reference/revision only)

In astrophysics, a radiation field can often be usefully approximated by that of a ‘black body’, for which the intensity is given by the Planck function:

$$I_\nu = B_\nu(T) = \frac{2h\nu^3}{c^2} \left\{ \exp\left(\frac{h\nu}{kT}\right) - 1 \right\}^{-1} \quad [\text{J m}^{-2} \text{s}^{-1} \text{Hz}^{-1} \text{sr}^{-1}]; \text{ or} \quad (1.16)$$

$$I_\lambda = B_\lambda(T) = \frac{2hc^2}{\lambda^5} \left\{ \exp\left(\frac{hc}{\lambda kT}\right) - 1 \right\}^{-1} \quad [\text{J m}^{-2} \text{s}^{-1} \text{m}^{-1} \text{sr}^{-1}] \quad (1.17)$$

(where  $B_\nu \, d\nu = B_\lambda \, d\lambda$ ).

We have seen that

$$F_\nu = 2\pi \int_{-1}^{+1} I_\nu(\mu) \mu \, d\mu. \quad (1.9)$$

If we have a surface radiating like a black body then  $I_\nu = B_\nu(T)$ , and there is no  $\mu$  dependence, other than that the energy is emitted over the limits  $0 \leq \mu \leq 1$ ; thus the physical flux for a black-body radiator is given by

$$\begin{aligned} F_\nu = F_\nu^+ &= 2\pi \int_0^{+1} B_\nu(T) \mu \, d\mu = B_\nu \left. \frac{2\pi\mu^2}{2} \right|_0^{+1} \\ &= \pi B_\nu. \end{aligned} \tag{1.18}$$

(cp. eqtn. (1.11):  $F_\nu = \pi I_\nu$ )

### 1.6.1 Integrated flux

The total radiant energy flux is obtained by integrating eqtn. (1.18) over frequency,

$$\begin{aligned} \int_0^\infty F_\nu \, d\nu &= \int_0^\infty \pi B_\nu \, d\nu \\ &= \int_0^\infty \frac{2\pi h\nu^3}{c^2} \left\{ \exp\left(\frac{h\nu}{kT}\right) - 1 \right\}^{-1} \, d\nu. \end{aligned} \tag{1.19}$$

We can solve this by setting  $x = (h\nu)/(kT)$  (whence  $d\nu = [kT/h] \, dx$ ), so

$$\int_0^\infty F_\nu \, d\nu = \left(\frac{kT}{h}\right)^4 \frac{2\pi h}{c^2} \int_0^\infty \frac{x^3}{\exp(x) - 1} \, dx$$

The integral is now a standard form, which has the solution  $\pi^4/15$ , whence

$$\int_0^\infty F_\nu \, d\nu = \left(\frac{k\pi}{h}\right)^4 \frac{2\pi h}{15c^2} T^4 \tag{1.20}$$

$$\equiv \sigma T^4 \tag{1.21}$$

where  $\sigma$  is the Stefan-Boltzmann constant,

$$\sigma = \frac{2\pi^5 k^4}{15h^3 c^2} = 5.67 \times 10^{-5} \quad [\text{J m}^{-2} \text{K}^{-4} \text{s}^{-1}].$$

### 1.6.2 Approximate forms

There are two important approximations to the Planck function which follow directly from eqtn. 1.16:

$$B_\nu(T) \simeq \frac{2h\nu^3}{c^2} \left\{ \exp\left(\frac{h\nu}{kT}\right) \right\}^{-1} \quad \text{for } \frac{h\nu}{kT} \gg 1 \tag{1.22}$$

(Wien approximation), and

$$B_\nu(T) \simeq \frac{2\nu^2 kT}{c^2} \quad \text{for } \frac{h\nu}{kT} \ll 1 \tag{1.23}$$

(Rayleigh-Jeans approximation;  $\exp(h\nu/kT) \simeq 1 + h\nu/kT$ ).

The corresponding wavelength-dependent versions are, respectively,

$$\begin{aligned} B_\lambda(T) &\simeq \frac{2hc^2}{\lambda^5} \left\{ \exp\left(\frac{hc}{\lambda kT}\right) \right\}^{-1}, \\ B_\lambda(T) &\simeq \frac{2ckT}{\lambda^4}. \end{aligned}$$

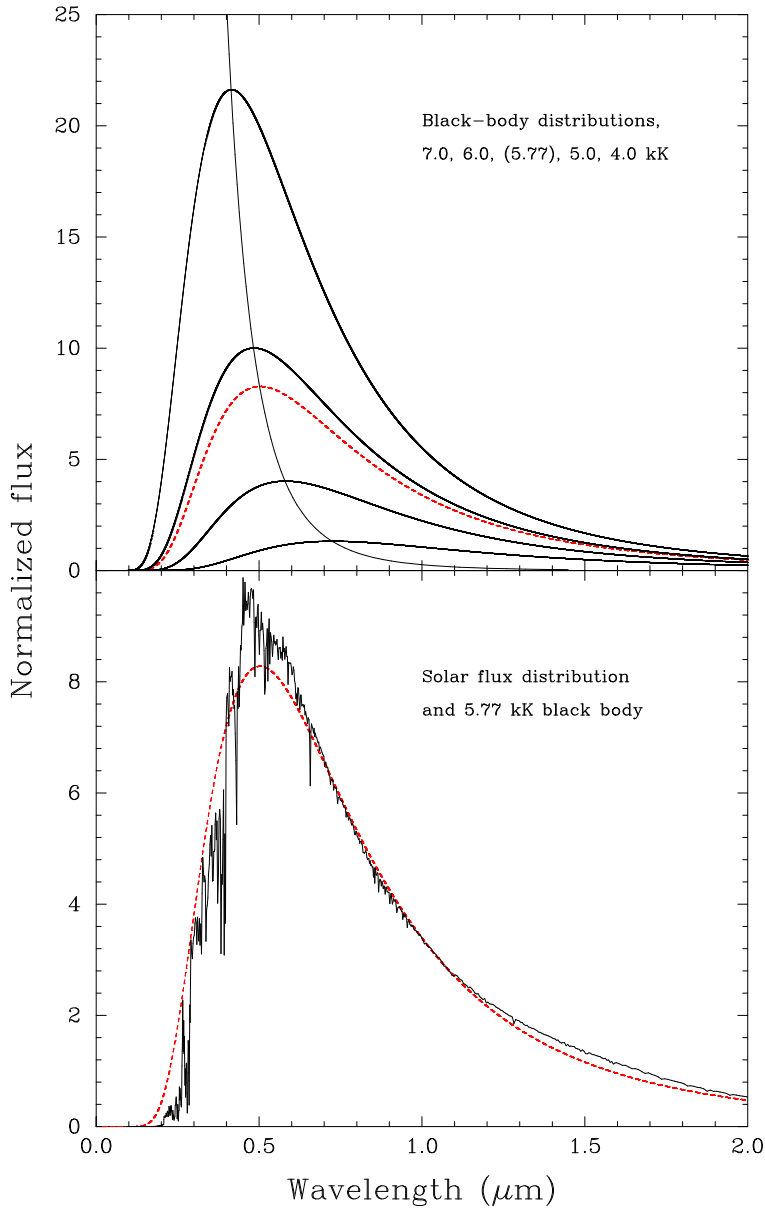


Figure 1.2: *Upper panel:* Flux distributions for black bodies at several different temperatures. A hotter black body radiates more energy at *all* wavelengths than a cooler one, but the increase is greater at shorter wavelengths. The peak of the black-body distribution migrates blueward with increasing temperature, in accordance with Wien's law (also plotted).

*Lower panel:* Flux distribution for the Sun (actually, a Kurucz solar model) compared with a black-body distribution at the same temperature. The black body is a reasonable, though far from perfect, match to the model, the main differences arising because of line blocking in the sun at short wavelengths. This energy must come out elsewhere, and appears as an excess over the black body at long wavelengths.

(Flux units are  $10^7 \text{ J m}^{-2} \text{ s}^{-1} \mu\text{m}^{-1}$ .)

The Wien approximation to the Planck function is very good at wavelengths shortwards of and up to the peak of the flux distribution; but one generally needs to go something like  $\sim 10\times$  the peak wavelength before the long-wavelength Rayleigh-Jeans approximation is satisfactory.

### 1.6.3 Wien's Law

Wien's displacement law (not to be confused with the Wien approximation!) relates the black-body temperature to the wavelength of peak emission. To find the peak, we differentiate eqn. (1.17) with respect to wavelength, and set to zero:

$$\frac{\partial B}{\partial \lambda} = 8hc \left( \frac{hc}{\lambda^7 kT} \frac{\exp\{hc/\lambda kT\}}{(\exp\{hc/\lambda kT\} - 1)^2} - \frac{1}{\lambda^6} \frac{5}{\exp\{hc/\lambda kT\} - 1} \right) = 0$$

whence

$$\frac{hc}{\lambda_{\max} kT} (1 - \exp\{-hc/\lambda_{\max} kT\})^{-1} - 5 = 0$$

An analytical solution of this equation can be obtained in terms of the Lambert  $W$  function; we merely quote the result,

$$\frac{\lambda_{\max}}{\mu\text{m}} = \frac{2898}{T/\text{K}}$$

We expect the Sun's output to peak around 500 nm (for  $T_{\text{eff}} = 5770$  K) – just where the human eye has peak sensitivity, for obvious evolutionary reasons.

## 1.7 Radiation Energy Density, $U_\nu$

Consider some volume of space containing a given number of photons; the photons have energy, so we can discuss the density of radiant energy. From eqn. (1.1), and referring to Fig. 1.1,

$$dE_\nu = I_\nu(\theta) dS dt d\nu d\Omega.$$

We can eliminate the time dependence<sup>2</sup> by noting that there is a single-valued correspondence<sup>3</sup> between time and distance for radiation. Defining a characteristic length  $\ell = ct$ ,  $dt = d\ell/c$ , and

$$\begin{aligned} dE_\nu &= I_\nu(\theta) dS \frac{d\ell}{c} d\nu d\Omega \\ &= \frac{I_\nu(\theta)}{c} dV d\nu d\Omega \end{aligned} \tag{1.24}$$

where the volume element  $dV = dS d\ell$ . The mean radiation energy density per unit frequency per unit volume is then

$$\begin{aligned} U_\nu d\nu &= \frac{1}{V} \int_V \int_\Omega dE_\nu \\ &= \frac{1}{c} \int_\Omega I_\nu d\nu d\Omega \end{aligned}$$

<sup>2</sup>Assuming that no time dependence exists; that is, that for every photon leaving some volume of space, a compensating photon enters. This is an excellent approximation under many circumstances.

<sup>3</sup>Well, *nearly* single-valued; the speed at which radiation propagates actually depends on the refractive index of the medium through which it moves – e.g., the speed of light in water is only  $^{3/4}$ .

whence

$$\begin{aligned}
 U_\nu &= \frac{1}{c} \int I_\nu d\Omega \\
 &= \frac{4\pi}{c} J_\nu \quad [\text{J m}^{-3} \text{ Hz}^{-1}] \quad [\text{from eqtn. (1.2): } J_\nu = 1/4\pi \int I_\nu d\Omega]
 \end{aligned} \tag{1.25}$$

Again, this is explicitly frequency dependent; the *total* energy density is obtained by integrating over frequency:

$$U = \int_0^\infty U_\nu d\nu.$$

For black-body radiation,  $J_\nu (= I_\nu) = B_\nu$ , and

$$U = \int_0^\infty \frac{4\pi}{c} B_\nu d\nu$$

but  $\int \pi B_\nu = \sigma T^4$  (eqtn. (1.21)) so

$$\begin{aligned}
 U &= \frac{4\sigma}{c} T^4 \equiv aT^4 \\
 &= 7.55 \times 10^{-16} T^4 \quad \text{J m}^{-3}
 \end{aligned} \tag{1.26}$$

where  $T$  is in kelvin,  $\sigma$  is the Stefan-Boltzmann constant and  $a$  is the ‘radiation constant’. Note that the energy density of black-body radiation is a *fixed quantity* (for a given temperature).

For a given form of spectrum, the *energy* density in radiation must correspond to a specific *number* density of photons:

$$N_{\text{photon}} = \int_0^\infty \frac{U_\nu}{h\nu} d\nu.$$

For the particular case of a black-body spectrum,

$$N_{\text{photon}} \simeq 2 \times 10^7 T^3 \quad \text{photons m}^{-3}. \tag{1.27}$$

Dividing eqtn. (1.26) by (1.27) gives the mean energy per photon for black-body radiation,

$$\overline{h\nu} = 3.78 \times 10^{-23} T = 2.74kT \tag{1.28}$$

(although there is, of course, a broad spread in energies of individual photons).

## 1.8 Radiation Pressure

A photon carries momentum  $E/c (= h\nu/c)$ .<sup>4</sup> Momentum flux (momentum per unit time, per unit area) is a *pressure*.<sup>5</sup> If photons encounter a surface at some angle  $\theta$  to the normal, the component of momentum perpendicular to the surface per unit time per unit area is that pressure,

$$dP_\nu = \frac{dE_\nu}{c} \times \cos\theta \frac{1}{dt dA d\nu}$$

(where we have chosen to express the photon pressure ‘per unit frequency’); but the specific intensity is

$$I_\nu = \frac{dE_\nu}{dA \cos\theta d\Omega d\nu dt}, \quad (1.1)$$

whence

$$dP_\nu = \frac{I_\nu}{c} \cos^2\theta d\Omega$$

i.e.,

$$P_\nu = \frac{1}{c} \int I_\nu \mu^2 d\Omega \quad [\text{J m}^{-3} \text{ Hz}^{-1} \equiv \text{Pa Hz}^{-1}] \quad (1.29)$$

We know that

$$\int d\Omega = \int_0^{2\pi} \int_{-1}^{+1} d\mu d\phi \quad (1.4)$$

so

$$P_\nu = \frac{2\pi}{c} \int_{-1}^{+1} I_\nu \mu^2 d\mu;$$

however, the  $K$  integral is

$$K_\nu = \frac{1}{2} \int_{-1}^{+1} I_\nu(\mu) \mu^2 d\mu \quad (1.14)$$

(from Section 1.4), hence

$$P_\nu = \frac{4\pi}{c} K_\nu \quad (1.30)$$

<sup>4</sup>Classically, momentum is mass times velocity. From  $E = mc^2 = h\nu$ , the photon rest mass is  $h\nu/c^2$ , and its velocity is  $c$ , hence momentum is  $h\nu/c$ .

<sup>5</sup>Dimensional arguments show this to be true; in the SI system, momentum has units of  $\text{kg m s}^{-1}$ , and momentum flux has units of  $\text{kg m s}^{-1}$ ,  $\text{m}^{-2}$ ,  $\text{s}^{-1}$ ; i.e.,  $\text{kg m}^{-1} \text{s}^{-2}$ ,  $= \text{N m}^{-2} = \text{Pa}$  – the units of pressure. Pressure in turn is force per unit area (where force is measured in Newtons,  $= \text{J m}^{-1} = \text{kg m s}^{-2}$ ).

For an *isotropic* radiation field  $K_\nu = 1/3I_\nu = 1/3J_\nu$  (eqn. (1.15)), and so

$$P_\nu = \frac{4\pi}{3c}I_\nu = \frac{4\pi}{3c}J_\nu.$$

In this isotropic case we also have

$$U_\nu = \frac{4\pi}{c}J_\nu = \frac{4\pi}{c}I_\nu$$

(eqn. (1.25)) so – for an isotropic radiation field – the radiation pressure is

$$P_\nu = \frac{1}{3}U_\nu$$

or, integrating over frequency (using  $\int U_\nu d\nu = aT^4 = 4\sigma/cT^4$ ; eqn. (1.26)),

$$P_R = \frac{1}{3}aT^4 = \frac{4\sigma}{3c}T^4 \quad [\text{J m}^{-3} \equiv \text{N m}^{-2} \equiv \text{Pa}]. \quad (1.31)$$

In that equation (1.31) expresses the relationship between pressure and temperature, it is the equation of state for radiation.

Note that in the isotropic case,  $P_\nu$  (or  $P_R$ ) is a scalar quantity – it has magnitude but not direction (like air pressure, locally, on Earth). For an *anisotropic* radiation field, the radiation pressure has a direction (normally outwards from a star), and is a vector quantity. (This *directed* pressure, or force per unit area, becomes important in luminous stars, where the force becomes significant compared to gravity; Section 10.9.)

## Section 2

# The interaction of radiation with matter

As a beam of radiation traverses astrophysical material (such as a stellar interior, a stellar atmosphere, or interstellar space), energy can be added or subtracted – the process of ‘radiative transfer’. A large number of detailed physical processes can contribute to these changes in intensity, and we will consider some of these processes in subsequent sections. First, though, we concentrate on general principles.

### 2.1 Emission: increasing intensity

A common astrophysical<sup>1</sup> definition of the (monochromatic) emissivity is the energy generated per unit volume,<sup>2</sup> per unit time, per unit frequency, per unit solid angle:

$$j_\nu = \frac{dE_\nu}{dV dt d\nu d\Omega} \quad [\text{J m}^{-3} \text{ s}^{-1} \text{ Hz}^{-1} \text{ sr}^{-1}]; \quad (2.1)$$

If an element of distance along a line (e.g., the line of sight) is  $ds$ , then the change in specific intensity along that element resulting from the emissivity of a volume of material of unit cross-sectional area is

$$dI_\nu = +j_\nu(s) ds \quad (2.2)$$

---

<sup>1</sup>Other definitions of ‘emissivity’ occur in physics.

<sup>2</sup>The emissivity can also be defined per unit mass (or, in principle, per particle).

## 2.2 Extinction: decreasing intensity

‘Extinction’ is a general term for the removal of light from a beam. Two different classes of process contribute to the extinction: absorption and scattering. Absorption (sometimes called ‘true absorption’) results in the destruction of photons; scattering merely involves redirecting photons in some new direction. For a beam directed towards the observer, scattering still has the effect of diminishing the recorded signal, so the two types of process can be treated together for the present purposes.

The amount of intensity removed from a beam by extinction in (say) a gas cloud must depend on

- The initial strength of the beam (the more light there is, the more you can remove)
- The number of particles (absorbers)
- The microphysics of the particles – specifically, how likely they are to absorb (or scatter) an incident photon. This microphysics is characterized by an effective cross-section per particle presented to the radiation.

By analogy with eqtn. (2.2), we can write the change in intensity along length  $ds$  as

$$dI_\nu = -a_\nu n I_\nu ds \tag{2.3}$$

for a number density of  $n$  extinguishing particles per unit volume, with  $a_\nu$  the ‘extinction coefficient’, or *cross-section* (in units of area) per particle.

## 2.3 Opacity

In astrophysical applications, it is customary to combine the cross-section per particle (with dimensions of area) and the number of particles into either the extinction per unit mass, or the extinction per unit volume. In the former case we can set

$$a_\nu n \equiv \kappa_\nu \rho$$

and thus write eqtn. (2.3) as

$$dI_\nu = -\kappa_\nu \rho(s) I_\nu ds$$

for mass density  $\rho$ , where  $\kappa_\nu$  is the (monochromatic) mass extinction coefficient or, more usually, the *opacity* per unit mass (dimensions of area per unit mass; SI units of  $\text{m}^2 \text{kg}^{-1}$ ).

For opacity per unit volume we have

$$a_\nu n \equiv k_\nu$$

whence

$$dI_\nu = -k_\nu I_\nu ds.$$

The volume opacity  $k_\nu$  has dimensions of area per unit volume, or SI units of  $\text{m}^{-1}$ . It has a straightforward and useful physical interpretation; the mean free path for a photon moving through a medium with volume opacity  $k_\nu$  is

$$\ell_\nu \equiv 1/k_\nu. \tag{2.4}$$

[In the literature,  $\kappa$  is often used generically to indicate opacity, regardless of whether ‘per unit mass’ or ‘per unit volume’, and the sense has to be inferred from the context. (You can always do this by looking at the dimensions involved.)]

### 2.3.1 Optical depth

We can often calculate, but rarely measure, opacity as a function of position along a given path. Observationally, often all that is accessible is the cumulative effect of the opacity integrated along the line of sight; this is quantified by the *optical depth*,

$$\tau_\nu = \int_0^D k_\nu(s) ds = \int_0^D \kappa_\nu \rho(s) ds = \int_0^D a_\nu n(s) ds \tag{2.5}$$

over distance  $D$ .

### 2.3.2 Opacity sources

At the atomic level, the processes which contribute to opacity are:

- bound-bound absorption (photoexcitation – line process);
- bound-free absorption (photoionization – continuum process);
- free-free absorption (continuum process); and
- scattering (continuum process).

Absorption process can be thought of as the destruction of photons (through conversion into other forms of energy, whether radiative or kinetic).

Scattering is the process of photon absorption followed by prompt re-emission through the inverse process. For example, resonance-line scattering is photo-excitation from the ground state to an excited state, followed quickly by radiative decay. Continuum scattering processes include electron scattering and Rayleigh scattering.

Under most circumstances, scattering involves re-emission of a photon with virtually the same energy (in the rest frame of the scatterer), but in a new direction.<sup>3</sup>

Calculation of opacities is a major task, but at the highest temperatures ( $T \gtrsim 10^7$  K) elements are usually almost fully ionized, so free-free and electron-scattering opacities dominate. Under these circumstances,  $\kappa \simeq \text{constant}$ . Otherwise, a parameterization of the form

$$\kappa = \kappa_0 \rho^a T^b \tag{2.6}$$

is convenient for analytical or illustrative work.

---

<sup>3</sup>In Compton scattering, energy is transferred from a high-energy photon to the scattering electron (or vice versa for inverse Compton scattering). These processes are important at X-ray and  $\gamma$ -ray energies; at lower energies, classical Thomson scattering dominates. For our purposes, ‘electron scattering’ can be regarded as synonymous with Thomson scattering.

# Rate coefficients and rate equations (reference/revision only)

Before proceeding to consider specific astrophysical environments, we review the coefficients relating to *bound-bound* (line) transitions. Bound-free (ionization) process will be considered in sections 5 (photoionization) and 11.2 (collisional ionization).

## Einstein (radiative) coefficients

Einstein (1916) proposed that there are three purely radiative processes which may be involved in the formation of a spectral line: induced emission, induced absorption, and spontaneous emission, each characterized by a coefficient reflecting the probability of a particular process.

- [1]  $A_{ji}$  ( $s^{-1}$ ): the Einstein coefficient, or transition probability, for spontaneous decay from an upper state  $j$  to a lower state  $i$ , with the emission of a photon (radiative decay); the time taken for an electron in state  $j$  to spontaneously decay to state  $i$  is  $1/A_{ji}$  on average

If  $n_j$  is the number density of atoms in state  $j$  then the change in the number density of atoms in that state per unit time due to spontaneous emission will be

$$\frac{dn_j}{dt} = - \sum_{i < j} A_{ji} n_j$$

while level  $i$  is populated according to

$$\frac{dn_i}{dt} = + \sum_{j > i} A_{ji} n_j$$

- [2]  $B_{ij}$  ( $s^{-1} J^{-1} m^2 sr$ ): the Einstein coefficient for radiative excitation from a lower state  $i$  to an upper state  $j$ , with the absorption of a photon.

$$\frac{dn_i}{dt} = - \sum_{j > i} B_{ij} n_i I_\nu,$$

$$\frac{dn_j}{dt} = + \sum_{i < j} B_{ij} n_i I_\nu$$

- [3]  $B_{ji}$  ( $s^{-1} J^{-1} m^2 sr$ ): the Einstein coefficient for radiatively induced de-excitation from an upper state to a lower state.

$$\frac{dn_j}{dt} = - \sum_{i < j} B_{ji} n_j I_\nu,$$

$$\frac{dn_i}{dt} = + \sum_{j > i} B_{ji} n_j I_\nu$$

where  $I_\nu$  is the specific intensity at the frequency  $\nu$  corresponding to  $E_{ij}$ , the energy difference between excitation states.

For reference, we state, without proof, the relationships between these coefficients:

$$A_{ji} = \frac{2h\nu^3}{c^2} B_{ji};$$

$$B_{ij} g_i = B_{ji} g_j$$

where  $g_i$  is the statistical weight of level  $i$ .

In astronomy, it is common to work not with the Einstein  $A$  coefficient, but with the absorption oscillator strength  $f_{ij}$ , where

$$A_{ji} = \frac{8\pi^2 e^2 \nu^2}{m_e c^3} \frac{g_i}{g_j} f_{ij}$$

and  $f_{ij}$  is related to the absorption cross-section by

$$a_{ij} \equiv \int a_\nu d\nu = \frac{\pi e^2}{m_e c} f_{ij}.$$

Because of the relationships between the Einstein coefficients, we also have

$$B_{ij} = \frac{4\pi^2 e^2}{m_e h \nu c} f_{ij},$$

$$B_{ji} = \frac{4\pi^2 e^2}{m_e h \nu c} \frac{g_i}{g_j} f_{ij}$$

## Collisional coefficients

For collisional processes we have analogous coefficients:

- [4]  $C_{ji}$  ( $\text{m}^3 \text{s}^{-1}$ ): the coefficient for collisional de-excitation from an upper state to a lower state.

$$\frac{dn_j}{dt} = - \sum_{j>i} C_{ji} n_j n_e,$$

$$\frac{dn_i}{dt} = + \sum_{i<j} C_{ji} n_j n_e$$

(for excitation by electron collisions)

- [5]  $C_{ij}$  ( $\text{m}^3 \text{s}^{-1}$ ): the coefficient for collisional excitation from a lower state to an upper state.

$$\frac{dn_i}{dt} = - \sum_{j>i} C_{ij} n_i n_e,$$

$$\frac{dn_j}{dt} = + \sum_{i<j} C_{ij} n_i n_e$$

These coefficients are related through

$$\frac{C_{ij}}{C_{ji}} = \frac{g_j}{g_i} \exp \left\{ - \frac{h\nu}{kT_{\text{ex}}} \right\}$$

for excitation temperature  $T_{\text{ex}}$ .

The rate coefficient has a Boltzmann-like dependence on the kinetic temperature

$$C_{ij}(T_k) = \left( \frac{2\pi}{T_k} \right)^{1/2} \frac{h^2}{4\pi^2 m_e^{3/2}} \frac{\Omega(ij)}{g_i} \exp \left\{ \frac{-\Delta E_{ij}}{kT_k} \right\}$$

$$\propto \frac{1}{\sqrt{T_e}} \exp \left\{ \frac{-\Delta E_{ij}}{kT_k} \right\} \quad [\text{m}^3 \text{s}^{-1}] \quad (2.7)$$

where  $\Omega(1, 2)$  is the so-called ‘collision strength’.

## Statistical Equilibrium

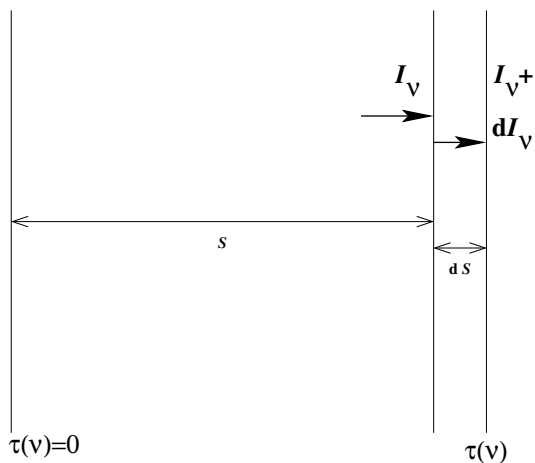
Overall, for any ensemble of atoms in equilibrium, the number of de-excitations from any given excitation state must equal the number of excitations into that state – the principle of *statistical equilibrium*. That is,

$$\sum_{j>i} B_{ij} n_i I_\nu + \sum_{j\neq i} C_{ij} n_j n_e = \sum_{j>i} A_{ji} n_j + \sum_{j>i} B_{ji} n_j I_\nu + \sum_{j\neq i} C_{ji} n_j n_e \quad (2.8)$$

## Section 3

# Radiative transfer

### 3.1 Radiative transfer along a ray



Consider a beam of radiation from a distant point source (e.g., an unresolved star), passing through some intervening material (e.g., interstellar gas). The intensity change as the radiation traverses the element of gas of thickness  $ds$  is the intensity added, less the intensity taken away (per unit frequency, per unit time, per unit solid angle):

$$dI_\nu \left( \frac{dA d\nu d\omega dt}{ds} \right) = + j_\nu \frac{ds dA d\nu d\omega dt}{ds} - k_\nu I_\nu \frac{ds dA d\nu d\omega dt}{ds}$$

i.e.,

$$dI_\nu = (j_\nu - k_\nu I_\nu) ds,$$

or

$$\frac{dI_\nu}{ds} = j_\nu - k_\nu I_\nu, \tag{3.1}$$

which is the basic form of *the Equation of Radiative Transfer*.

The ratio  $j_\nu/k_\nu$  is called the *Source Function*,  $S_\nu$ . For systems in thermodynamic equilibrium  $j_\nu$  and  $k_\nu$  are related through the Kirchhoff relation,

$$j_\nu = k_\nu B_\nu(T),$$

and so in this case (though not in general) the source function is given by the Planck function

$$S_\nu = B_\nu$$

Equation (3.1) expresses the intensity of radiation as a function of position. In astrophysics, we often can't establish exactly where the absorbers are; for example, in the case of an absorbing interstellar gas cloud of given physical properties, the same absorption lines will appear in the spectrum of some background star, regardless of where the cloud is along the line of sight. It's therefore convenient to divide both sides of eqn. 3.1 by  $k_\nu$ ; then using our definition of optical depth, eqn. (2.5), gives a more useful formulation,

$$\frac{dI_\nu}{d\tau_\nu} = S_\nu - I_\nu. \tag{3.2}$$

### 3.1.1 Solution 1: $j_\nu = 0$

We can find simple solutions for the equation of transfer under some circumstances. The very simplest case is that of absorption only (no emission;  $j_\nu = 0$ ), which is appropriate for interstellar absorption lines (or headlights in fog); just by inspection, eqn. (3.1) has the straightforward solution

$$I_\nu = I_\nu(0) \exp \{-\tau_\nu\}. \tag{3.3}$$

We see that an optical depth of 1 results in a reduction in intensity of a factor  $e^{-1}$  (i.e., a factor  $\sim 0.37$ ).

### 3.1.2 Solution 2: $j_\nu \neq 0$

To obtain a more general solution to transfer along a line we begin by guessing that

$$I_\nu = \mathcal{F} \exp \{C_1 \tau_\nu\} \tag{3.4}$$

where  $\mathcal{F}$  is some function to be determined, and  $C_1$  some constant; differentiating eqn. 3.4,

$$\begin{aligned} \frac{dI_\nu}{d\tau_\nu} &= \exp\{C_1\tau_\nu\} \frac{d\mathcal{F}}{d\tau_\nu} + \mathcal{F}C_1 \exp\{C_1\tau_\nu\} \\ &= \exp\{C_1\tau_\nu\} \frac{d\mathcal{F}}{d\tau_\nu} + C_1 I_\nu, & = S_\nu - I_\nu \text{ (eqn. 3.2)}. \end{aligned}$$

Identifying like terms we see that  $C_1 = -1$  and that

$$S_\nu = \exp\{-\tau_\nu\} \frac{d\mathcal{F}}{d\tau_\nu},$$

i.e.,

$$\mathcal{F} = \int_0^{\tau_\nu} S_\nu \exp\{t_\nu\} dt_\nu + C_2$$

where  $t$  is a dummy variable of integration and  $C_2$  is some constant. Referring back to eqn. (3.4), we now have

$$I_\nu(\tau_\nu) = \exp\{-\tau_\nu\} \int_0^{\tau_\nu} S_\nu(t_\nu) \exp\{t_\nu\} dt_\nu + I_\nu(0) \exp\{-\tau_\nu\}$$

where the constant of integration is set by the boundary condition of zero extinction ( $\tau_\nu = 0$ ). In the special case of  $S_\nu$  independent of  $\tau_\nu$  we obtain

$$I_\nu = I_\nu(0) \exp\{-\tau_\nu\} + S_\nu (1 - \exp\{-\tau_\nu\})$$

## 3.2 Radiative Transfer in Stellar Atmospheres

Having established the principles of the simple case of radiative transfer along a ray, we turn to more general circumstances, where we have to consider radiation coming not just from one direction, but from arbitrary directions. The problem is now three-dimensional in principle; we could treat it in cartesian ( $xyz$ ) coördinates,<sup>1</sup> but because a major application is in spherical objects (stars!), it's customary to use spherical polar coördinates.

Again consider a beam of radiation travelling in direction  $s$ , at some angle  $\theta$  to the radial direction in a stellar atmosphere (Fig. 3.1). If we neglect the curvature of the atmosphere (the 'plane parallel approximation') and any azimuthal dependence of the radiation field, then the intensity change along this particular ray is

$$\frac{dI_\nu}{ds} = j_\nu - k_\nu I_\nu, \tag{3.1}$$

as before.

We see from the figure that

$$dr = \cos\theta ds \equiv \mu ds$$

---

<sup>1</sup>We could also treat the problem as time-dependent; but we won't ... A further complication that we won't consider is motion in the absorbing medium (which introduces a directional dependence in  $k_\nu$  and  $j_\nu$ ); this directionality is important in stellar winds, for example.

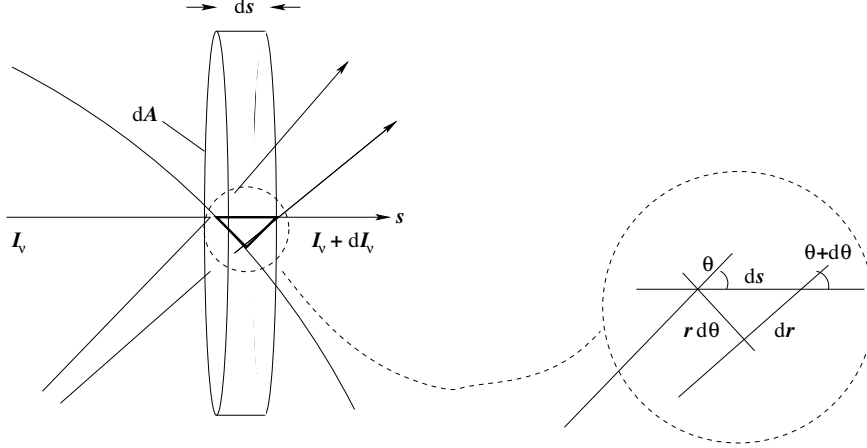


Figure 3.1: Geometry used in radiative-transfer discussion, section 3.2.

so the transfer in the radial direction is described by

$$\frac{\mu}{k_\nu} \frac{dI_\nu}{dr} = \frac{j_\nu}{k_\nu} - I_\nu, \quad (3.5)$$

(where we've divided through by  $k_\nu$ ); and since  $j_\nu/k_\nu = S_\nu$  and  $d\tau_\nu = -k_\nu dr$  (eqtn. 2.5, measuring distance in the radial direction, and introducing a minus because the sign convention in stellar-atmosphere work is such that optical depth *increases* with *decreasing*  $r$ ) we have

$$\mu \frac{dI_\nu}{d\tau_\nu} = S_\nu - I_\nu. \quad (3.6)$$

This is the standard formulation of the equation of transfer in plane-parallel stellar atmospheres.

For *arbitrary* geometry we have to consider the full three-dimensional characterization of the radiation field; that is

$$\frac{dI_\nu}{ds} = \frac{\partial I_\nu}{\partial r} \frac{dr}{ds} + \frac{\partial I_\nu}{\partial \theta} \frac{d\theta}{ds} + \frac{\partial I_\nu}{\partial \phi} \frac{d\phi}{ds}, \quad (3.7)$$

where  $r, \theta, \phi$  are our spherical polar coordinates. This is our most general formulation, but in the case of stellar atmospheres we can often neglect the  $\phi$  dependence; and we rewrite the  $\theta$  term by noting not only that

$$dr = \cos \theta ds \equiv \mu ds$$

but also that

$$-r d\theta = \sin \theta ds.$$

(The origin of the minus sign may be clarified by reference to Fig. 3.1; for increasing  $s$  we have increasing  $r$ , but *decreasing*  $\theta$ , so  $r d\theta$  is negative for positive  $ds$ .)

Using these expressions in eqtn. (3.7) gives a two-dimensional form,

$$\frac{dI_\nu}{ds} = \frac{\partial I_\nu}{\partial r} \cos \theta - \frac{\partial I_\nu}{\partial \theta} \frac{\sin \theta}{r}$$

but this is also

$$= j_\nu - k_\nu I_\nu$$

so, dividing through by  $k_\nu$  as usual,

$$\begin{aligned} \frac{\cos \theta}{k_\nu} \frac{\partial I_\nu}{\partial r} + \frac{\sin \theta}{k_\nu r} \frac{\partial I_\nu}{\partial \theta} &= \frac{j_\nu}{k_\nu} - I_\nu \\ &= S_\nu - I_\nu \end{aligned}$$

Once again, it's now useful to think in terms of the optical depth measured *radially inwards*:

$$d\tau = -k_\nu dr,$$

which gives us the customary form of the equation of radiative transfer for use in *extended* stellar atmospheres, for which the plane-parallel approximation fails:

$$\frac{\sin \theta}{\tau_\nu} \frac{\partial I_\nu}{\partial \theta} - \mu \frac{\partial I_\nu}{\partial \tau_\nu} = S_\nu - I_\nu. \quad (3.8)$$

We recover our previous, plane-parallel, result if the atmosphere is very thin compared to the stellar radius. In this case, the surface curvature shown in Fig. 3.1 becomes negligible, and  $d\theta$  tends to zero. Equation (3.8) then simplifies to

$$\mu \frac{\partial I_\nu}{\partial \tau_\nu} = I_\nu - S_\nu, \quad (3.6)$$

which is our previous formulation of the equation of radiative transfer in plane-parallel stellar atmospheres.

## 3.3 Energy transport in stellar interiors

### 3.3.1 Radiative transfer

In optically thick environments – in particular, stellar interiors – radiation is often the most important transport mechanism,<sup>2</sup> but for large opacities the radiant energy doesn't flow directly outwards; instead, it *diffuses* slowly outwards.

The same general principles apply as led to eqn. (3.6); there is no azimuthal dependence of the radiation field, and the photon mean free path is (very) short compared to the radius. Moreover, we can make some further simplifications. First, the radiation field can be treated as isotropic to a very good approximation. Secondly, the conditions appropriate to 'local thermodynamic equilibrium' (LTE; Sec. 11.1) apply, and the radiation field is very well approximated by black-body radiation.

---

<sup>2</sup>Convection can also be a significant means of energy transport under appropriate conditions, and is discussed in Section 3.3.3.

**Box 3.1.** It may not be immediately obvious that the radiation field in stellar interiors is, essentially, isotropic; after all, outside the energy-generating core, the full stellar luminosity is transmitted across any spherical surface of radius  $r$ . However, if this flux is small compared to the local mean intensity, then isotropy is justified.

The flux at an interior radius  $r$  (outside the energy-generating core) must equal the flux at  $R$  (the surface); that is,

$$\pi F = \sigma T_{\text{eff}}^4 \frac{R^2}{r^2}$$

while the mean intensity is

$$J_\nu(r) \simeq B_\nu(T(r)) = \sigma T^4(r).$$

Their ratio is

$$\frac{F}{J} = \left( \frac{T_{\text{eff}}}{T(r)} \right)^4 \left( \frac{R}{r} \right)^2.$$

Temperature rises rapidly below the surface of stars, so this ratio is always small; for example, in the Sun,  $T(r) \simeq 3.85$  MK at  $r = 0.9R_\odot$ , whence  $F/J \simeq 10^{-11}$ . That is, the radiation field is isotropic to better than 1 part in  $10^{11}$ .

We recall that, in general,  $I_\nu$  is direction-dependent; i.e., is  $I_\nu(\theta, \phi)$  (although we have generally dropped the explicit dependence for economy of nomenclature). Multiplying eqn. (3.6) by  $\cos \theta$  and integrating over solid angle, using  $d\Omega = \sin \theta d\theta d\phi = d\mu d\phi$ , then

$$\frac{d}{d\tau_\nu} \int_0^{2\pi} \int_{-1}^{+1} \mu^2 I_\nu(\mu, \phi) d\mu d\phi = \int_0^{2\pi} \int_{-1}^{+1} \mu I_\nu(\mu, \phi) d\mu d\phi - \int_0^{2\pi} \int_{-1}^{+1} \mu S_\nu(\mu, \phi) d\mu d\phi;$$

or, for axial symmetry,

$$\frac{d}{d\tau_\nu} \int_{-1}^{+1} \mu^2 I_\nu(\mu) d\mu = \int_{-1}^{+1} \mu I_\nu(\mu) d\mu - \int_{-1}^{+1} \mu S_\nu(\mu) d\mu.$$

Using eqtns. (1.14) and (1.9), respectively, for the first two terms, and supposing that the emissivity has no preferred direction (as is true to an excellent approximation in stellar interiors; Box 3.1) so that the source function is isotropic (and so the final term is zero), we obtain

$$\frac{dK_\nu}{d\tau_\nu} = \frac{F_\nu}{4\pi}$$

or, from eqn. (1.15),

$$\frac{1}{3} \frac{dI_\nu}{d\tau_\nu} = \frac{F_\nu}{4\pi}.$$

In LTE we may set  $I_\nu = B_\nu(T)$ , the Planck function; and  $d\tau_\nu = -k_\nu dr$  (where again the minus arises because the optical depth is measured inwards, and decreases with increasing  $r$ ). Making these substitutions, and integrating over frequency,

$$\int_0^\infty F_\nu d\nu = -\frac{4\pi}{3} \int_0^\infty \frac{1}{k_\nu} \frac{dB_\nu(T)}{dT} \frac{dT}{dr} d\nu \quad (3.9)$$

To simplify this further, we introduce the *Rosseland mean opacity*,  $\bar{k}_R$ , defined by

$$\frac{1}{\bar{k}_R} \int_0^\infty \frac{dB_\nu(T)}{dT} d\nu = \int_0^\infty \frac{1}{k_\nu} \frac{dB_\nu(T)}{dT} d\nu.$$

Recalling that

$$\int_0^\infty \pi B_\nu \, d\nu = \sigma T^4 \quad (1.21)$$

we also have

$$\begin{aligned} \int_0^\infty \frac{dB_\nu(T)}{dT} \, d\nu &= \frac{d}{dT} \int_0^\infty B_\nu(T) \, d\nu \\ &= \frac{4\sigma T^3}{\pi} \end{aligned}$$

so that eqn. 3.9 can be written as

$$\int_0^\infty F_\nu \, d\nu = -\frac{4\pi}{3} \frac{1}{\bar{k}_R} \frac{dT}{dr} \frac{acT^3}{\pi} \quad (3.10)$$

where  $a$  is the radiation constant,  $4\sigma/c$ .

The luminosity at some radius  $r$  is given by

$$L(r) = 4\pi r^2 \int_0^\infty F_\nu \, d\nu$$

so, finally,

$$L(r) = -\frac{16\pi}{3} \frac{r^2}{\bar{k}_R} \frac{dT}{dr} acT^3, \quad (3.11)$$

which is our adopted form of the equation of radiative energy transport.

**Box 3.2.** The radiative energy density is  $U = aT^4$  (eqn. 1.26), so that  $dU/dT = 4aT^3$ , and we can express eqn. (3.10) as

$$\begin{aligned} F &= \int_0^\infty F_\nu \, d\nu \\ &= -\frac{c}{3\bar{k}_R} \frac{dT}{dr} \frac{dU}{dT} \\ &= -\frac{c}{3\bar{k}_R} \frac{dU}{dr} \end{aligned}$$

This ‘diffusion approximation’ shows explicitly how the radiative flux relates to the energy gradient; the constant of proportionality,  $c/3\bar{k}_R$ , is called the diffusion coefficient. The larger the opacity, the less the flux of radiative energy, as one might intuitively expect.

### 3.3.2 Convection in stellar interiors

Energy transport can take place through one of three standard physical processes: radiation, convection, or conduction. In the rarified conditions of interstellar space, radiation is the only significant mechanism; and gases are poor conductors, so conduction is generally negligible even in stellar interiors (though not in, e.g., neutron stars). In stellar interiors (and some stellar atmospheres) energy transport by convection can be very important.

## Conditions for convection to occur

We can rearrange eqn. (3.11) to find the temperature gradient where energy transport is radiative:

$$\frac{dT}{dr} = -\frac{3}{16\pi} \frac{\bar{k}_R}{r^2} \frac{L(r)}{acT^3},$$

If the energy flux isn't contained by the temperature gradient, we have to invoke another mechanism – convection – for energy transport. (Conduction is negligible in ordinary stars.) Under what circumstances will this arise?

Suppose that through some minor perturbation, an element (or cell, or blob, or bubble) of gas is displaced upwards within a star. It moves into surroundings at lower pressure, and if there is no energy exchange it will expand and cool adiabatically. This expansion will bring the system into pressure equilibrium (a process whose timescale is naturally set by the speed of sound and the linear scale of the perturbation), but not *necessarily* temperature equilibrium – the cell (which arose in deeper, hotter layers) may be hotter and less dense than its surroundings. If it is less dense, then simple buoyancy comes into play; the cell will continue to rise, and convective motion occurs.<sup>3</sup>

We can establish a condition for convection by considering a discrete bubble of gas moving upwards within a star, from radius  $r$  to  $r + dr$ . We suppose that the pressure and density of the ambient background and within the bubble are  $(P_1, \rho_1)$ ,  $(P_2, \rho_2)$  and  $(P_1^*, \rho_1^*)$ ,  $(P_2^*, \rho_2^*)$ , respectively, at  $(r)$ ,  $(r + dr)$ .

The condition for adiabatic expansion is that

$$PV^\gamma = \text{constant}$$

where  $\gamma = C_P/C_V$ , the ratio of specific heats at constant pressure and constant volume. (For a monatomic ideal gas, representative of stellar interiors,  $\gamma = 5/3$ .) Thus, for a blob of constant mass ( $V \propto \rho^{-1}$ ),

$$\begin{aligned} \frac{P_1^*}{(\rho_1^*)^\gamma} &= \frac{P_2^*}{(\rho_2^*)^\gamma}; \text{ i.e.,} \\ (\rho_2^*)^\gamma &= \frac{P_2^*}{P_1^*} (\rho_1^*)^\gamma. \end{aligned}$$

A displaced cell will continue to rise if  $\rho_2^* < \rho_2$ . However, from our discussion above, we suppose that  $P_1^* = P_1$ ,  $\rho_1^* = \rho_1$  initially; and that  $P_2^* = P_2$  finally. Thus

---

<sup>3</sup>Another way of looking at this is that the entropy (per unit mass) of the blob is conserved, so the star is unstable if the ambient entropy per unit mass decreases outwards.

convection will occur if

$$(\rho_2^*)^\gamma = \frac{P_2}{P_1} (\rho_1)^\gamma < \rho_2.$$

Setting  $P_2 = P_1 - dP$ ,  $\rho_2 = \rho_1 - d\rho$ , we obtain the condition

$$\rho_1 \left(1 - \frac{dP}{P_1}\right)^{1/\gamma} < \rho_1 - d\rho.$$

If  $dP \ll P_1$ , then a binomial expansion gives us

$$\left(1 - \frac{dP}{P}\right)^{1/\gamma} \simeq 1 - \frac{1}{\gamma} \frac{dP}{P}$$

(where we have dropped the now superfluous subscript), and so

$$\begin{aligned} -\frac{\rho}{\gamma} \frac{dP}{P} &< -d\rho, \text{ or} \\ -\frac{1}{\gamma} \frac{1}{P} \frac{dP}{dr} &< -\frac{1}{\rho} \frac{d\rho}{dr} \end{aligned} \tag{3.12}$$

However, the equation of state of the gas is  $P \propto \rho T$ , i.e.,

$$\begin{aligned} \frac{dP}{P} &= \frac{d\rho}{\rho} + \frac{dT}{T}, \text{ or} \\ \frac{1}{P} \frac{dP}{dr} &= \frac{1}{\rho} \frac{d\rho}{dr} + \frac{1}{T} \frac{dT}{dr}; \end{aligned}$$

thus, from eqn. (3.12),

$$\begin{aligned} \frac{1}{P} \frac{dP}{dr} &< \frac{1}{\gamma} \frac{1}{P} \frac{dP}{dr} + \frac{1}{T} \frac{dT}{dr} \\ &< \left(\frac{\gamma}{\gamma-1}\right) \frac{1}{T} \frac{dT}{dr}, \text{ or} \\ \frac{d(\ln P)}{d(\ln T)} &< \frac{\gamma}{\gamma-1} \end{aligned} \tag{3.13}$$

for convection to occur.

### Schwarzschild criterion

Start with adiabatic EOS

$$P\rho^{-\gamma} = \text{constant} \tag{3.14}$$

i.e.,

$$\frac{d \ln \rho}{d \ln P} = \frac{1}{\gamma} \tag{3.15}$$

To rise, the cell density must decrease more rapidly than the ambient density; i.e.,

$$\frac{d \ln \rho_c}{d \ln P_c} > \frac{d \ln \rho_a}{d \ln P_a} \quad (3.16)$$

Gas law,  $P = nkT = \rho kT/\mu$  gives

$$\frac{d \ln \rho}{d \ln P} = 1 + \frac{d \ln \mu}{d \ln P} - \frac{d \ln T}{d \ln P} \quad (3.17)$$

whence the Schwarzschild criterion for convection,

$$\frac{d \ln T_a}{d \ln P_a} > 1 - \frac{1}{\gamma} + \frac{d \ln \mu}{d \ln P}. \quad (3.18)$$

### 3.3.3 Convective energy transport

Convection is a complex, hydrodynamic process. Although much progress is being made in numerical modelling of convection over short timescales, it's not feasible at present to model convection in detail in stellar-evolution codes, because of the vast disparities between convective and evolutionary timescales. Instead, we appeal to simple parameterizations of convection, of which mixing-length 'theory' is the most venerable, and the most widely applied.

We again consider an upwardly moving bubble of gas. As it rises, a temperature difference is established with the surrounding (cooler) gas, and in practice some energy loss to the surroundings must occur.

XXXWork in progress

PART II: THE DIFFUSE NEUTRAL  
INTERSTELLAR MEDIUM

## Section 4

# Introduction: Gas and Dust in the ISM

### 4.1 Gas

The interstellar medium (ISM) is a complex, dynamic environment. In order to reduce this complexity to a tractable summary of the broad characteristics of the ISM, we identify four gas-phase constituents that are in approximate pressure equilibrium. We describe each of these as ‘ionized’ or ‘neutral’, referring to the dominant state of the dominant element, i.e., hydrogen. (Note, however, that there are is some always some ionized hydrogen even in ‘neutral’ regions, because of X-ray and cosmic-ray ionization; and there are always some neutral hydrogen atoms even in ‘ionized’ regions, because of continual recombination; see Section 5).

- (i) *Hot, ionized gas*, occupying most of the volume of the ISM, with  
number density  $n \sim 10^3 \text{ m}^{-3}$ ;  
kinetic temperature  $T_k \sim 10^6\text{K}$ ;  
filling factor  $f \sim 70\%$ ;  
( $nT \sim 10^9 \text{ m}^{-3} \text{ K}$ ).

A probable origin for this hot gas is overlapping old supernova remnants.

- (ii) *Cold, neutral gas*, occupying a smaller volume fraction but providing most of the mass, in the form of ‘clouds’ with  
number density  $n \sim 10^7 \text{ m}^{-3}$ ;  
kinetic temperature  $T_k \sim 30\text{--}100\text{K}$ ;  
( $nT \sim 10^9 \text{ m}^{-3} \text{ K}$ ).

Characteristic length scales are of order  $\sim\text{pc}$ . As well as atoms (and dust grains) they contain some simple molecules (such as  $\text{H}_2$  and  $\text{CO}$ )

At the interface between the hot ionized gas and cool neutral clouds are an outer

- (iii) *Warm, ionized medium* (with an ionization fraction  $X \sim 0.7$ , generated by photoionization), and an inner
- (iv) *Warm, neutral medium* ( $X \sim 0.1$ , maintained by X-rays and cosmic rays), each with  $n \sim 10^5 \text{ m}^{-3}$  and  $T_k \sim 8000\text{K}$  ( $nT \sim 10^9 \text{ m}^{-3} \text{ K}$ ).

There are, in addition, two important gas-phase components *not* in pressure equilibrium:

- (v) *Molecular clouds* are colder, denser regions in which hydrogen is predominantly molecular (not atomic), and other molecules are present (typically detected by their microwave emission).  $n \sim 10^9\text{--}10^{13} \text{ m}^{-3}$  and  $T_k \sim 10\text{--}50\text{K}$ ; typical length scales again  $\sim \text{pc}$ , with larger clouds tending to have lower densities. A large cloud ( $r \sim 30\text{pc}$ ,  $\rho \sim 10^9 \text{ m}^{-3}$ ) has a mass of  $\sim 10^6 M_\odot$ . These clouds have large optical depths in the visible, and are studied through their long-wavelength emission. Smaller, denser clouds may be star-forming.
- (vi) *Photoionized regions* (H II regions and planetary nebulae) – discussed in detail later (page 37 *et seq.*).

This summary is not exhaustive, but accounts for most of the ISM.

## 4.2 Dust

The colder regions, at least, contain interstellar dust in addition to the gas. There is extensive evidence for this dust in the ISM:

- (i) Interstellar absorption (‘holes’ in the sky)
- (ii) Interstellar reddening
- (iii) Solid-state spectral features (e.g., the  $10\text{-}\mu\text{m}$  ‘silicate’ feature)
- (iv) Reflection nebulae
- (v) Depletion of elements from the gas phase

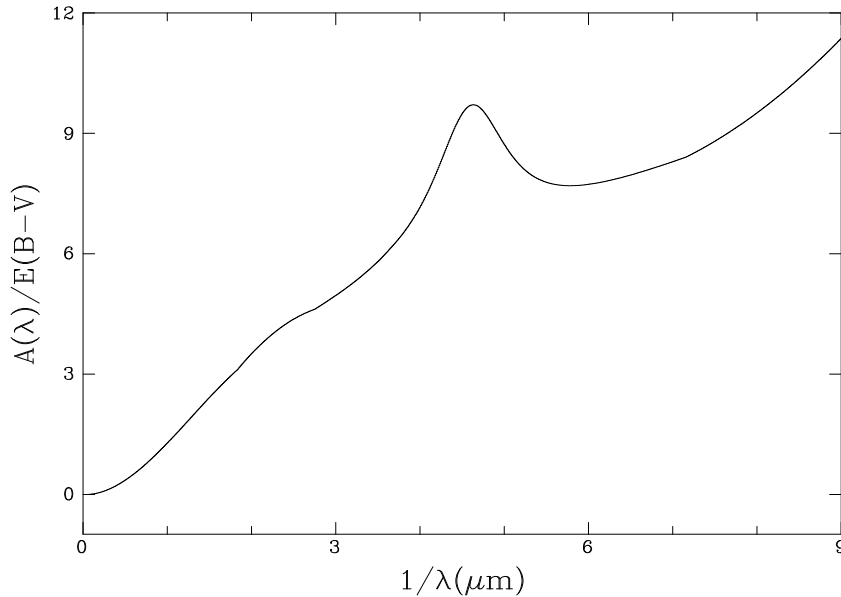


Figure 4.1: The normalized interstellar extinction curve.

Dust grains are intermingled with gas throughout the ISM, with one dust grain for, roughly, every  $\sim 10^{12}$  atoms. Dust grains show a power-law size distribution,

$$n(r) \propto r^{-3.5}, \quad (4.1)$$

derived from an analysis of the interstellar extinction curve, discussed below. Although there is a large range, ‘typical’ grain sizes are of order  $10^2$  nm ( $0.1 \mu\text{m}$ ).

#### 4.2.1 The normalized interstellar extinction curve

Extinction by dust is the removal of continuum light from starlight, including both absorption and scattering.<sup>1</sup> When ‘extinction’ is used without qualification in interstellar astrophysics, it is often this continuous dust extinction that is meant.<sup>2</sup>

Extinction removes a *fraction* of incident radiation (not an absolute amount; eqn. 3.3). Since removing a fixed fraction of radiation corresponds to a fixed magnitude change, dust extinction is conventionally expressed in magnitudes, as a function of wavelength:

$$m(\lambda) = m_0(\lambda) + A(\lambda) \quad (4.2)$$

---

<sup>1</sup>Recall: an *absorbed* photon is destroyed, with its energy used in ejecting an electron, or converted into internal energy of the dust grain; while a *scattered* photon is re-emitted, normally in a different direction to that which it came in.

<sup>2</sup>The distinction between the smallest dust grains and the largest molecules is moot. Particularly in the infrared, there is structure in the extinction curve (on scales much larger than that of atomic absorption lines) that is attributable to large molecules, such as polycyclic aromatic hydrocarbons.

where  $m(\lambda)$  is the observed magnitude,  $m_0(\lambda)$  is the magnitude which would be observed in the absence of extinction, and  $A(\lambda)$  is the extinction (a positive quantity). Of course, it is not possible to separate the two terms on the right-hand side of eqn. (4.2). Fortunately, however, the wavelength dependence of extinction comes to our aid. If we observe at two wavelengths then

$$m(\lambda_2) - m(\lambda_1) = m_0(\lambda_2) - m_0(\lambda_1) + A(\lambda_2) - A(\lambda_1) \quad (4.3)$$

The left-hand side is an observed quantity, while  $m_0(\lambda_2) - m_0(\lambda_1)$  can be estimated from observations of unreddened stars of the same spectral type as the target; these stars are assumed to have the same temperature, and the same intrinsic colours, as the target.

The differential extinction,  $A(\lambda_2) - A(\lambda_1)$  still depends on the absolute extinction (it's bigger for more heavily reddened stars). It is convenient to take out this dependence by normalizing the extinction curve such that

$$A(B) - A(V) \equiv E(B - V) \equiv 1$$

where  $\lambda_B \simeq 440\text{nm}$  and  $\lambda_V \simeq 550\text{nm}$ .<sup>3</sup> Then for any other wavelength

$$\frac{A(\lambda) - A(V)}{A(B) - A(V)} = \frac{E(\lambda - V)}{E(B - V)} = \frac{A(\lambda)}{E(B - V)} - \frac{A(V)}{E(B - V)} \quad (4.4)$$

We plot this quantity against  $1/\lambda$  (Fig. 4.1). The general trend is one of increasing extinction towards shorter wavelengths (at least, down to the Lyman edge at 91.2 nm), with little large-scale structure excepting the so-called ‘2200Å bump’. In particular, because the extinction is greater at  $B$  than at  $V$ , a star which undergoes extinction appears *reddened*; and interstellar *reddening* is generally used synonymously with interstellar extinction.

The form of the curve is a function of the chemical composition of the grains, and their size distribution. The overall shape is fairly constant along diffuse sightlines in our Galaxy, but there are significant differences in denser environments, and in galaxies with different metallicities (e.g., the 2200Å bump is much weaker in many SMC sightlines, presumably a consequence of the lower metallicity there).

#### 4.2.2 The ratio of total to selective extinction.

The normalization to unit  $E(B - V)$  in eqn. (4.4) has the advantage that we can compare the differential extinction curves of different stars (per unit  $E(B - V)$ ); but the unknown value of the constant term  $A(V)/E(B - V)$  means that we don't know the *absolute* extinction at any wavelength.

---

<sup>3</sup>The precise value of the ‘effective wavelength’ of a filter depends on then colour of the target being observed.

Differential extinction (e.g.  $E(B - V)$ ) may be referred to as a *selective* extinction. The *total* extinction at any wavelength (e.g.  $V$ ) is found by extrapolating the extinction curve in the infrared and assuming that

$$A(\lambda) \rightarrow 0 \text{ as } \lambda \rightarrow \infty$$

(which is a prediction of scattering theory, verified by everyday experience – brick walls are transparent to radio waves). The intercept on the  $y$  axis equals  $-R$ , where

$$R = \frac{A(V)}{E(B - V)}$$

is referred to as ‘the’ ratio of total to selective extinction. A value close to  $R = 3.1$  is found for diffuse clouds in general, although larger values are found in dense clouds (where the grain composition is different—e.g. ice mantles). In fact,  $R$  is a crude size indicator—optical theory shows that bigger dust grains produce a bigger value of  $R$ .

### 4.3 Other ingredients

We have already mentioned the diffuse radiation field arising from the integrated light of stars; the ISM is also permeated by the cosmic microwave background, and by a flux of high-energy cosmic rays (which can play an important role in ionization and dissociation in dense clouds, where few photons penetrate).

## PART III: IONIZED NEBULAE

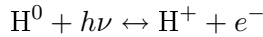


## Section 5

# Ionization equilibrium in H II Regions

Photons with energies  $h\nu > 13.6\text{eV}$  ( $= I_{\text{H}}$ , the ground-state ionization potential for hydrogen) may photoionize neutral hydrogen atoms. Excess energy  $h\nu - I_{\text{H}}$  is carried away as kinetic energy of the ejected electron (and hence goes into heating the gas).

The inverse process is recombination, and in equilibrium



where essentially all ionizations are from the  $n = 1$  level, but recombinations are to *all* levels. We will consider these processes in some detail, considering a pure hydrogen nebula.

### 5.1 Recombination

Recombination may occur to any level (principal quantum number  $n$ ), and is followed by cascading down to the  $n = 1$  level. The rate of recombinations per unit volume into level  $n$ ,  $\dot{n}_n$ , depends on the density *squared*, and on the electron temperature:

$$\dot{n}_n = n_e n_p \alpha_n(T_e) \simeq n_e^2 \alpha_n(T_e) \quad [\text{m}^{-3} \text{ s}^{-1}]. \quad (5.1)$$

where  $\alpha_n(T_e)$  is the *recombination coefficient* (to level  $n$  at electron temperature  $T_e$ ).

Obviously, the recombination rate is proportional to the number of available protons,  $n_p$ , and the number of available electrons,  $n_e$ ; and for a pure hydrogen nebula,  $n_p = n_e$ . The temperature dependence of  $\alpha_n(T_e)$  arises for two reasons:

- (i) The higher the temperature the faster the electrons, and the more likely they are to encounter a proton; but,
- (ii) the faster the electron the less likely it is to be ‘captured’ by the proton.

The latter term is more important, so the recombination coefficient is *smaller* at higher temperatures.

For the purpose of calculating the overall ionization balance, we evidently need the rate of recombinations to *all* levels (so called ‘case A recombination’):

$$\dot{n}_A = \sum_{n=1}^{\infty} n_e n_p \alpha_n(T_e) \equiv n_e n_p \alpha_A(T_e)$$

However – recombination to  $n = 1$  will always result in a photon with  $h\nu > 13.6\text{eV}$  (i.e., a Lyman continuum photon), which will quickly be re-absorbed in a photoionization. Thus recombinations to  $n = 1$  may be followed by ionizations from  $n = 1$ .<sup>1</sup> In the ‘on the spot’ approximation, photons generated in this way are assumed to be re-absorbed quickly and locally, and thus have no overall effect on the ionization balance.

In case B recombination, we therefore do *not* include recombination direct to the ground state;

$$\dot{n}_B = \sum_{n=2}^{\infty} n_e n_p \alpha_n(T_e) \equiv n_e n_p \alpha_B(T_e). \quad (5.2)$$

A reasonable numerical approximation to detailed calculations is

$$\alpha_B(T_e) \simeq 2 \times 10^{-16} T_e^{-3/4} \text{ m}^3 \text{ s}^{-1}. \quad (5.3)$$

## 5.2 Ionization

The lifetime of an excited level in the hydrogen atom ( $1/A_{ji}$ ) is  $\sim 10^{-6}$ – $10^{-8}$ s. This is very much less than the ionization timescale, so the probability of a photoionization from an excited state is negligible; essentially *all* ionization is from the ground state.

Suppose a star is embedded in a gas of uniform mass density. Then consider a volume element  $dV$  in a thin shell of thickness  $dr$  at distance  $r$  from the ionizing star.

Let the number of photons from the star crossing unit area of the shell per unit time be

$$N_P(\nu) \quad (\text{m}^{-2} \text{ s}^{-1});$$

then the photoionization rate from level 1 is

$$\begin{aligned} \dot{n}_1 &= \int_{\nu_0}^{\infty} a_\nu n(\text{H}^0) N_P(\nu) d\nu \\ &= \bar{a}_1 n(\text{H}^0) N_P(I) \quad (\text{m}^{-3} \text{ s}^{-1}). \end{aligned} \quad (5.4)$$

---

<sup>1</sup>In principle, recombination of sufficiently energetic electrons to other levels can also result in ionizing photons, but this is a rare outcome in practice.

where  $\nu_0$  is the photon frequency corresponding to the ground-state ionization potential of hydrogen ( $h\nu = 13.6$  eV)  $N_P(I)$  is the number of ionizing photons,  $a_\nu$  is the ground-state photoionization cross-section (in units of  $\text{m}^2$ ), and  $\bar{a}_1$  is the value of  $a_\nu$  averaged over frequency. In practice,

$$a_\nu \simeq a_0(\nu_0/\nu)^3$$

for hydrogen (and hydrogen-like atoms), where  $a_0$  is the cross-section at  $\nu_0$ . The photoionization cross-section therefore peaks at  $a_0$ ; the flux of ionizing photons also typically peaks near  $\nu_0$ . It's therefore not too inaccurate (and certainly convenient) to assume

$$\bar{a}_1 \simeq a_0 = 6.8 \times 10^{-22} \text{ m}^2.$$

### 5.3 Ionization equilibrium

We first introduce  $x$ , the degree of ionization, defined by

$$n_p [= n(\text{H}^+)] = n_e = xn(\text{H})$$

where  $n(\text{H})$  is the *total* number of hydrogen nuclei,  $n_p + n(\text{H}^0)$ ; that is,  $x = 0$  for a neutral gas,  $x = 1$  for a fully ionized gas, and, in general,

$$n(\text{H}^0) = (1 - x)n(\text{H})$$

The condition of *ionization equilibrium* is that the number of recombinations equals the number of (ground-state) ionizations:

$$\dot{n}_R (\equiv \dot{n}_B) = \dot{n}_I.$$

That is

$$n_e n_p \alpha_B(T_e) = a_0(1 - x) n(\text{H}) N_P(I)$$

(from eqtns. (5.2) and (5.4)). Noting that, for our pure hydrogen nebula,

$$n_e n_p = n_p^2 = x^2 n^2(\text{H})$$

we obtain

$$\frac{x^2}{(1 - x)} = \frac{N_P(I)}{n(\text{H})} \frac{a_0}{\alpha_B(T_e)}. \tag{5.5}$$

To estimate the photon flux  $N_P$  at a typical point in the nebula, we assume simple inverse-square dilution of the stellar flux [a good approximation except *very* near the star

(where the geometry is slightly more complex) and near the edge of the nebula (where absorption becomes important<sup>2</sup>):

$$N_P \simeq \frac{S_*}{4\pi r^2} \quad [\text{m}^{-2} \text{ s}^{-1}] \quad (5.6)$$

where  $S_*$  is the rate at which the star emits ionizing photons ( $\text{s}^{-1}$ ). For representative numbers,

$$\begin{aligned} n(\text{H}) &= 10^8 \text{ m}^{-3} \\ r &= 1 \text{ pc} \quad (3.08568025 \times 10^{16} \text{ m}) \\ S_* &= 10^{49} \text{ s}^{-1} \end{aligned}$$

(where  $S_*$  corresponds roughly to an O6.5 main-sequence star – similar to the ionizing star in the Orion nebula), eqtn. (5.6) gives

$$N_P \simeq 8 \times 10^{14} \quad \text{m}^{-2} \text{ s}^{-1}$$

and eqtn. (5.5) becomes

$$\frac{x^2}{(1-x)} \simeq 3 \times 10^4 \quad (5.7)$$

(for  $T_e \sim 10^4\text{K}$ ). We can solve this (e.g., by Newton-Raphson), giving  $(1-x) = 3 \times 10^{-5}$ ; but we can see by simple inspection that  $x \simeq 1$  – i.e., where the gas is ionized it is, essentially, *fully* ionized.

## 5.4 Nebular size and mass; the ‘Strömgren Sphere’

There is a simple physical limit to the size of a photoionized nebula; the total number of (case B) recombinations per unit time within a nebula must equal the total number of ionizing photons emitted by the star per unit time; that is, for a homogeneous nebula,

$$\frac{4}{3}\pi R_S^3 n_e n_p \alpha_B(T_e) = S_* \quad (5.8)$$

where  $R_S$  is the (ionized) nebular radius, or *Strömgren radius*,

$$R_S = \left[ \frac{3}{4\pi} \frac{S_*}{n_e^2 \alpha_B(T_e)} \right]^{1/3} \quad (5.9)$$

where we’ve used the fact that  $n_p = n_e$ . The ionized volume is called the *Strömgren sphere*. Again adopting  $S_* = 10^{49} \text{ s}^{-1}$  (and using  $T_e \simeq 10^4\text{K}$  in eqtn. (5.3) to evaluate  $\alpha_B$ ) we find

$$R_S \simeq 7 \times 10^5 n_e^{-2/3} \quad \text{m}^{-2} \text{ pc}$$

---

<sup>2</sup>Recall that the attenuation is *exponential*, so there is a fairly rapid swieth from ‘ionized’ to ‘neutral’ as the flux of ionizing photons rapidly diminishes.

For typical densities, Strömngren radii are of order  $\sim 10^0\text{--}10^2$  pc.

The mass is the volume times the (mass) density:

$$\begin{aligned} M_S &= \frac{4}{3}\pi R_S^3 n_e m(\text{H}) \\ &= \frac{S_* m(\text{H})}{n_e \alpha_B(T_e)} \end{aligned}$$

(from eqtn. (5.8)). Typical values are of order  $\sim 10^3 M_\odot$ , with a large dispersion.



## Section 6

# The Radio-Frequency Continuum

Free-free emission (or *bremstrahlung*) is generated by the deceleration of thermal electrons in the electric field of ions. This is a continuous process in wavelength, but the emission is most readily observed in the radio regime, where it dominates the emission from an ionized gas. Here we will discuss its application to ionized nebulae.

Self-absorption of free-free emission within the nebula can be significant, and must be taken into account – i.e., we must consider the radiative transfer within the nebula. To do this we recall definitions from Section 1

- $I_\nu$ , the (*specific*) *intensity* of radiation – the rate of energy flow energy,
  - per unit frequency,
  - per unit area,
  - per unit solid angle,
  - per unit time.

SI Units are thus  $\text{J Hz}^{-1} \text{m}^{-2} \text{sr}^{-1} \text{s}^{-1}$  ( $= \text{J m}^{-2} \text{sr}^{-1}$ )

- $j_\nu$ , the *emission coefficient* – the radiant energy emitted by the gas,
  - per unit frequency,
  - per unit volume,
  - per unit solid angle,
  - per unit time.

Units are thus  $\text{J Hz}^{-1} \text{m}^{-3} \text{sr}^{-1} \text{s}^{-1}$  ( $= \text{J m}^{-3} \text{sr}^{-1}$ )

- $k_\nu$ , the *absorption coefficient*, or opacity per unit volume.

From Section 3.1, the equation of radiative transfer can be written as

$$\frac{dI_\nu}{ds} = j_\nu - k_\nu I_\nu, \tag{3.1}$$

where the ratio  $j_\nu/k_\nu$  is the *Source Function*,  $S_\nu$ . For systems in thermodynamic equilibrium, the source function is given by the Planck function,  $B_\nu$ , and  $j_\nu$  and  $k_\nu$  are related through the Kirchhoff relation,

$$j_\nu = k_\nu B_\nu(T); \quad \text{i.e., } S_\nu = B_\nu$$

(Section 11.1). Because free-free radiation is an essentially collisional process, in this respect the nebula is in thermodynamic equilibrium, and we can use  $S_\nu = B_\nu$ . Then eqtn. (3.1) can be written in the form

$$\frac{dI_\nu}{d\tau_\nu} = B_\nu(T_e) - I_\nu$$

(cp. eqtn. (3.2)), where we have use the definition of optical depth,

$$d\tau_\nu = k_\nu ds.$$

The solution of this first-order differential equation is

$$I_\nu = B_\nu(T_e)(1 - \exp\{-\tau_\nu\}). \quad (6.1)$$

where  $\tau_\nu$  is the total optical depth through the region. Note that we have made two implicit assumptions –

- $T_e$  is constant throughout the region
- $I_\nu = 0$  at  $\tau_\nu = 0$ ; i.e., there is no external or background radiation.

There are two obvious limiting forms of eqtn. (6.1):

1. For  $\tau_\nu \gg 1$ ,  $\exp\{-\tau_\nu\} \rightarrow 0$ , and

$$I_\nu \simeq B_\nu(T_e) \quad (6.2)$$

2. For  $\tau_\nu \ll 1$ ,  $\exp\{-\tau_\nu\} \rightarrow [1 - \tau_\nu]$  and

$$I_\nu \simeq B_\nu(T_e)\tau_\nu \quad (6.3)$$

### **Free-free opacity (reference only)**

From Allen (AQ), the free-free opacity is given by:

$$k_{\text{ff}} = \frac{4\pi}{3\sqrt{3}} \frac{Z^2 e^6}{hcm_e^2 v_e} \frac{g_{\text{ff}}}{\nu^3} n_e n_i \quad [\text{m}^{-1}]$$

where  $g_{\text{ff}}$  is the free-free gaunt factor. Using

$$v_e = \sqrt{\frac{\pi kT}{2m_e}}.$$

as the mean velocity, and allowing for stimulated emission,

$$k_\nu = 3.692 \times 10^8 \frac{Z^2 g_{\text{ff}} n_e n_i}{\nu^3 \sqrt{T}} \left[ 1 - \exp \left\{ -\frac{h\nu}{kT} \right\} \right]$$

for electron velocity  $v_e$ , ionic charge  $Z$ , electron and ion densities  $n_e n_i$ , and cgs units throughout ( $\lambda$  in cm). Normally  $n_e \simeq n_i \simeq n(\text{H})$  (and certainly  $n_e, n_i \propto n(\text{H})$ ); then expanding the exponential term,

$$\exp \left\{ -\frac{h\nu}{kT} \right\} \simeq 1 - \frac{h\nu}{kT} + \frac{1}{2} \left( \frac{h\nu}{kT} \right)^2 \dots$$

gives

$$k_{\text{ff}} \propto g_{\text{ff}} \nu^{-2} T^{-3/2} n^2(\text{H})$$

In the case of free-free radiation at radio wavelengths, the opacity can be approximated by

$$k_\nu \propto \nu^{-2.1} T_e^{-1.35} n_e n_p$$

(where we have made allowance for the weak  $\nu, T$  dependences of  $g_{\text{ff}}$ ), so that for a pure-hydrogen nebula ( $n_e = n_p$ )

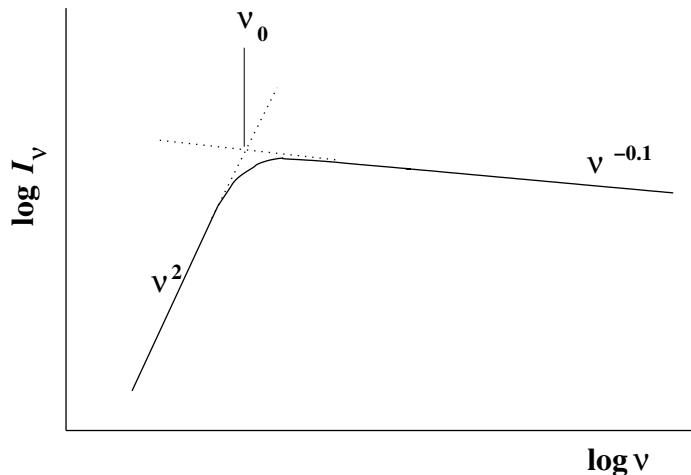
$$\tau_\nu = k_\nu L \propto \nu^{-2.1} T_e^{-1.35} n_e^2 L \tag{6.4}$$

for path length  $L$  through the nebula; the quantity  $n_e^2 L$  is a fixed quantity, called the *Emission Measure* (usually expressed in units of  $\text{m}^{-6} \text{pc}$ ), for a given nebula. Note that the optical depth is smaller at higher frequencies (shorter wavelengths).

At radio frequencies we can use the Rayleigh-Jeans approximation to the Planck function (eqtn. 1.23),

$$B_\nu(T_e) = \frac{2h\nu^3}{c^2} \frac{1}{\exp\{h\nu/kT_e\}} \simeq \frac{2kT_e}{c^2} \nu^2 \tag{6.5}$$

[since  $(h\nu)/(kT_e) \ll 1$  for small  $\nu$ , so  $\exp\{(h\nu)/(kT_e)\} \simeq 1 + (h\nu)/(kT_e)$ ].



In the optically thin limit (small optical depth; high frequencies, short wavelengths) eqtns. (6.4), (6.5) and (6.3) give

$$I_\nu \propto \nu^{-0.1} T_e^{-0.35} n_e^2 L$$

while in the optically thick limit (large optical depths; small frequencies, long wavelengths) eqtns. (6.4), (6.5) and (6.2) give

$$I_\nu \propto \nu^2 T_e.$$

That is, we can determine the nebular temperature, directly (and independent of distance<sup>1</sup> from the intensity at optically thick frequencies; then knowing  $T_e$ , we can determine the emission measure from the emission at any optically thin frequency (or from eqtn. (6.4) by determining the ‘turnover frequency’,  $\nu_0$ , at which the optical depth is unity).

---

<sup>1</sup>For a spatially resolved source; cf. section 1.3

## Section 7

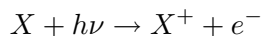
# Heating & Cooling in the Interstellar Medium

### 7.1 Heating

In general terms, we can imagine two categories of heating processes in the *diffuse* ISM:<sup>1</sup> large-scale (mechanical, e.g., cloud-cloud collisions), and ‘microscopic’ (absorption of photon energy by gas or dust). The second dominates under most circumstances, but, in any event, we should note that collisions normally enforce a Maxwellian velocity distribution of particles (eqtn. 8.15), and the kinetic temperature serves as the most useful characterization of ‘the’ temperature.

#### 7.1.1 Photoionization

The principal source of heating in the gas phase is photoionization – the ejection of an electron from some species  $X$  (a parent atom, ion, or molecule):



The ejected electron carries away some energy which goes into heating the gas; that energy is the difference between the photon energy and the ionization potential,  $h\nu - \text{IP}$ .

#### Ionized gas

In H II regions, photoionization of hydrogen dominates (because of its abundance); the gas is heated through the energy of freed electrons,  $E = h\nu - I_{\text{H}}$  (where  $I_{\text{H}}$  is the ionization potential

---

<sup>1</sup>We exclude molecular clouds from this treatment, where cosmic rays are a significant heating source.

of hydrogen, 13.6eV, corresponding to  $\lambda \leq 91.2\text{nm}$ ).

The heating rate  $G$  (for ‘Gain’) – that is, the energy input to the gas (per unit volume per unit time) – is

$$G = \dot{n}_I Q (= \dot{n}_R Q \text{ in equilibrium}) \quad [\text{J m}^{-3} \text{s}^{-1}] \quad (7.1)$$

where  $Q$  is the average energy input into the gas per hydrogen photoionization ( $= \overline{h\nu} - I_{\text{H}}$ ) and  $\dot{n}_I$ ,  $\dot{n}_R$  are the hydrogen ionization and recombination rates ( $\dot{n}$  meaning  $dn/dt$ ). As in Section 5, we write the recombination rate as

$$\dot{n}_R = n_e n_p \alpha_{\text{B}}(T_e) \quad [\text{m}^{-3} \text{s}^{-1}] \quad (5.2)$$

where  $\alpha_{\text{B}}$  is the case B recombination coefficient for hydrogen, for which numerical values are given by equation (5.3).

## Neutral gas

By definition, hydrogen is almost entirely neutral in the ‘diffuse neutral clouds’ (some ionization is produced by cosmic rays and X-rays). This means there must be a negligible density of photons with energies  $\geq 13.6\text{eV}$ , and as a result only species with  $\text{IP} < 13.6\text{eV}$  can be photoionized in neutral clouds.

Of such species, neutral carbon is the most important, with  $\text{IP} = 11.3\text{eV}$ , corresponding to photons with wavelengths shortward of 110nm. (Neutral nitrogen and oxygen, for example, have IPs of 14.4eV and 13.6eV, and so they remain largely un-ionized.)

However, photoionization of  $\text{C}^0$  (and other species) is not an effective heating mechanism, because

- (i) carbon is not very abundant ( $\sim 10^{-4}$  by number compared to hydrogen);
- (ii) only photons with wavelengths in the narrow wavelength range 91.2–110.0nm can ionize;
- (iii) The maximum energy release per ionization is only  $13.6 - 11.3\text{eV} = 2.3\text{eV}$  (and so the *average* energy release is only  $\sim 1\text{eV}$ ).

### 7.1.2 Photoejection

The dominant heating mechanism in the neutral ISM is, in fact, photoejection of electrons from interstellar dust grains. The energy of the ejected electron is

$$E_{\text{pe}} = h\nu - W$$

where  $h\nu$  is an average photon energy for the diffuse interstellar radiation field and  $W$  is the grain *work function* (analogous to the ionization potential). For typical values of  $h\nu \simeq 11\text{eV}$

and  $W \simeq 5\text{eV}$ , about  $6\text{eV}$  is available, per photoejection, for heating the gas. Grain photoejection is thus more effective than photoionization (primarily because  $W < \text{IP}$ ).

The heating rate for photoejection, for grains of radius  $r$ , is given by

$$G = \int \left\{ n(\text{H}) A_{\text{d}}(r) \int_{\nu_W}^{\nu_0} \left[ \frac{F_{\nu}}{h\nu} \phi_{\text{d}}(\nu, r) y_{\text{pe}}(\nu, r) \right] E_{\text{pe}}(\nu) d\nu \right\} dr \quad (7.2)$$

Here

$n(\text{H})$  is the hydrogen-atom number density,

$A_{\text{d}}(r)$  is the dust-grain projected surface area per hydrogen (so  $n(\text{H})\bar{A}_{\text{d}}$  is the total dust-grain surface area per unit volume);

$F_{\nu}/h\nu$  is the flux of photons with frequency  $\nu$  incident on the grain surface;

$\phi_{\text{d}}(\nu)$  is the average photon absorption efficiency of the grains ( $0 \leq \phi_{\text{d}}(\nu) \leq 1$ ; this measures how many incident photons are actually absorbed);

$y_{\text{pe}}(\nu)$  is the photoelectric efficiency, or quantum yield (measuring how many electrons are ejected per photoabsorption);

$E_{\text{pe}}(\nu)$  is the mean energy of a photoejected electron as a function of energy of the incident photon;

$\nu_0$  is the frequency corresponding to the IP of hydrogen ( $3.289 \times 10^{15} \text{ s}^{-1}$ ), corresponding in turn to the photon energy available in diffuse, *neutral* clouds; and

$\nu_W$  is the frequency corresponding to the grain work function.

To see the physical significance of eqtn. (7.2) we can rewrite it schematically as

$$G = n(\text{H})\bar{A}_{\text{d}} F_{\text{pe}} \bar{E}_{\text{pe}} \quad (7.3)$$

where

$n(\text{H})\bar{A}_{\text{d}}$  is the available grain area per unit volume of space,

$F_{\text{pe}}$  is the flux of photoejected electrons (per unit grain surface area), averaged over frequency, for which observations of the diffuse radiation field suggest

$$F_{\text{pe}} \simeq 2 \times 10^{11} y_{\text{pe}} \bar{\phi}_{\text{d}} \text{ m}^{-2} \text{ s}^{-1}.$$

where the numerical constant is a measure of the photon density in the diffuse radiation field, and

$\bar{E}_{\text{pe}}$  is the average energy of the ejected photoelectrons.

For the UV frequencies of interest, the mean dust absorption efficiency is  $\bar{\phi}_{\text{d}} \simeq 1$ . Typical values of  $y_{\text{pe}}$  are a few tenths, for average grain sizes and incident photon energies  $\gtrsim 10\text{eV}$ . However, smaller grains have larger yields; the mean free path for slowing a photoelectron (before it can escape) is of order 10nm, and so, for dust grains of radius  $\sim 5\text{nm}$ ,  $y_{\text{pe}} \simeq 1$ .

Since small grains dominate the size distribution (eqn. (4.1); as usual in astronomy, there are lots of little 'uns and not many big 'uns), photoejection can be an efficient heating mechanism. If we adopt  $\bar{E}_{\text{pe}} = 5\text{eV}$  and  $A_{\text{d}} = 10^{-25} \text{ m}^2$  per H atom, we find

$$G \simeq 2 \times 10^{-32} y_{\text{pe}} n(\text{H}) \text{ J s}^{-1} \quad (7.4)$$

where  $y_{\text{pe}} \simeq 0.1\text{--}1.0$ .

## 7.2 Cooling processes

Cooling processes fundamentally involve the conversion of kinetic energy (thermal motion) to radiant energy (photons) which can escape from the system – the inverse of heating processes. This typically occurs through collisional excitation, followed by radiative decay. Because hydrogen and helium require rather high energies (i.e., high temperatures) for collisional excitation from the ground state, cooling in interstellar gas is mostly through metal lines. Moreover, if the radiative decay is in an ‘allowed’ transition, the resulting photon is liable to be re-absorbed elsewhere in the gas (in a photo-excitation), and so is inefficient as a coolant. The most important cooling lines therefore result from collisional excitation of ‘forbidden’ (or semiforbidden) transitions.

We designate the lower level of some species  $I$  with number density  $n(I)$ , as  $i$ , and an excited upper level as  $j$ . The *collisional excitation rate* from level  $i$  to  $j$ , resulting from collisions with some particle  $X$  (typically an electron in ionized gas, or a hydrogen atom in diffuse neutral gas), is

$$\dot{n}_{ij} = n_X n_i(I) C_{ij}(T_{\text{k}}) \quad [\text{m}^{-3} \text{ s}^{-1}] \quad (7.5)$$

where  $C_{ij}(T_{\text{k}})$  is the *rate coefficient* for collisional excitation, at kinetic temperature  $T_{\text{k}}$  (with typical values of order  $\sim 10^{-4}\text{--}10^{-2} \text{ m}^3 \text{ s}^{-1}$ ).

We recall that this rate coefficient (and hence the collisional excitation rate) has a Boltzmann-like dependence on the kinetic temperature,

$$\begin{aligned} C_{ij}(T_{\text{k}}) &= \left(\frac{2\pi}{T_{\text{k}}}\right)^{1/2} \frac{h^2}{4\pi^2 m_e^{3/2}} \frac{\Omega(ij)}{g_i} \exp\left\{\frac{-\Delta E_{ij}}{kT_{\text{k}}}\right\} \\ &\propto \frac{1}{\sqrt{T_{\text{k}}}} \exp\left\{\frac{-\Delta E_{ij}}{kT_{\text{k}}}\right\} \quad [\text{m}^3 \text{ s}^{-1}] \end{aligned} \quad (2.7)$$

If each excitation is followed by radiative decay (and emission of a forbidden-line photon of energy  $\Delta E_{ij}$ ), then the rate of energy loss is

$$L_{ij} = \dot{n}_{ij} \Delta E_{ij} = n_X n_i(I) C_{ij}(T_e) \Delta E_{ij} \quad [\text{J m}^{-3} \text{ s}^{-1}] \quad (7.6)$$

Note that cooling is a two-body collisional process, and the loss rate depends on the product of the densities of both bodies involved. Since each density depends on the overall density, cooling is a density *squared* process; this contrasts with photo-heating, which only involves a single particle (plus a photon).

### 7.2.1 Cooling of the neutral ISM

In the cool, neutral ISM:

(i) The electron densities are low (these are neutral clouds!), so it is impacts of atoms that are most important. Hydrogen impacts dominate because of its abundance and relatively low mass (resulting in relatively high speeds).

(ii) Because kinetic temperatures are low, the transitions that are excited in the diffuse ISM must be low-energy transitions, often corresponding to splitting of ground-state levels of the atom by the fine-structure interaction. (Not all atoms/ions undergo fine-structure splitting of the ground state; e.g.,  $\text{C}^0$  and  $\text{O}^0$  do, but  $\text{N}^0$  doesn't.)

Because the transitions<sup>2</sup> involve only small energy changes, the emitted photons are typically in the far-IR:

Ion/Spectrum	Transition	Collider	$\Delta E/k$	$\lambda$ ( $\mu\text{m}$ )
$\text{Si}^+ / [\text{Si II}]$	${}^2P_{3/2} \rightarrow {}^2P_{1/2}$	(H), e	413K	34.8
$\text{O}^0 / [\text{O I}]$	${}^3P_1 \rightarrow {}^3P_2$	H, e	228K	63.2
	${}^3P_0 \rightarrow {}^3P_1$	H, e	99K	146
$\text{C}^+ / [\text{C II}]$	${}^2P_{3/2} \rightarrow {}^2P_{1/2}$	$\text{H}_2$ , H, e	92K	158

One of the most important single coolants in diffuse neutral clouds is the C II 158- $\mu\text{m}$  line, with  $\Delta E/k = 92\text{K}$ . The cooling rate  $L$  (for ‘Loss’) associated with the transition is, from eqtn. (7.6),

$$L(\text{C II}) = \text{const} \times n(\text{H})n(\text{C}) T_k^{-1/2} \exp(-92/T_k) \text{ m}^3 \text{ J s}^{-1}$$

(for excitation by neutral hydrogen), but we can write

$$n(\text{C}) = n(\text{H})a(\text{C})\delta(\text{C})$$

---

<sup>2</sup>Notation: (multiplicity)<sub>(L quantum number)<sub>(J)</sub></sub>

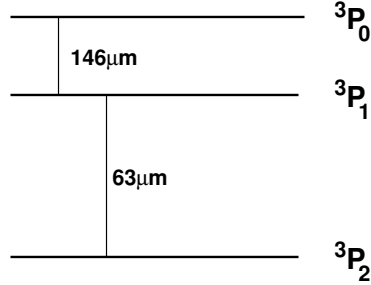


Figure 7.1: Schematic structure for  $O^0$

where  $a(C)$  is the abundance (by number) of carbon relative to hydrogen and  $\delta(C)$  is the *depletion factor* for gaseous carbon, which accounts for the fact that a significant fraction of carbon may be locked up in dust grains (and hence absent from the gas phase). Inserting appropriate numerical values for the various constants (including an assumed ‘cosmic’ abundance for carbon) we obtain

$$\begin{aligned}
 L(C \text{ II}) &= 8 \times 10^{-40} n^2(\text{H}) \delta(C) \exp(-92/T) \text{ m}^3 \text{ J s}^{-1} \\
 &= 2.5 \times 10^{-40} n^2(\text{H}) \delta(C) \text{ m}^3 \text{ J s}^{-1} \quad \text{at } 80\text{K}.
 \end{aligned}
 \tag{7.7}$$

The depletion factor  $\delta(C)$  is not particularly well known; clearly,  $\delta(C) \leq 1$ , and probably  $\delta(C) \sim 0.1$ .

### 7.2.2 Cooling of the ionized gas

The importance of collisional excitation of forbidden lines of metals followed by radiative decay as a coolant in H II gas can be seen directly in the spectra of photoionized nebulae; the total flux in forbidden lines of metals exceeds that in the hydrogen lines. The efficiency of collisional excitation (in this case, by free electrons) is sufficiently high that it more than offsets the low abundances of metals compared to hydrogen.

We consider oxygen (one of the most important coolants of ionized gas) as an example. The IP of  $O^0$ , 13.6eV, is almost the same as that of hydrogen, so where hydrogen is ionized, so is oxygen. (The IP of  $O^+$  is 35.1eV, so only the hotter O stars can produce  $O^{2+}$ .)

All the labelled transitions in fig. 7.2 are *forbidden* (as electric dipole transitions; they can occur as magnetic dipole transitions or electric quadrupole transitions, with transition probabilities  $A_{ji} \sim 1 \text{ s}^{-1}$  [compare with allowed transitions,  $A_{ji} \sim 10^8 \text{ s}^{-1}$ ]). They are not observed in the laboratory, where collisional de-excitation occurs before radiative decay can take place. However, at the much lower densities of nebulae, radiative decays can occur more rapidly than collisional de-excitations.

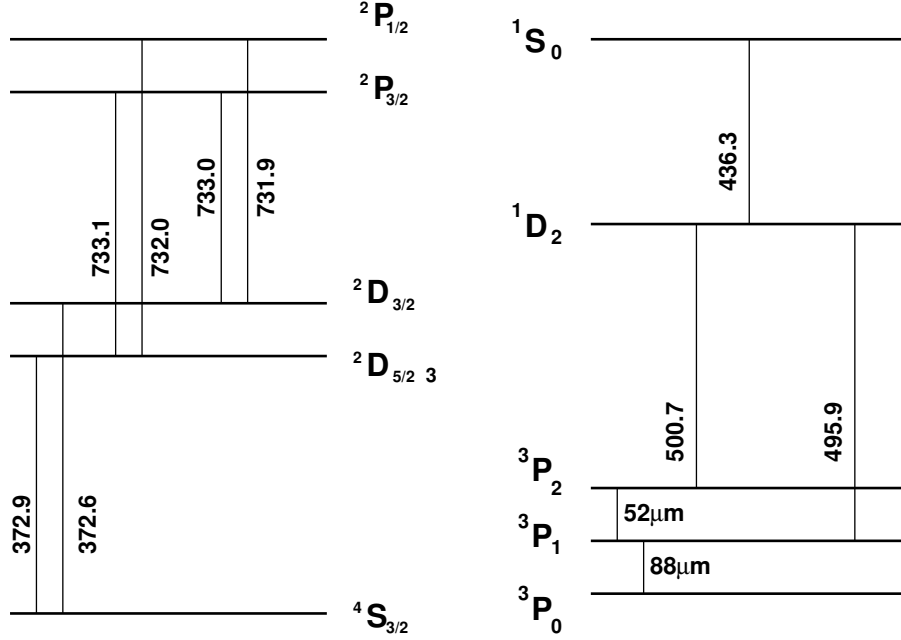


Figure 7.2: Simplified energy-level diagram for  $O^+$  (left) and  $O^{2+}$  (right). Unlabelled O II and O III wavelengths are in nm.

Since the oscillator strengths are small the probability of a photon from a forbidden transition being re-absorbed is small; these photons readily escape from (and hence cool) the nebula.

As in Section 7.2, if each excitation is followed by radiative decay (and emission of a forbidden-line photon of energy  $\Delta E_{ij}$ ), then the rate of energy loss is

$$L_{ij} = \dot{n}_{ij} \Delta E_{ij} = n_e n_i(I) C_{ij}(T_e) \Delta E_{ij} \quad [\text{J m}^{-3} \text{ s}^{-1}]. \quad (7.6)$$

If we consider cooling due to collisional excitation to  $2D_{5/2}$  and  $2D_{3/2}$  in  $O^+$  (the 372.9 and 372.6 nm lines, fig. 7.2), then

$$L(O^+) \simeq 1.1 \times 10^{-33} y(O^+) \frac{n^2(\text{H})}{\sqrt{T_e}} \exp \left\{ \frac{-3.89 \times 10^4}{kT_e} \right\} \quad \text{J m}^{-3} \text{ s}^{-1} \quad (7.8)$$

where  $y(O^+)$  is the ionization fraction,  $n(O^+)/n(O)$ ; we have used  $n_e \simeq n(\text{H})$  and an oxygen abundance by number  $n(\text{H})/n(\text{O}) \equiv A(\text{O}) = 6 \times 10^{-4}$ ; and we assume negligible depletion onto dust in the ionized gas ( $\delta(\text{O}) = 0$ ). Again note the strong (exponential) dependence of the cooling rate on temperature.

## 7.3 Equilibrium Temperatures

### 7.3.1 The Diffuse Neutral ISM

In equilibrium we require

$$G = L;$$

i.e., from eqtns. (7.4) and (7.7),

$$2 \times 10^{-32} y_{\text{pe}} n(\text{H}) = 8 \times 10^{-40} n^2(\text{H}) \delta(\text{C}) \exp(-92/T). \quad (7.9)$$

For  $n(\text{H}) \sim 10^8 \text{ m}^{-3}$  and  $y_{\text{pe}} \simeq \delta(\text{C}) \simeq 0.1$  we obtain an equilibrium temperature of  $\sim 70\text{K}$  – in accord with observations. Although this is only a rough calculation, it does argue that we have not overlooked any important processes, and that in the diffuse, neutral ISM heating by absorption of photons by dust grains (with subsequent photoejection of electrons) is balanced by collisional excitation of low-lying levels in gas-phase species (followed by radiative decay).

### 7.3.2 Ionized gas

#### A *pure hydrogen nebula*

For illustration we first consider cooling of a *pure hydrogen* nebula by recombination (the electron energies are too low for significant cooling by collisional excitation of hydrogen). On average, each recombination removes  $\sim \frac{3}{2}kT_e$  (the average kinetic energy of the recombining electrons) of energy from the gas. The total loss per unit volume per unit time is therefore

$$L = \frac{3}{2}kT_e \dot{n}_R \quad [\text{J m}^{-3} \text{ s}^{-1}] \quad (7.10)$$

In equilibrium  $L = G$ , and

$$G = \dot{n}_R Q; \quad (7.11)$$

hence

$$T_e = \frac{2}{3} \frac{Q}{k}. \quad (7.11)$$

where  $Q$  is the average energy input into the gas per hydrogen photoionization; its value evidently depends on the radiation field emitted from the star,<sup>3</sup>

$$Q = \frac{\int_{\nu_0}^{\infty} \frac{4\pi J_{\nu}}{h\nu} h(\nu - \nu_0) d\nu}{\int_{\nu_0}^{\infty} \frac{4\pi J_{\nu}}{h\nu} d\nu} \quad (7.12)$$

$$\equiv \frac{3}{2}kT_{e,i} \quad (7.13)$$

---

<sup>3</sup>And on the distance from the star (because of the  $\nu^{-3}$  dependence of the photoionization cross-section, which means that photons near the ionization edge are absorbed close to the star; hence the radiation field hardens with distance from the star)

where  $T_{e,i}$  is the initial kinetic temperature of the ejected photoelectron. As a rough approximation, we suppose that the star radiates like a black body at temperature  $T_*$ ; the mean photon energy is then

$$\overline{h\nu} = 2.7kT_*. \quad (1.28)$$

but only those with energies greater than  $h\nu_0$  contribute to heating. Numerical integration of eqn. (7.12) shows that, roughly,  $T_{e,i} \simeq T_*$  whence

$$Q \simeq \frac{3}{2}kT_* \quad (7.14)$$

So we see, from eqtns. (7.11) and (7.14), that if cooling were solely by recombination we would expect

$$T_e \simeq T_*$$

Typical values for O-type stars are  $T_* \simeq 30\text{--}50\text{kK}$ ; the implied electron temperatures in the nebula are *much higher* than observed values ( $\sim 10^4\text{K}$ ). To reconcile observed and computed temperatures, we need additional cooling processes.

For a *pure hydrogen* nebula, we have three possibilities:

- Free-free radiation* (bremsstrahlung),
- Collisional excitation* of hydrogen, and
- Collisional ionization* of hydrogen.

However, none of these processes are important coolants in practice. It's therefore necessary to relax the assumption of a pure hydrogen nebula; the crucial cooling mechanism is collisional excitation of forbidden lines of *metals*.

### A more realistic calculation

As before (Section 7.3.1), to estimate an equilibrium temperature we set  $G = L$ ; from eqtns. (7.1) and (5.2), and using  $Q \simeq \frac{3}{2}kT_*$  (eqn. 7.14),

$$G(= \dot{n}_I Q) = \dot{n}_R Q \simeq n_e^2 \alpha_B(T_e) \frac{3}{2}kT_*$$

and using eqn. (7.8) for the cooling rate  $L$  we find

$$T_e^{1/4} \exp \left\{ \frac{-3.89 \times 10^4}{kT_e} \right\} = 3.75 \times 10^{-6} T_*$$

Numerically,	Stellar Temp.	Equilbm. Nebular
	$T_*$ (K)	Temp, $T_e$ (K)
	$2 \times 10^4$	7500
	$4 \times 10^4$	8600
	$6 \times 10^4$	9300

which is in satisfactory agreement with observations.

Note that over the entire factor-3 range of relevant stellar temperatures (cooler stars don't produce ionized nebulae; hotter 'normal' stars aren't found), the nebular temperature only varies by  $\sim 20\%$ . Why? First, as  $T_e$  increases, the recombination rate decreases, and so the number density of neutral hydrogen goes down. A decrease in neutral hydrogen number density reduces the rate of heating. Secondly, as  $T_e$  increases, the cooling rate, eqn. (2.7), goes up. Both effects oppose the trend to increasing  $T_e$ . This feedback mechanism, or 'thermostat' regulates the temperatures of H II regions.

A notable consequence of the importance of metals to cooling is that H II regions in low-metallicity environments (like the SMC) are significantly warmer than those in our Galaxy.

## Thermalization in the gas (for reference only)

A pure hydrogen nebula contains neutral hydrogen atoms, protons, and electrons.

Photoionization continuously injects energy into the nebula, through the energy of the photoelectrons, which is determined by the energy distribution of ionizing photons ( $E = h\nu - \text{I.P.}$ ) – that is, by the effective temperature of the ionizing star(s).

Following photoejection of the electron, collisions redistribute the electron energy among all particles, thereby increasing the kinetic temperature. (The 'collisions' are not physical impacts, of course, but Coulomb interactions.) This happens so quickly (compared to ionization/recombination timescales) that it can be regarded as essentially instantaneous, but the energy redistribution is nonetheless hierarchical:

- The ejected electrons first share their energy with other electrons
- The electrons transfer energy to the protons, until equipartition of energy is achieved. (This is a slower process because the mass difference between electrons and protons makes the energy transfer inefficient.)
- Finally, the neutrals (which are less affected by coulomb interactions) gain energy

## Section 8

# Line Broadening

Absorption and emission lines in spectra are not infinitely narrow, but are broadened by a number of processes. These processes can be grouped under three broad headings:

- microscopic processes
- macroscopic processes
- instrumental processes

‘Microscopic’ processes are broadening mechanisms that occur on length scales smaller than the photon mean free path. Typically such processes operate on an atomic (or molecular) scale, and they are described in the following paragraphs. These microscopic processes change the line strength (profile function) for a fixed number of absorbers, as discussed in the context of interstellar lines in Section 9.1. They are the principal topic of this section.

Macroscopic broadening involves the redistribution of absorption through processes that operate on length scales greater than the photon mean free path; an example is rotational broadening of stellar absorption lines. They do *not* change the overall line strength, but merely redistribute a fixed amount of absorption to different wavelengths.

Instrumental broadening is a form of macroscopic broadening, but is usually considered separately as it is not of astrophysical origin

At this point we should explicitly note, and thereby attempt to avoid, possible ambiguities in the meaning of ‘absorption profile’. There is (i) the wavelength- (or frequency-)dependent profile of an *observed* absorption line, and (ii) the frequency-dependent probability of absorption by, or absorption cross-section of, some given absorber. Once we’re aware of this

difference, confusion is unlikely, but nevertheless these notes will generally stick to the convention where the former is the ‘line profile’ and the latter is the ‘absorption profile’.

We’ve already encountered the absorption profile  $a_\nu$  in Section 2.2; it is, in effect, the probability of an atom, or group of atoms, absorbing or scattering an incident photon, as a function of frequency (or wavelength). It is often convenient to split the absorption profile into two parts: a measure of overall line strength, and a description of the frequency dependence; that is,

$$a_\nu \equiv a_0 \phi_\nu$$

where  $\phi_\nu$  is the normalized profile function (or normalized absorption profile) — normalized such its area, integrated over all frequencies, is unity.

The primary microscopic processes responsible for the finite breadth of the absorption function are:

- (i) Natural broadening, intrinsic to the transition and resulting from the Heisenberg uncertainty principle. This gives rise to a Lorentzian absorption cross-section.
- (ii) Thermal (Doppler) broadening, due to random thermal motions of the atoms. For a Maxwellian velocity distribution, the 1-D projected velocity distribution is Gaussian.

Other processes may contribute to line broadening; if these arise from physical changes on length scales less than the photon mean free path, they change the profile function. Such small-scale processes are generally brought together under the label of

- (iii) ‘microturbulent’ broadening – an ad hoc description of nonthermal motions. typically *assumed* also to be characterized by a Gaussian line-of-sight velocity distribution.

As we shall see in Section 9, the foregoing processes influence the strength of a line profile, even if all other parameters (such as number of absorbers) are fixed. Processes that act on length scales longer than a photon mean free path (like stellar rotation) may change the shape, but not the overall strength, of an absorption line.

## 8.1 Natural Line Broadening

From the Uncertainty Principle, any given atomic energy level  $i$  does not have a perfectly defined energy  $E_i$ , but is rather a superposition of possible states spread<sup>1</sup> around  $E_i$ . As a

---

<sup>1</sup> $t\Delta E \simeq h/(2\pi)$ , where  $t$  is the time an electron occupies the higher-energy state.

result, transitions of electrons between any two energy levels do not correspond to any exact, specific energy difference; equivalently, absorption of photons does not take place at one exact, unique frequency/wavelength, but over a (small) range.

For reference, the *classical* result for an absorption cross-section,<sup>2</sup>  $a(\omega)$ , is:

$$a(\omega) = \frac{8\pi e^4}{3m_e^2 c^4} \left[ \frac{\omega^4}{(\omega^2 - \omega_0^2)^2 + \gamma^2 \omega^2} \right], \quad (8.1)$$

where

$$\begin{aligned} \omega &= 2\pi\nu && \text{is the angular frequency,} \\ \omega_0 &= 2\pi\nu_0 && \text{and } \nu_0 \text{ is the line-centre frequency,} \end{aligned}$$

and

$$\begin{aligned} \gamma &= \left( \frac{2e^2}{3m_e c^3} \right) \omega_0^2 \\ &= \left( \frac{8\pi^2 e^2}{3m_e c^3} \right) \nu_0^2 \\ &= 2.47 \times 10^{-22} \nu_0^2 \text{ s}^{-1} \end{aligned} \quad (8.2)$$

is the classical damping constant.

This classical form (eqtn. (8.1)) applies in ‘real world’ absorption lines, but with two modifications. First, we replace the classical damping coefficient,  $\gamma$ , by the quantum-mechanical damping constant  $\Gamma$ , the sum of all transition probabilities for natural decay from each of the lower and upper levels of the transition:

$$\Gamma = \Gamma_i + \Gamma_j \quad (8.3)$$

where

$$\Gamma_i = \sum_{\ell < i} A_{i\ell}, \quad (8.4)$$

$$\Gamma_j = \sum_{\ell < j} A_{j\ell}$$

and the Einstein coefficient  $A_{i\ell}$  is the probability (in units of  $\text{s}^{-1}$ ) of a transition from the upper level,  $i$ , to lower level  $\ell$ . The resulting profile for the absorption cross-section of a transition between two states reflects the intrinsic energy widths of *both* states.

Secondly, we incorporate the *oscillator strength*,  $f$ , as a correction/scaling factor, whence eqtn. (8.1) becomes

$$a_\nu = \frac{8\pi e^4}{3m_e^2 c^4} f \left[ \frac{\nu^4}{(\nu^2 - \nu_0^2)^2 + [\Gamma/(2\pi)]^2 \nu^2} \right]. \quad (8.5)$$

Line absorption is only important near the resonance frequency,  $\nu_0$ , so we can simplify eqtn. (8.5) by substituting

$$\begin{aligned} (\nu^2 - \nu_0^2)^2 &= (\nu + \nu_0)^2 (\nu - \nu_0)^2 \\ &\simeq (2\nu_0)^2 (\nu - \nu_0)^2 \end{aligned} \quad (8.6)$$

---

<sup>2</sup>Derived in PHAS2116?

giving

$$a_\nu \simeq \frac{2\pi e^4}{3m_e^2 c^4} f \left[ \frac{\nu_0^2}{(\nu - \nu_0)^2 + [\Gamma/(4\pi)]^2} \right] \quad (8.7)$$

or

$$a_\nu \equiv a_0 \phi_\nu;$$

i.e., the absorption cross-section can be expressed as a frequency-independent set of physical constants ( $a_0$ ), and a frequency-dependent function,

$$\phi_\nu = \frac{C}{(\nu - \nu_0)^2 + [\Gamma/(4\pi)]^2}. \quad (8.8)$$

The constant  $C$  is required to satisfy the normalization condition, and can be determined from it:

$$\int_0^\infty \phi_\nu d\nu \equiv 1 \quad (8.9)$$

whence

$$1 = C \int_0^\infty \frac{d\nu}{(\nu - \nu_0)^2 + (\Gamma/4\pi)^2}$$

which is of the form

$$1 = C \int_0^\infty \frac{dx}{x^2 + b^2} \quad (8.10)$$

with

$$x = (\nu - \nu_0), \quad b = \Gamma/4\pi. \quad (8.11)$$

We can solve this as standard integral,

$$\int_{-\infty}^{+\infty} \frac{dx}{x^2 + b^2} = \frac{\pi}{b}$$

giving

$$C = \frac{\Gamma}{4\pi^2} \quad (8.12)$$

Thus from eqtn. (8.8) we obtain our final result for the *shape* of the normalized absorption cross-section for damping constant  $\Gamma$ :

$$\begin{aligned} \phi_\nu &= \frac{\Gamma/(4\pi^2)}{(\nu - \nu_0)^2 + [\Gamma/(4\pi)]^2} \\ &= \frac{\Gamma}{4\pi^2(\nu - \nu_0)^2 + (\Gamma/2)^2} \end{aligned} \quad (8.13)$$

which is, as anticipated, a natural, or Lorentz, function, with  $\Gamma$  the quantum-mechanical damping constant (the sum of all transition probabilities for natural decay from each of the lower and upper levels of the transition).

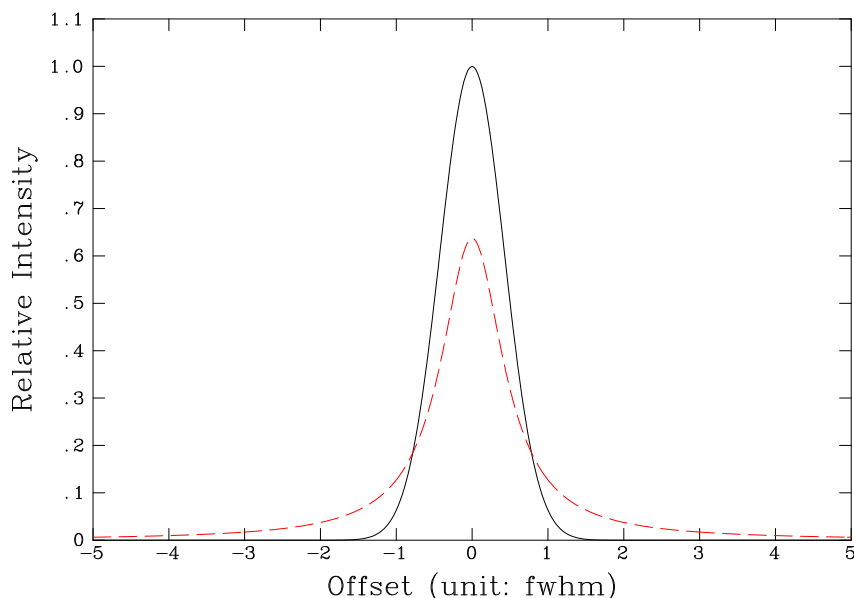


Figure 8.1: Gaussian (solid) and Lorentz (dashed) profiles, each normalized unit area and to FWHM=1. The Lorentzian has much more extensive wings.

### 8.1.1 Peak value and width

We can characterize a function by its area ( $\equiv 1$  in this case), the peak (line-centre) value, and the full-width at half maximum, FWHM. The maximum value of  $\phi_\nu$  occurs when  $\nu = \nu_0$ , whence

$$\phi_0 = 4/\Gamma$$

(from eqtn. (8.13)). The value of the function at half-maximum is thus  $2/\Gamma$ ; to find the corresponding full width at half maximum we therefore substitute  $\phi_\nu = 2/\Gamma$  into eqtn. (8.13), giving

$$\frac{\Gamma^2}{2} = 4\pi^2(\nu_{1/2} - \nu_0)^2 + \left(\frac{\Gamma}{2}\right)^2$$

whence  $(\nu_{1/2} - \nu_0)^2 = \Gamma^2/16\pi^2$ , or

$$\nu_{1/2} = \nu_0 \pm \Gamma/4\pi.$$

The *full*-width at half maximum (FWHM), in frequency units, is  $2\nu_{1/2}$ , or

$$\Delta\nu_{1/2} = \frac{\Gamma}{2\pi}$$

For allowed transitions, typical values might be in the region of  $\sim 10^{-5}$  nm or less.

## 8.2 Thermal Line Broadening

In a gas at kinetic temperature  $T_k$ , individual atoms will have random motions away from or towards the observer, leading to red- or blue-wards frequency shifts.

If the (natural) absorption coefficient for a stationary atom is  $a_\nu$  at some frequency  $\nu$ , then for an atom moving at velocity  $v$  the same absorption occurs at observed frequency

$$\nu_D = \nu \left(1 - \frac{v}{c}\right) = \nu - \nu \frac{v}{c}$$

(where the ‘D’ subscript can be taken as standing for Doppler, or Displaced). At a given observed frequency  $\nu$ , the total absorption coefficient is the product of the absorption coefficient of atoms moving at some velocity,  $v$ , times the fraction of atoms at that velocity,  $f(v)$ , integrated over velocity:

$$a_\nu = \int_{-\infty}^{+\infty} a \left(\nu - \nu \frac{v}{c}\right) f(v) dv. \quad (8.14)$$

We want to express this thermally broadened cross-section  $a_\nu$  as a function of the observable quantity  $\nu$  (instead of  $v$ ), which requires some algebra.

Where the distribution of particle velocities is established by collisions (as is almost always the case in normal astrophysical environments, like the interstellar medium, or in stars), the gas particles follow a Maxwellian velocity distribution characterized by kinetic temperature  $T_k$ :

$$f(V) dV = 4\pi \left(\frac{m}{2\pi k T_k}\right)^{3/2} V^2 \exp\left(-\frac{1}{2} \frac{mV^2}{k T_k}\right) dV \quad (8.15)$$

where  $V$  is the space velocity ( $V^2 = v_x^2 + v_y^2 + v_z^2$ ) for particles of mass  $m$ . The mean squared velocity is

$$\begin{aligned} \langle V^2 \rangle &= \frac{\int_0^\infty V^2 f(V) dV}{\int_0^\infty f(V) dV} \\ &= \frac{3kT_k}{m} \end{aligned}$$

and the mean kinetic energy is therefore

$$\frac{1}{2} m \langle V^2 \rangle = \frac{3}{2} k T_k$$

(which effectively defines ‘kinetic temperature’). The higher the temperature, or the less the particle mass, the greater the mean velocity (and the spread in velocities).

For line formation, we’re usually interested not in the space velocity, but in the line-of-sight component of the velocity distribution; that is, the projection of eqtn. (8.15) onto a single axis, which is a gaussian:

$$f(v) dv = \frac{1}{\sqrt{\pi}} \left(\frac{m}{2kT_k}\right)^{1/2} \exp\left\{-\frac{mv^2}{2kT_k}\right\} dv \quad (8.16)$$

for a particle of mass  $m$  at temperature  $T_k$ ; then the (line of sight) *thermal* (doppler) *width* is defined as

$$v_{\text{th}} \equiv \sqrt{\frac{2kT_k}{m}} \quad (8.17)$$

or, in frequency units,

$$\Delta\nu_{\text{th}} = \nu_0 \frac{v_{\text{th}}}{c} = \frac{\nu_0}{c} \sqrt{\frac{2kT_k}{m}} \quad (8.18)$$

Using eqtns. (8.16) and (8.17) in eqtn. (8.14) gives

$$a_\nu = \frac{1}{\sqrt{\pi}} \frac{1}{v_{\text{th}}} \int_{-\infty}^{\infty} a \left( \nu - \nu \frac{v}{c} \right) \exp \left\{ -\frac{mv^2}{2kT_k} \right\} dv \quad (8.19)$$

We now switch between velocity space and frequency space by setting

$$\nu' \equiv \nu \frac{v}{c}$$

giving, from eqtn. (8.19),

$$a_\nu = \frac{1}{\sqrt{\pi}} \frac{1}{\Delta\nu_{\text{th}}} \int_0^\infty a (\nu - \nu') \exp \left\{ -\left( \frac{\nu'}{\Delta\nu_{\text{th}}} \right)^2 \right\} d\nu' \quad (8.20)$$

The natural line width is much less than the thermal width and so here – where we're focussing on the form of the thermal broadening, and not the combined effects of natural+thermal – it can be approximated here by a  $\delta$  function (i.e., an infinitely narrow intrinsic line of unit area) at the doppler-shifted position,

$$a_\nu \simeq a_0 \delta(\nu - \nu_0).$$

This means the integral has to be evaluated at only a single point, and gives our final form for the thermally (or doppler) broadened profile,

$$a_\nu = \frac{a_0}{\sqrt{\pi}} \frac{1}{\Delta\nu_{\text{th}}} \exp \left\{ -\left( \frac{\nu - \nu_0}{\Delta\nu_{\text{th}}} \right)^2 \right\}, \quad (8.21)$$

where all the terms are constant except  $(\nu - \nu_0)$ , for given  $m$  and  $T_k$ . Eqtn. (8.21) therefore again has the general form

$$a_\nu = a_0 \phi_\nu,$$

with

$$\phi_\nu = \frac{1}{\sqrt{\pi}} \frac{1}{\Delta\nu_{\text{th}}} \exp \left\{ -\left( \frac{\nu - \nu_0}{\Delta\nu_{\text{th}}} \right)^2 \right\}. \quad (8.22)$$

Note that  $\phi_\nu$  is a *normalized* gaussian which already satisfies

$$\int_0^\infty \phi_\nu d\nu = 1$$

(and that, in effect, the algebra we have carried out has simply converted a gaussian velocity distribution of particles into a gaussian profile for the absorption cross-section).

### 8.2.1 Peak value and width

The peak value of  $\phi_\nu$ , at  $\nu = \nu_0$ , is given by eqtn. (8.22)

$$\begin{aligned}\phi_0 &= \frac{1}{\sqrt{\pi}} \frac{1}{\Delta\nu_{\text{th}}} \\ &= \frac{1}{\sqrt{\pi}} \frac{c}{\nu_0} \frac{1}{v_{\text{th}}} \\ &= \frac{1}{\sqrt{\pi}} \frac{c}{\nu_0} \left( \frac{m}{2kT_k} \right)^{1/2}.\end{aligned}\tag{8.23}$$

At half maximum  $\phi_{\nu(1/2)} = 0.5\phi_0$ :

$$\frac{1}{2} \left[ \frac{1}{\sqrt{\pi}} \frac{c}{\nu_0} \sqrt{\frac{m}{2kT_k}} \right] = \left[ \frac{1}{\sqrt{\pi}} \frac{c}{\nu_0} \sqrt{\frac{m}{2kT_k}} \right] \exp \left\{ -\frac{mc^2}{2kT_k} \left( \frac{\nu_{1/2} - \nu_0}{\nu_0} \right)^2 \right\}$$

(where the left-hand side comes from eqtn. 8.23 and the right-hand side from eqtns. 8.22 and 8.18), giving

$$(\nu_{1/2} - \nu_0)^2 = \nu_0^2 \left( \frac{2kT_k}{mc^2} \right) \ln 2$$

so that

$$\begin{aligned}\text{FWHM} &= \frac{2\nu_0}{c} \left[ \frac{2kT_k}{m} \ln 2 \right]^{1/2} \\ \text{i.e., } \Delta\nu_{1/2} &= 2(\ln 2)^{1/2} \Delta\nu_{\text{th}} \\ &= 1.665 \Delta\nu_{\text{th}}\end{aligned}$$

in frequency units; or

$$\begin{aligned}\Delta v &= \Delta\nu \frac{c}{\nu_0} = 1.665 \Delta\nu_{\text{th}} \frac{c}{\nu_0} \\ &= 1.665 \Delta v_{\text{th}} \frac{\nu_0}{c} \frac{c}{\nu_0}\end{aligned}$$

i.e.,

$$\Delta v = 1.665 \left( \frac{2kT_k}{m} \right)^{1/2}$$

For example, for  $\text{H}\alpha$  ( $n = 3 \rightarrow 2$ ),  $m = m(\text{H})$ :

at 60K,  $\Delta v = 1.7 \text{ km s}^{-1}$  ( $\Delta\lambda = 0.0036\text{nm}$ )

at 6000K,  $\Delta v = 17 \text{ km s}^{-1}$  ( $\Delta\lambda = 0.036\text{nm}$ )

(Heavier elements will have smaller thermal line widths. For comparison, the natural width for  $\text{H}\alpha$  is  $\sim 2 \times 10^{-5}\text{nm}$ , justifying our ‘ $\delta$  function’ approximation.)

### 8.3 ‘Turbulent’ Broadening

The final broadening process is not well defined physically; it is, if you like, ‘the other stuff’. This might include internal motions within an interstellar cloud, or even non-physical effects (like unrecognized overlapping or unresolved lines from different clouds). Without a firm physical model for these additional sources of velocity dispersion, it is customary to adopt a gaussian line-of-sight velocity distribution, largely as a matter of convenience (and because this assumption appears consistent with observation in general – which doesn’t make it true!).

We know that the root-mean-square (rms) *line-of-sight* (1-D) thermal doppler velocity dispersion arising from a Maxwellian velocity distribution is

$$v_{\text{th}} \equiv \sqrt{2 \frac{kT_{\text{k}}}{m}} \quad (8.17)$$

We characterize the line-of-sight turbulent velocity distribution as gaussian, with an rms value  $v_{\text{turb}}$ ; then the *total* doppler broadening is obtained simply by adding the thermal and turbulent widths in quadrature,

$$v_{\text{D}}^2 = v_{\text{turb}}^2 + v_{\text{th}}^2$$

and the form of the gaussian component of the absorption profile is unchanged.

In stellar physics, this turbulence is usually described as ‘microturbulence’, and is supposed to operate on length scales shorter than the photon mean free path. (Processes operating on length scales much longer than the mean free path modify the observed line profile, but not the absorption profile. Where a complete physical description of such large-scale processes does not exist, or is unwieldy – as in surface ‘granulation’ or convective cells – they may be characterised as ‘macroturbulence’.) In studies of the interstellar medium, it’s customary to use a line-broadening parameter  $b$ , defined as

$$\begin{aligned} b &= \left[ 2 \frac{kT_{\text{k}}}{m} + 2v_{\text{turb}}^2 \right]^{1/2} \\ &= [v_{\text{th}}^2 + 2v_{\text{turb}}^2]^{1/2} \end{aligned} \quad (8.24)$$

in the interstellar case discussed in Section 9; clearly, as

$$v_{\text{th}} \rightarrow 0, \quad b \rightarrow \sqrt{2} v_{\text{turb}}$$

$$v_{\text{turb}} \rightarrow 0, \quad b \rightarrow v_{\text{th}}.$$

As for thermal broadening,

$$\begin{aligned}\text{FWHM} &= 2(\ln 2)^{1/2} b \\ &= 1.665 b \\ &= 1.665 \left[ \frac{2kT_k}{m} + 2v_{\text{turb}}^2 \right]^{1/2}\end{aligned}\tag{8.25}$$

Can  $v_{\text{turb}}$  and  $v_{\text{th}}$  be separately determined? In principle, yes, because all elements should share the same turbulent broadening, but will undergo different (mass-dependent) thermal broadening. In practice, this is very difficult, because the turbulence is frequently the dominant term.

## 8.4 Combined results

Combining (convolving) gaussian and lorentzian gives voigt.

## Section 9

# Interstellar absorption lines

We can study diffuse interstellar clouds through the absorption lines they produce in the spectra of background stars. Because of the low densities in the ISM, most atoms are in the *ground state*; that is, the configuration with the lowest possible energy. As a consequence, most atomic or ionic lines observed in the ISM are *resonance lines*, corresponding to transitions of a valence electron from the ground state to some (usually) low-lying excited state. In practice, this photo-excitation is quickly followed by a de-excitation back to the ground state, with emission of a photon of almost the same wavelength as the incident photon – a scattering.

These resonance lines generally occur in the UV part of the spectrum, shortwards of  $3000\text{\AA}$  or so, because the energy gaps from ground states to first excited states are quite large (although there are a few important transitions in the optical – e.g., the Ca *H* & *K* lines at  $3933.7$ ,  $3968.5\text{\AA}$  and the Na *D* lines at  $5890.0$ ,  $5895.9\text{\AA}$ ).

OB stars make particularly good background sources for interstellar-line studies because

Their spectral energy distributions peak in the UV;

They are intrinsically luminous (so are observable over relatively large distances)

They typically have rather broad photospheric lines (so that the narrow interstellar lines are easily identified and measured).

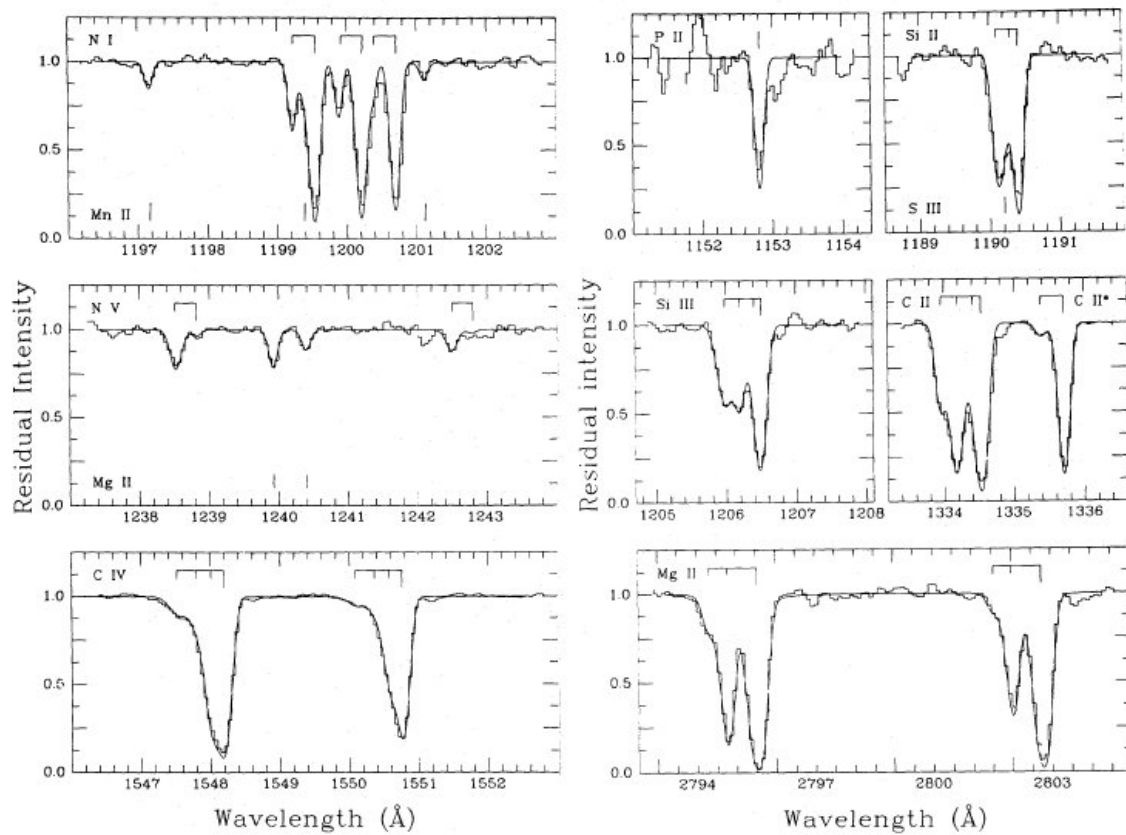


Figure 9.1: Some interstellar lines in the UV spectrum of HD 50896.

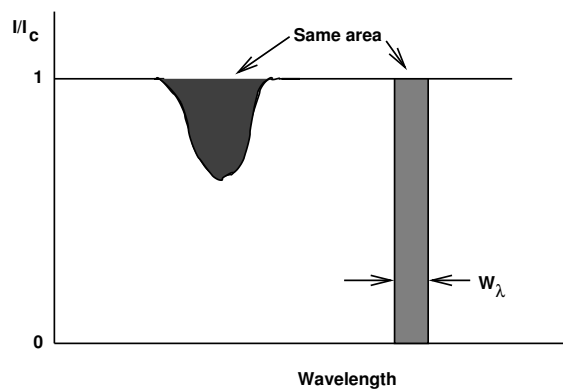


Figure 9.2: The equivalent width.

## 9.1 The transformation between observed and theoretical quantities

### 9.1.1 Equivalent width

Because of the low temperatures of diffuse interstellar clouds, the thermal line broadening is small (sec. 8.2), and the lines are intrinsically narrow ( $\sim$ few km s<sup>-1</sup>) – too narrow to be resolved by typical spectrographs. Since we can't usually study the intrinsic spectral-line profiles, it's often necessary to characterize the absorption by a simple line-strength measurement, the *equivalent width*.

[Equivalent width is conserved through instrumental broadening, because that broadening is characterized by a function  $\varphi_\nu$  (or  $\varphi_\lambda$ ) which obeys the normalization

$$\int \varphi_\nu d\nu \equiv 1;$$

that is, instrumental effects just redistribute equivalent width over frequency, without changing the actual value.]

The equivalent width,  $W_\lambda$ , is defined as

$$\begin{aligned} W_\lambda &= \int_0^\infty \left( \frac{I_\lambda^C - I_\lambda}{I_\lambda^C} \right) d\lambda \\ &= \int_0^\infty \left( 1 - \frac{I_\lambda}{I_\lambda^C} \right) d\lambda \end{aligned} \tag{9.1}$$

where  $I_\lambda^C$  is the (interpolated) continuum intensity<sup>1</sup> and  $I_\lambda$  the actual intensity through the spectral-line profile; the quantity  $I_\lambda/I_\lambda^C$  is usually called the 'rectified intensity' (and is, obviously, dimensionless).

An equivalent 'frequency' version can be constructed:

$$\begin{aligned} W_\nu &= \int_0^\infty \left( \frac{I_\nu^C - I_\nu}{I_\nu^C} \right) d\nu \\ &= \int_0^\infty \left( 1 - \frac{I_\nu}{I_\nu^C} \right) d\nu. \end{aligned} \tag{9.2}$$

The formal integration limits 0– $\infty$  apply only to the line of interest; they can be used in a theoretical calculation, but in practice for an observation the integration is truncated at the edges of the line (the term in brackets being zero elsewhere).

---

<sup>1</sup>This is extremely commonplace usage, but rather sloppy in the context of the nomenclature outlined in Section 1. The 'intensity' here is nothing to do with the specific intensity, and is more closely allied to the physical flux. This 'intensity' is measured in units of 'counts per second per pixel', or something similar, rather than being in SI units.

Physically,  $W_\lambda$  is the width (in wavelength units) of the continuum that has the same area as the line. The total flux<sup>2</sup> in the line is  $W_\lambda \times I_\lambda^C$ . By convention (and in agreement with the above definitions), absorption-line equivalent widths take positive values, and emission lines negative ones.

### Equivalent Width to Optical Depth

The equivalent width of a line is evidently related to the optical depth along the line of sight. Although equivalent width is usually expressed in wavelength units, optical depth is usually expressed in frequency units. We can convert between the two by noting that

$$\begin{aligned}\Delta\lambda &= \Delta\nu \frac{d\lambda}{d\nu} \\ &= \Delta\nu \frac{c}{\nu^2} \\ &= \Delta\nu \frac{\lambda^2}{c};\end{aligned}$$

(where a minus sign has been compensated by an implicit change in ordinate direction; wavelength increases as frequency decreases) i.e.,

$$W_\lambda = W_\nu \frac{\lambda^2}{c}.$$

Recalling that  $I_\nu d\nu = I_\lambda d\lambda$ , we can then write eqtn. (9.2) as

$$W_\lambda = \frac{\lambda_0^2}{c} \int_0^\infty \left(1 - \frac{I_\nu}{I_\nu^C}\right) d\nu$$

or, since  $I_\nu = I_\nu^C \exp\{-\tau_\nu\}$  (eqtn. (3.3)) in the circumstances appropriate to interstellar-line formation,

$$W_\lambda = \frac{\lambda_0^2}{c} \int_0^\infty (1 - \exp\{-\tau_\nu\}) d\nu \tag{9.3}$$

*Eqtn. (9.3) is the basic relationship between  $W_\lambda$  and optical depth  $\tau_\nu$  (customarily expressed in wavelength and frequency units, respectively).*

### Optical Depth to Column Density

What we're really interested in is the *column densities* of different species – that is, the number of absorbers per unit area along a given sightline (in practice, normally measured in units of  $\text{cm}^{-2}$ ). We know that

$$\tau_\nu = \int_0^D k_\nu ds = \int_0^D a_\nu n_i(s) ds \tag{2.5}$$

---

<sup>2</sup>Again, loose terminology – this is *not* (normally) the physical flux.

with  $D$  the distance over which absorption occurs, and where  $k_\nu$  is the ‘volume’ opacity<sup>3</sup> for transition  $i \rightarrow j$ , with  $a_\nu$  the absorption cross-section ( $\text{m}^2$ ) and  $n_i$  ( $\text{m}^{-3}$ ) the number density (so  $\tau$  is dimensionless).

For a line transition from levels  $i$  to  $j$  the absorption cross-section is given by

$$a_\nu(ij) = \frac{c^2}{8\pi\nu^2} \frac{g_j}{g_i} A_{ji} \phi_\nu(s) \quad (= a_0 \phi_\nu(s)) \quad (9.4)$$

where  $g_i, g_j$  are statistical weights for the lower, upper levels;  $A_{ji}$  is the emission transition probability (Einstein coefficient); and  $\phi_\nu(s)$  is the normalized profile function at position  $s$ . It is usual, when considering absorption lines, to work not with the Einstein  $A$  coefficient, but with the absorption oscillator strength  $f_{ij}$ ; the two are related by

$$A_{ji} = \frac{8\pi^2 e^2 \nu^2}{m_e c^3} \frac{g_i}{g_j} f_{ij}. \quad (9.5)$$

so that

$$a_\nu(ij) = \frac{\pi e^2}{m_e c} f_{ij} \phi_\nu(s). \quad (9.6)$$

Substituting eqtn. (9.6) into the definition of optical depth, eqtn. (2.5),

$$\tau_\nu = \frac{\pi e^2}{m_e c} f_{ij} \int_0^d \phi_\nu(s) n_i(s) ds$$

or, if  $\phi_\nu$  is independent of  $s$ ,

$$= \frac{\pi e^2}{m_e c} \phi_\nu N_i f_{ij} \quad (9.7)$$

where  $N$  is the ‘column density’, the number of particles in a column of unit cross-section from the observer to the background source,

$\int_0^d \nu(s) n_i(s) ds$ . *In practice, column density is usually measured in units of ‘ $\text{cm}^{-2}$ ’.*

Eqtn. (9.7) is the relationship between optical depth (as a function of frequency) and column density; with

$$I_\nu = I_\nu^C \exp \{-\tau_\nu\} \quad (3.3)$$

it gives us the line profile; and on integrating the line profile (eqtn. (9.3)) it defines the relationship between the equivalent width,  $W_\lambda$  (an observable quantity), and the number of absorbing atoms,  $N$  (a quantity of astrophysical interest) – the so-called *Curve of Growth* (CoG).

Eqtn. (9.7) shows that the optical depth (hence the line profile) also depends on  $\phi_\nu$  – i.e., on the *shape* of the absorption profile. In other words, at some given frequency (e.g., the line centre) the optical depth can be greater or smaller, depending on  $\phi_\nu$ , for fixed  $N$ .

<sup>3</sup>In units of  $\text{m}^{-1}$ ; recall that one can also define opacity  $\kappa$  in terms of area per unit mass.

## Line formation (for reference only)

For a pure absorption line

$$I_\lambda = I_\lambda(0) \exp(-\tau_\lambda) \quad (3.3)$$

and (for a homogeneous medium)

$$\tau_\lambda = N_i a_\lambda \quad (9.8)$$

The absorption profile is, in general, the convolution of the natural broadening and the line-of-sight velocity distribution; that is, if the number of atoms in the column with velocities in the range  $v$  to  $v + dv$  is  $N_i \psi(v) dv$  then

$$a_\lambda = \frac{\lambda^4}{8\pi^2 c} \frac{g_j}{g_i} A_{ji} \int_{-\infty}^{+\infty} \frac{\Gamma_\lambda}{\Gamma_\lambda^2 + [\lambda - \lambda_0(1 + v/c)]^2} \psi(v) dv \quad (9.9)$$

where  $g$  is the statistical weight,  $A_{ji}$  is the transition probability,  $\Gamma$  is the damping constant,  $\Gamma_\lambda = \Gamma \lambda^2 / c$  and  $\lambda_0$  is the rest wavelength.

For the special case of a Gaussian line-of-sight velocity dispersion

$$\psi(v) = \frac{1}{b\sqrt{\pi}} \exp\left\{-\frac{(v - v_0)^2}{b^2}\right\}$$

and eqn. (9.9) reduces to

$$a_\lambda = \frac{\lambda^4}{8\pi^2 c} \frac{1}{b\sqrt{\pi}} \frac{g_j}{g_i} A_{ji} \int_{-\infty}^{+\infty} \frac{\alpha \exp(-y^2)}{\alpha^2 + (v - y)^2} dy \quad (9.10)$$

where

$$\alpha = \lambda_c \Gamma / b$$

$$y = (v - v_c) / b$$

and the subscript  $c$  indicates the line-centre wavelength/velocity. The Voigt function is

$$H(\alpha, v) = \frac{1}{\pi} \int_{-\infty}^{+\infty} \frac{\alpha \exp(-y^2)}{\alpha^2 + (v - y)^2} dy$$

so that eqn. (9.10) further reduces to

$$a_\lambda = \frac{\lambda^4}{8\pi c} \frac{1}{b\sqrt{\pi}} \frac{g_j}{g_i} A_{ji} H(\alpha, v)$$

The transition probability is related to the oscillator strength by

$$A_{ji} = \frac{8\pi^2 e^2 \nu^2}{m_e c} \frac{g_i}{g_j} f_{ij}$$

so our final expression for the absorption coefficient is

$$a_\lambda = \frac{\lambda^2 / c}{b\sqrt{\pi}} \frac{\pi e^2}{m_e c} f_{ij} H(\alpha, v)$$

where

$$a = \lambda_c \Gamma / b$$

$$v = c(\lambda - \lambda_c) / b\lambda_c$$

which allows us to calculate theoretical line profiles.

## 9.2 Interstellar Curve of Growth

The ‘curve of growth’ (CoG) is, essentially, a plot of line strength (expressed as equivalent width,  $W_\lambda$ ) as a function of column density of absorbers ( $N$ ). It is a standard tool in interstellar absorption-line studies. We first consider the general form of the CoG

### 9.2.1 Weak lines: optically thin limit

We first recall that

$$W_\lambda = \frac{\lambda_0^2}{c} \int_0^\infty (1 - \exp\{-\tau_\nu\}) d\nu \quad (9.3)$$

For weak lines,  $\tau_\nu \ll 1$ ; i.e.,  $(1 - \exp(-\tau_\nu)) \simeq \tau_\nu$ , and so, from eqn. (9.3),

$$W_\lambda \simeq \frac{\lambda_0^2}{c} \int_0^\infty \tau_\nu d\nu$$

or, using eqn. (9.7),

$$\begin{aligned} \frac{W_\lambda}{\lambda_0} &= \frac{\lambda_0}{c} \frac{\pi e^2}{m_e c} N_i f_{ij} \int \phi_\nu d\nu \\ &= \frac{\pi e^2}{m_e c^2} N_i \lambda_0 f_{ij} \end{aligned} \quad (9.11)$$

A plot of  $\log(W_\lambda/\lambda_0)$  versus  $\log(N_i f_{ij} \lambda_0)$  is a 1:1 straight line - this is the *linear part* of the CoG. Doubling  $N$  doubles  $W_\lambda$  for an optically thin line, *regardless of any details of the shape of the spectral-line profile*. Unfortunately, optically thin lines are often too weak to be reliably measured.

### 9.2.2 General case without damping – flat part of the CoG.

As the line strength increases, the line centre (doppler core) becomes ‘black’ – all the available light has been removed from the spectral-line profile, and an increase in  $N$  produces no significant change in  $W_\lambda$ . The line is said to be *saturated*, and this is correspondingly the ‘saturated part of the CoG’. (Eventually the damping wings become important and the line strength again increases.) The details *do* now depend on the spectral-line profile – for an intrinsically broader spectral line (e.g., high  $T_k$ ) the absorption is spread out over a greater velocity range, and a larger  $N$  is required before saturation becomes important.

Further analytical study becomes cumbersome, but we can illustrate the general role of broadening on the spectral-line profile with an analytic demonstration of the intuitively obvious fact that more strongly broadened lines saturate at higher  $N$  values. We know that

$$\tau_\nu = \frac{\pi e^2}{m_e c} N_i f_{ij} \phi_\nu \quad (9.7)$$

while from eqtn. (8.23), for a thermally broadened line,

$$\phi_0 = \frac{1}{\sqrt{\pi}} \frac{c}{\nu_0} \frac{1}{v_D}$$

which we can generalize to include gaussian turbulence (eqtn. (8.24)) to write

$$\phi_0 = \frac{1}{\sqrt{\pi}} \frac{\lambda_0}{b}.$$

Then the line-centre optical depth is

$$\begin{aligned} \tau_0 \equiv \tau_{\nu_0} &= \frac{\pi e^2}{m_e c} N_i f_{ij} \phi_0 \\ &= \frac{\sqrt{\pi} e^2}{m_e c} \frac{N_i f_{ij} \lambda_0}{b} \end{aligned} \quad (9.12)$$

which explicitly shows the dependence of the spectral-line profile on the broadening parameter  $b$  – for given  $N$ , the larger the  $b$  value, the smaller the line-centre optical depth  $\tau_0$  (and the smaller the degree of saturation). These effects are illustrated in Fig. 9.3

Writing  $\Delta\nu/(b/\lambda_0)$  as  $x$ , then, from eqtn. (9.3), after some manipulation we obtain

$$W_\lambda = \frac{\lambda_0^2}{c} \frac{b}{\lambda_0} \int_{-\infty}^{+\infty} (1 - \exp(-\tau_0 \exp(-x^2))) dx \quad (9.13)$$

For large  $\tau$  the integral in eqtn. (9.13) (which has to be evaluated numerically) approaches

$$W_\lambda \propto (\ln \tau_0)^{1/2}.$$

The dependence of  $W_\lambda$  on  $\tau_0$  (i.e., on  $N$ ; eqtn. (9.12)) is thus very small, and this region is therefore called the *flat part* of the CoG.<sup>4</sup>

### 9.2.3 Damping dominates – square root part of the CoG.

For very strong lines the gaussian core of the profile is saturated, but with increasing optical depth the Lorentzian *damping wings* of the Voigt profile,

$$\phi_\nu = \frac{\Gamma}{4\pi^2(\nu - \nu_0)^2 + (\Gamma/2)^2}, \quad (8.13)$$

---

<sup>4</sup>If we expand the first of the exponents in eqtn. (9.13) in a Taylor series, we get

$$W_\lambda = \pi^{1/2} b \lambda_0 \left( \frac{\tau_{\nu_0}}{1!\sqrt{1}} - \frac{\tau_{\nu_0}^2}{2!\sqrt{2}} + \frac{\tau_{\nu_0}^3}{3!\sqrt{3}} - \dots \right)$$

(Lundenburg 1930, Zs. Phys **65**, 200) Then, using eqtn. (9.12), for small  $\tau_{\nu_0}$  we get

$$\frac{W_\lambda}{\lambda_0} = \pi^{1/2} b \tau_{\nu_0} = \frac{\pi e^2}{m_e c} N_i f_{ij} \lambda_0$$

which shows that this general form recovers the optically thin limit, eqtn. (9.11).

become important.<sup>5</sup> When the damping wings dominate, it can be shown (with considerable algebra) that

$$\frac{W_\lambda}{\lambda_0} \propto (\lambda_0^2 N_i)^{1/2}$$

This delineates the *square-root* section of the CoG. Note that this region of the CoG is again independent of  $b$  (physically, no reasonable amount of gaussian turbulence is capable of desaturating the profile).

In the diffuse ISM, lines are not normally strong enough for damping wings to become significant (because stars behind large columns are heavily extinguished and therefore hard to observe). However, the *resonance line* of hydrogen, at 121.6nm, is an important exception, and is nearly always on the square root part of the CoG.

### 9.3 The Empirical Curve of Growth

A *theoretical* curve of growth is, in practice, a plot of  $\log(W_\lambda/\lambda)$  vs.  $\log(Nf\lambda)$ . Observationally, we can measure  $W_\lambda$ , and look up  $\lambda_0$  and  $f_{ij}$  – but we don't know the column density,  $N$ .

In order to derive the abundances of species in the gas phase of the ISM, we construct an *empirical* CoG. From observations of equivalent widths of different lines of a given atomic species, we plot  $\log(W_\lambda/\lambda_0)$  against  $\log(f_{ij}\lambda_0)$  for observed lines.

In principle, we should construct separate CoG for each species. This is because each element has a different mass; so for a given temperature, each element will have a different  $b$  value. Also, we have no *a priori* reason to suppose that different ions of a given element are formed at the same temperatures, or necessarily, in the same place. However, in practice the principal broadening process is often 'turbulence' not thermal, and so we may combine observations of different *dominant ions* (in the diffuse neutral ISM, those with  $IP < 13.6\text{eV}$ ). We do this by overlaying various empirical CoGs, and sliding them along the horizontal axis to obtain a smooth 'global' curve. This gives a much better sampling of the empirical CoG, since normally we only have a few lines of any one species, typically covering a small range in  $f\lambda$ .

If the shape of the curve indicates that the weaker lines are on the linear part of the CoG ( $N$  independent of  $b$ ) then we can determine  $N$  for those lines. Thus the empirical CoG can, in principle, yield column densities for all species on the CoG, independently of any model assumptions.

---

<sup>5</sup>The fwhm of the naturally-broadened Lorentzian is typically much narrower than that of the thermally-broadened Gaussian core. However, the relative strength of the Lorentzian at large distances from the line centre is much greater than that of the gaussian, so for large line strengths can dominate in the wings.

Unfortunately, lines weak enough to be certainly unsaturated are, in practice, often so weak as to be undetectable. We must then resort to overlaying the empirical CoG on a family of theoretical CoGs (calculated for a range of  $b$  values). It is normally possible to find a horizontal shift between the empirical and theoretical CoGs which gives a ‘best fit’. That shift yields  $\log N$ , the column density; and, as a by-product,  $b$  is also constrained. As before,  $\log N$  is most reliably determined if lines are observed on the steepest part of the CoG, *i.e.* on or near the linear part. If lines are present only on the flat part of the CoG there will be large uncertainties on  $\log N$ ; if there is only one line observed, the best we can do is use the linear formula to obtain a *lower limit* to  $N$ .

### 9.3.1 Results

Finally, what do we learn from such studies? Typically, we obtain column densities for a range of elements occurring in the diffuse, neutral ISM.<sup>6</sup> We can derive the relative abundances (ideally, relative to hydrogen), and compare them to the relative abundances in other environments – especially the sun and stars.

Typically, we find that most atoms of particular elements (like silicon, calcium, and iron) are apparently missing, or ‘depleted’, from the gas phase. Where are these missing atoms? We can assume that they are locked up in dust grains. This assumption is justified in a number of ways; for example, in high-velocity clouds, gas-phase abundances are often observed to be much more nearly solar. This is consistent with the idea that the clouds are accelerated by passing shock waves (e.g., from supernova remnants), which also shatter, or ‘sputter’, the dust grains, returning elements to the gas.

---

<sup>6</sup>Any given element may occur in a range of ionization stages, but there will normally be a ‘dominant ion’. In the diffuse neutral ISM, this will be the first stage required more than 13.6eV for further ionization.

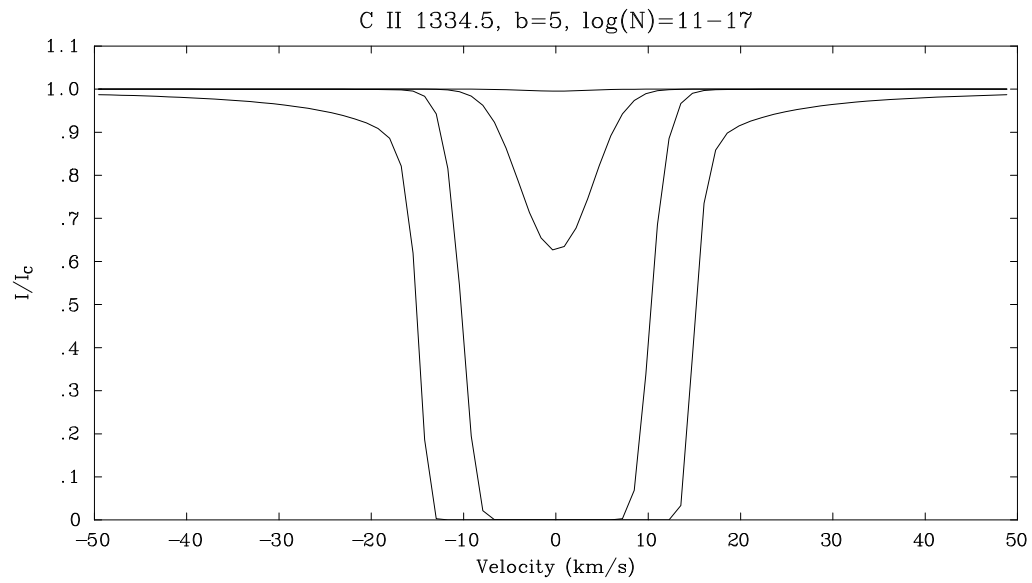
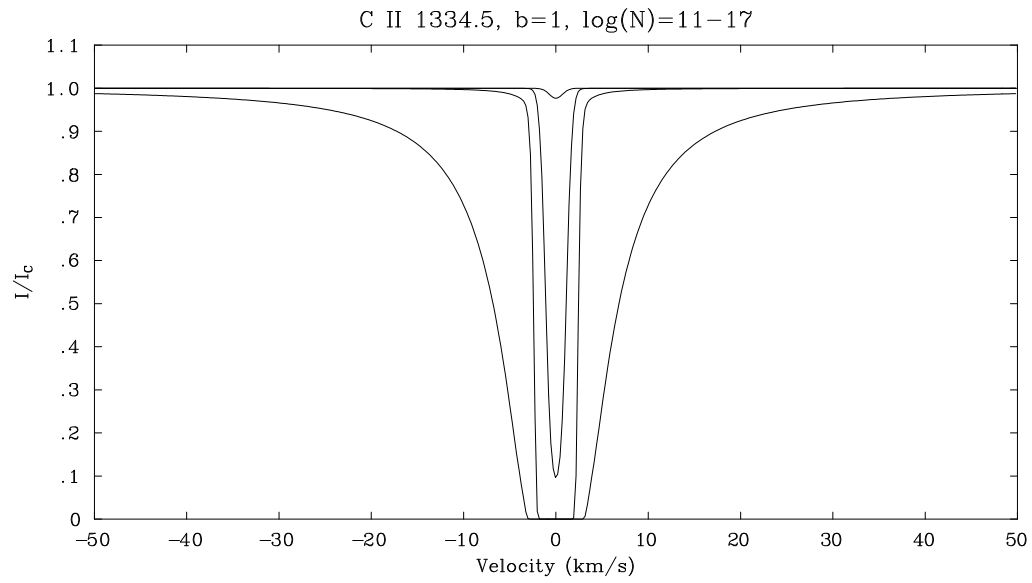


Figure 9.3: Calculated spectral-line profiles for increasing column densities and two different  $b$  values. Increasing line strengths correspond to column densities of 11, 13, 15, and 17 dex  $\text{cm}^{-2}$ .

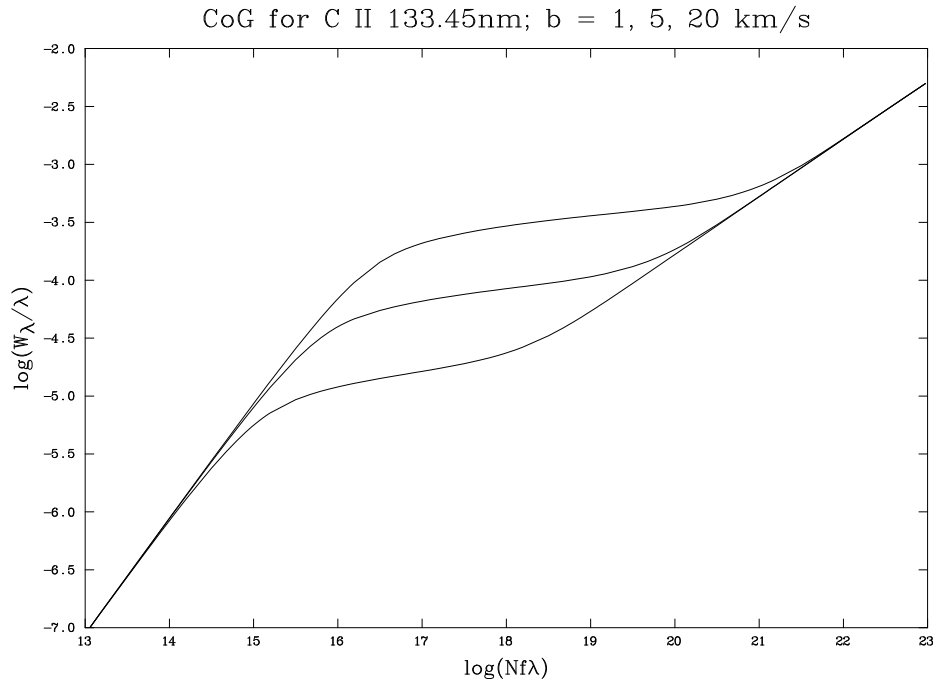


Figure 9.4: Theoretical curves of growth, illustrating the dependence on  $b$ .

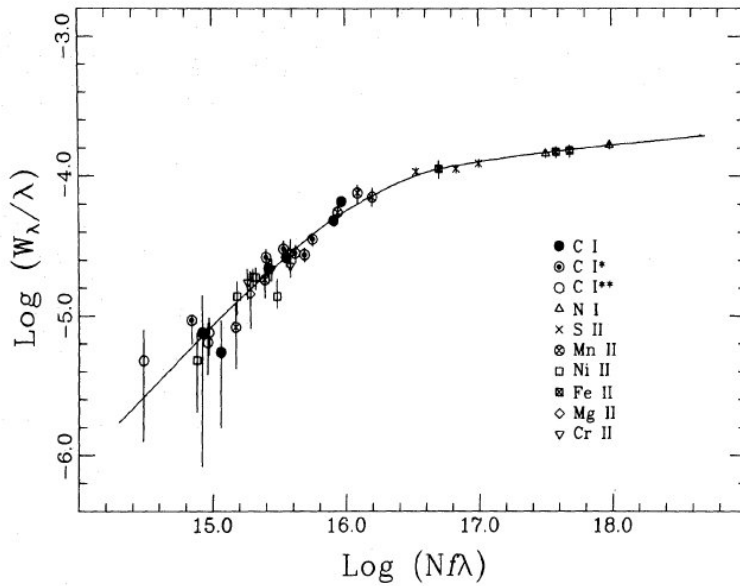


Figure 9.5: An empirical curve of growth for different lines in the spectrum of HD 50896. The solid line is a theoretical CoG with  $b = 10.5 \text{ km s}^{-1}$ .

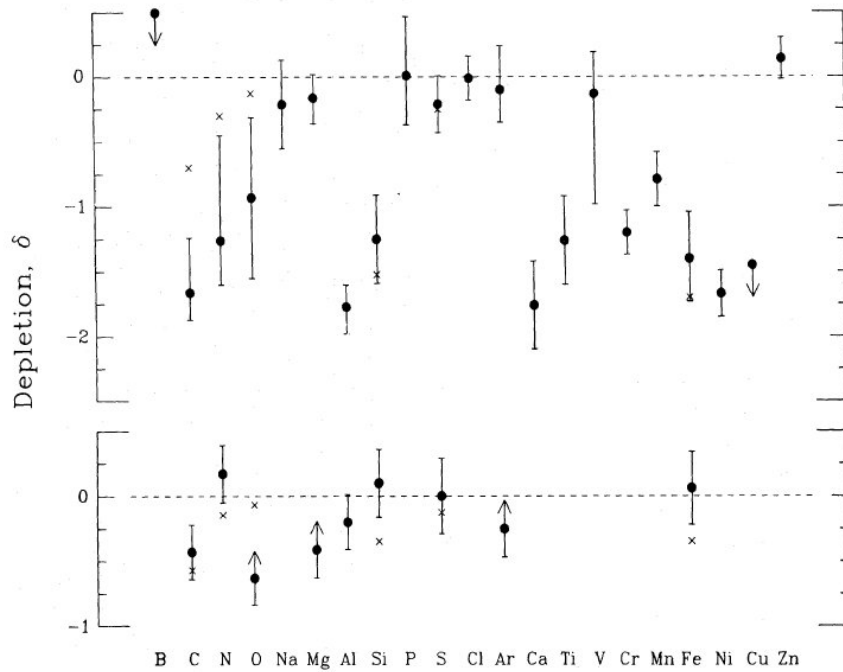


Figure 9.6: Depletions in the line of sight towards HD 50896 in two velocity systems. *Upper panel:* a ‘low velocity’ system, representing a typical diffuse interstellar sightline. Some elements, such as aluminium and calcium, are depleted by almost two orders of magnitude with respect to solar values (that is, something like 99 atoms out of every 100 are ‘missing’ – locked up in dust grains), while others, such as sulphur and zinc, are essentially undepleted. *Lower panel:* a ‘high velocity’ system, with a line-of-sight velocity of  $\sim 75 \text{ km s}^{-1}$ . No elements are significantly depleted, because dust grains have been destroyed in a high-velocity shock.

## 9.4 Summary

We've covered rather a lot of material in this section, so it's worth reviewing the major points (so we can see the wood as well as the trees...).

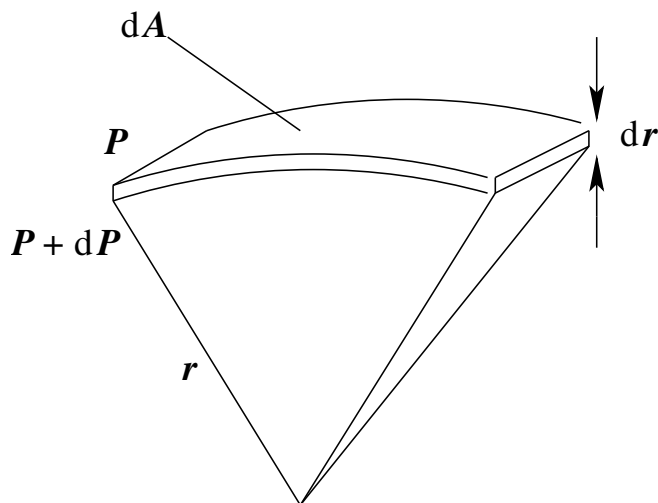
1. Bound-bound transitions in diffuse, interstellar gas clouds produce absorption lines in the spectra of background sources. These absorption lines can tell us something about the clouds – most importantly, the abundances of elements in the gas.
2. Of available background sources, OB stars are particularly useful for investigating the Galactic interstellar medium. (Distant quasars are often used in exactly the same way to investigate gas clouds at cosmological distances, and how metallicity evolves with age in the universe.)
3. Increasing column density (i.e., increasing numbers of absorbers along the line of sight) produces increasingly strong absorption lines. Column density is measured by  $N$ , the number of atoms (of a particular element in a particular stage of ionization), and line strength is measured by  $W_\lambda$ , the equivalent width (because the absorption lines are usually too narrow to measure their shapes in detail). In practice we don't simply plot  $N$  vs.  $W_\lambda$  (one good reason being that  $N$  for a given species is a fixed quantity along any given sightline), but instead plot  $\log(Nf\lambda)$  vs.  $\log(W_\lambda/\lambda)$  – the *Curve of Growth*.
4. The Curve of Growth has three main sections:
  - The *linear* part, for weak lines ( $W_\lambda/\lambda \propto Nf\lambda$ ).
  - The *flat* part, for intermediate-strength (saturated) lines ( $W_\lambda/\lambda \propto [\ln(Nf\lambda)]^{1/2}$  – a very weak dependence)
  - The *square-root* part, for strong (damped) lines ( $W_\lambda/\lambda_0 \propto (\lambda_0^2 N_i)^{1/2}$ ).
5. We can calculate a theoretical CoG (for a given line-of-sight velocity distribution of absorbers) or construct an empirical one. From the linear or square-root parts of the empirical CoG, or (less reliably) by comparison with the theoretical CoG, we can determine column densities in the line of sight. By comparing column densities of dominant ions of different elements (or by making corrections for unobserved ion stages) we can determine relative abundances.
6. We find that many elements are significantly *depleted* compared to solar abundances. The inference is that the 'missing' elements are locked up in the dust grains.

## PART IV: STARS – I

## Section 10

# The Equations of Stellar structure

### 10.1 Hydrostatic Equilibrium



Consider a volume element, density  $\rho$ , thickness  $dr$  and area  $dA$ , at distance  $r$  from a central point.

The gravitational force on the element is

$$\frac{Gm(r)}{r^2} \rho(r) dA dr$$

where  $m(r)$  is the total mass contained within radius  $r$ .

In *hydrostatic equilibrium* the volume element is supported by the (difference in the) pressure force,  $dP(r) dA$ ; i.e.,

$$dP(r) dA = \frac{-Gm(r)}{r^2} \rho(r) dA dr$$

or

$$\frac{dP(r)}{dr} = \frac{-Gm(r)\rho(r)}{r^2} = -\rho(r)g(r) \quad (10.1)$$

or

$$\frac{dP(r)}{dr} + \rho(r)g(r) = 0$$

which is the equation of hydrostatic equilibrium. (Note the minus sign, which arises because increasing  $r$  goes with decreasing  $P(r)$ .)

More generally, the gravitational and pressure forces may not be in equilibrium, in which case there will be a nett acceleration. The resulting equation of motion is simply

$$\frac{dP(r)}{dr} + \rho(r)g(r) = \rho(r)a \quad (10.2)$$

where  $a$  is the acceleration,  $d^2r/dt^2$ .

Note that we have not specified the nature of the supporting pressure; in stellar interiors, it is typically a combination of gas pressure,

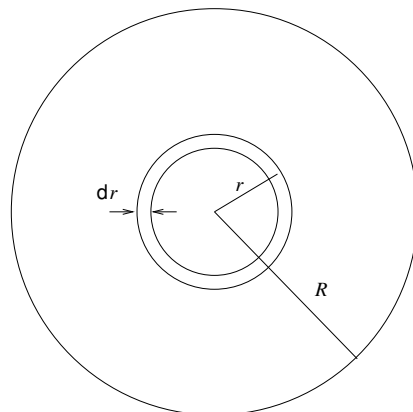
$$P = nkT,$$

and radiation pressure

$$P_R = \frac{4\sigma}{3c}T^4 \quad (1.31)$$

(Section 10.8). Turbulent pressure may be important under some circumstances.

## 10.2 Mass Continuity



The quantities  $m(r)$  and  $\rho(r)$  in eqn. (10.1) are clearly not independent, but we can easily derive the relationship between them. The mass in a spherical shell of thickness  $dr$  is

$$dm = 4\pi r^2 dr \times \rho(r).$$

Thus

$$\frac{dm}{dr} = 4\pi r^2 \rho(r); \tag{10.3}$$

the *Equation of Mass Continuity*.<sup>1</sup>

## Spherical symmetry

Implicit in eqn. (10.3) is the assumption of spherical symmetry. This assumption is reasonable as long as the centrifugal force arising from rotation is small compared to Newtonian gravity. The centrifugal force is a maximum at the equator, so for a star of mass  $M_*$  and equatorial radius  $R_e$  our condition for spherical symmetry is

$$\frac{mv_e^2}{R_e} = m\omega^2 R_e \ll \frac{GM_* m}{R_e^2}$$

for a test particle of mass  $m$  at the equator, where the rotational velocity is  $v_e$  (equatorial angular velocity  $\omega$ ); that is,

$$\omega^2 \ll \frac{GM_*}{R_e^3}, \text{ or, equivalently,} \tag{10.4}$$

$$v_e \ll \sqrt{\frac{GM_*}{R_e}} \text{ giving} \tag{10.5}$$

$$P_{\text{rot}} \gg 2\pi \sqrt{\frac{GM_*}{R_e^3}} \tag{10.6}$$

This condition is true for most stars; e.g., for the Sun,

$$P_{\text{rot}} \simeq 25.4 \text{ d (at the equator);}$$

$$2\pi \sqrt{\frac{GM_*}{R_e^3}} = 10^4 \text{ s} \simeq 0.1 \text{ d.}$$

However, a few stars (such as the emission-line B stars) *do* rotate so fast that their shapes are significantly distorted. The limiting case is when the centrifugal acceleration equals the gravitational acceleration at the equator:

$$\frac{GM_* m}{R_e^2} = \frac{mv_{\text{max}}^2}{R_e},$$

or

$$v_{\text{max}} = \sqrt{\frac{GM_*}{R_e}}$$

Equating the potential at the pole and the equator,

$$\frac{GM_*}{R_p} = \frac{GM_*}{R_e} + \frac{v_e^2}{2}$$

whence  $R_e = 1.5R_p$  in this limiting case.

---

<sup>1</sup>Note that this returns the right answer for the total mass:

$$M_* = \int_0^{R_*} dm = \int_0^{R_*} 4\pi r^2 \rho(r) dr = \frac{4}{3}\pi R^3 \bar{\rho}(R)$$

## Moving media

Equation 10.3 applies when hydrostatic equilibrium holds. If there is a flow (as in the case of stellar winds for example), the equation of mass continuity reflects different physics. In spherical symmetry, the amount of material flowing through a spherical shell of thickness  $dr$  at some radius  $r$  must be the same for all  $r$ . Since the flow at the surface,  $4\pi R_*^2 \rho(R_*) v(R_*)$  is the stellar mass-loss rate  $\dot{M}$ , we have

$$\dot{M} = 4\pi r^2 \rho(r) v(r)$$

## 10.3 Energy continuity

The increase in luminosity in going from  $r$  to  $r + dr$  is just the energy generation within the corresponding shell:

$$\begin{aligned} dL &= L(r + dr) - L(r) \\ &= 4\pi r^2 dr \rho(r) \epsilon(r); \end{aligned}$$

i.e.,

$$\frac{dL}{dr} = 4\pi r^2 \rho(r) \epsilon(r) \tag{10.7}$$

where  $\rho(r)$  is the mass density and  $\epsilon(r)$  is the energy generation rate per unit mass at radius  $r$ .

Stars don't have to be in energy equilibrium moment by moment (e.g., if the gas is getting hotter or colder), but equilibrium must be maintained on longer timescales.

Evidently, the stellar luminosity is given by integrating eqn. (10.7):

$$L = \int_0^{R_*} 4\pi r^2 \rho(r) \epsilon(r) dr$$

if we make the approximation that the luminosity (measured at the surface) equals the instantaneous energy-generation rate (in the interior). This assumption holds for most of a star's lifetime, since the energy diffusion timescale is short compared to the nuclear timescale (see discussions in Sections 12.3 and 12.4).

The equations of hydrostatic equilibrium ( $dP/dr$ ), mass continuity ( $dm/dr$ ), and energy continuity ( $dL/dr$ ), can be used (together with suitable boundary conditions) as a basis for the calculation of stellar structures.

## 10.4 Virial Theorem

The virial theorem expresses the relationship between gravitational and thermal energies in a 'virialised system' (which may be a star, or a cluster of galaxies). There are several ways to

obtain the theorem (e.g., by integrating the equation of hydrostatic equilibrium; see Section 10.4); the approach adopted here, appropriate for stellar interiors, is particularly direct.

The total thermal energy of a star is

$$U = \int_V \left( \frac{3}{2} kT(r) \right) n(r) dV \quad (10.8)$$

(mean energy per particle, times number of particles per unit volume, integrated over the volume of the star); but

$$V = \frac{4}{3} \pi r^3 \quad \text{whence} \quad dV = 4\pi r^2 dr$$

and

$$P = nkT$$

so

$$U = \int_0^{R_*} \frac{3}{2} 4\pi r^2 P(r) dr.$$

Integrating by parts,

$$\begin{aligned} U &= \frac{3}{2} \left[ 4\pi P(r) \frac{r^3}{3} \right]_0^{R_*} && - \frac{3}{2} \int_{P_C}^{P_S} 4\pi \frac{r^3}{3} dP \\ &= 0 && - \int_{P_C}^{P_S} 2\pi r^3 dP \end{aligned}$$

where  $P_S$ ,  $P_C$  are the surface and central pressures, and the first term vanishes because  $P_S \simeq 0$ ; but, from hydrostatic equilibrium and mass continuity,

$$dP = \frac{-Gm(r)\rho(r)}{r^2} \times \frac{dm}{4\pi r^2 \rho(r)} \quad (10.1, 10.3)$$

so

$$\begin{aligned} U &= \int_0^{M_*} 2\pi r^3 \frac{Gm(r)}{r^2} \frac{dm}{4\pi r^2} \\ &= \frac{1}{2} \int_0^{M_*} \frac{Gm(r)}{r} dm. \end{aligned} \quad (10.9)$$

However, the total gravitational potential energy (defined to be zero for a particle at infinity) is

$$\Omega = - \int_0^{M_*} \frac{Gm(r)}{r} dm; \quad (10.10)$$

comparing eqtns. (10.9) and (10.10) we see that

$$\boxed{2U + \Omega = 0 \quad - \quad \text{the Virial Theorem.}} \quad (10.11)$$

## An alternative derivation

From hydrostatic equilibrium and mass conservation,

$$\frac{dP(r)}{dr} = -\frac{Gm(r)\rho(r)}{r^2}, \quad (10.1)$$

$$\frac{dm}{dr} = 4\pi r^2 \rho(r) \quad (10.3)$$

we have that

$$\frac{dP(r)}{dm} = -\frac{Gm(r)}{4\pi r^4}.$$

Multiplying both sides by  $\frac{4}{3}\pi r^3 \equiv V$  gives us

$$\begin{aligned} V dP &= -\frac{4}{3}\pi r^3 \frac{Gm}{4\pi r^4} dm \\ &= -\frac{1}{3}Gmr dm. \end{aligned}$$

Integrating over the entire star,

$$\int_0^{R_*} V dP = PV|_0^{R_*} - \int_0^{V(R_*)} P dV, = \frac{1}{3}\Omega$$

but  $P \rightarrow 0$  as  $r \rightarrow R_*$ , so

$$3 \int_0^{V(R_*)} P dV + \Omega = 0.$$

We can write the equation of state in the form

$$P = (\gamma - 1)\rho u$$

where  $\gamma$  is the ratio of specific heats and  $u$  is the specific energy (i.e., internal [thermal] energy per unit mass);

$$3 \int_0^{V(R_*)} (\gamma - 1)\rho u dV + \Omega = 0.$$

Now  $\rho u$  is the internal energy per unit volume, so integrating over volume gives us the total thermal energy,  $U$ ; and

$$3(\gamma - 1)U + \Omega = 0.$$

For an ideal monatomic gas,  $\gamma = 5/3$ , and we recover eqn. (10.11).

### 10.4.1 Implications

Suppose a star contracts, resulting in a more negative  $\Omega$  (from eqn. (10.10); smaller  $r$  gives bigger  $|\Omega|$ ). The virial theorem relates the change in  $\Omega$  to a change in  $U$ :

$$\Delta U = -\frac{\Delta\Omega}{2}.$$

Thus  $U$  becomes more positive; i.e., the star gets hotter as a result of the contraction. This is as one might intuitively expect, but note that only *half* the change in  $\Omega$  has been accounted for; the remaining energy is ‘lost’ – in the form of radiation.

Overall, then, the effects of gravitational contraction are threefold (in addition to the trivial fact that the system gets smaller):

- (i) The star gets hotter
- (ii) Energy is radiated away
- (iii) The total energy of the system,  $T$ , decreases (formally, it becomes more negative – that is, more tightly bound);

$$\begin{aligned}
 \Delta T &= \Delta U + \Delta \Omega \\
 &= -\Delta \Omega / 2 + \Delta \Omega \\
 &= \frac{1}{2} \Delta \Omega
 \end{aligned}$$

These results have an obvious implication in star formation; a contracting gas cloud heats up until, eventually, thermonuclear burning may start. This generates heat, hence gas pressure, which opposes further collapse as the star comes in to hydrostatic equilibrium.

### 10.4.2 Red Giants

The evolution of solar-type main-sequence stars is a one of the most dramatic features of stellar evolution. All numerical stellar-evolution models predict this transition, and yet we lack a *simple*, didactic physical explanation:

“Why do some stars evolve into red giants though some do not? This is a classic question that we consider to have been answered only unsatisfactorily. This question is related, in a more general context, to the formation of core-halo structure in self-gravitating systems.” – *D. Sugimoto & M. Fujimoto (ApJ, 538, 837, 2000)*

Nevertheless, semi-phenomenological descriptions afford some insight; these can be presented in various degrees of detail, of which the most straightforward argument is as follows.

We simplify the stellar structure into an inner core and an outer envelope, with masses and radii  $M_c, M_e$  and  $R_c, R_e (= R_*)$  respectively. At the end of core hydrogen burning, we suppose that core contraction happens quickly – faster than the Kelvin-Helmholtz timescale, so that the Virial Theorem holds, and thermal and gravitational potential energy are conserved to a satisfactory degree of approximation. We formalize this supposition by writing

$$\begin{aligned}
 \Omega + 2U &= \text{constant} && \text{(Virial theorem)} \\
 \Omega + U &= \text{constant} && \text{(Energy conservation)}
 \end{aligned}$$

These two equalities can only hold simultaneously if both  $\Omega$  and  $U$  are individually constant, summed over the whole star. In particular, the total gravitational potential energy is constant

Stars are centrally condensed, so we make the approximation that  $M_c \gg M_e$ ; then, adding the core and envelope,

$$|\Omega| \simeq \frac{GM_c^2}{R_c} + \frac{GM_c M_e}{R_*}$$

We are interested in evolution, so we take the derivative with respect to time,

$$\frac{d|\Omega|}{dt} = 0 = -\frac{GM_c^2}{R_c^2} \frac{dR_c}{dt} - \frac{GM_c M_e}{R_*^2} \frac{dR_*}{dt}$$

i.e.,

$$\frac{dR_*}{dR_c} = -\frac{M_c}{M_e} \left( \frac{R_*}{R_c} \right)^2.$$

The negative sign demonstrates that as the core *contracts*, the envelope must *expand* – a good rule of thumb throughout stellar evolution, and, in particular, what happens at the end of the main sequence for solar-type stars.

## 10.5 Mean Molecular Weight

The ‘mean molecular weight’,  $\mu$ , is<sup>2</sup> simply the average mass of particles in a gas, expressed in units of the hydrogen mass,  $m(\text{H})$ . That is, the mean mass is  $\mu m(\text{H})$ ; since the number density of particles  $n$  is just the mass density  $\rho$  divided by the mean mass we have

$$n = \frac{\rho}{\mu m(\text{H})} \quad \text{and} \quad P = nkT = \frac{\rho}{\mu m(\text{H})} kT \quad (10.12)$$

In order to evaluate  $\mu$  we adopt the standard astronomical nomenclature of

$X$  = mass fraction of hydrogen

$Y$  = mass fraction of helium

$Z$  = mass fraction of metals.

(where implicitly  $X + Y + Z \equiv 1$ ). For a fully ionized gas of mass density  $\rho$  we can infer number densities:

Element:	H	He	Metals
No. of nuclei	$\frac{X\rho}{m(\text{H})}$	$\frac{Y\rho}{4m(\text{H})}$	$\frac{Z\rho}{\overline{Am}(\text{H})}$
No. of electrons	$\frac{X\rho}{m(\text{H})}$	$\frac{2Y\rho}{4m(\text{H})}$	$\frac{(\overline{A}/2)Z\rho}{\overline{Am}(\text{H})}$

<sup>2</sup>Elsewhere we’ve used  $\mu$  to mean  $\cos \theta$ . Unfortunately, both uses of  $\mu$  are completely standard; but fortunately, the context rarely permits any ambiguity about which ‘ $\mu$ ’ is meant. And why ‘molecular’ weight for a potentially molecule-free gas? Don’t ask me. . .

where  $\bar{A}$  is the average atomic weight of metals ( $\sim 16$  for solar abundances), and for the final entry we assume that  $A_i \simeq 2Z_i$  for species  $i$  with atomic number  $Z_i$ .

The total number density is the sum of the numbers of nuclei and electrons,

$$n \simeq \frac{\rho}{m(\text{H})} (2X + 3Y/4 + Z/2) \equiv \frac{\rho}{\mu m(\text{H})} \quad (10.13)$$

(where we have set  $Z/2 + Z/\bar{A} \simeq Z/2$ , since  $\bar{A} \gg 2$ ). We see that

$$\mu \simeq (2X + 3Y/4 + Z/2)^{-1}. \quad (10.14)$$

We can drop the approximations to obtain a more general (but less commonly used) definition,

$$\mu^{-1} = \sum_i \frac{Z_i + 1}{A_i} f_i$$

where  $f_i$  is the mass fraction of element  $i$  with atomic weight  $A_i$  and atomic number  $Z_i$ .

For a fully ionized pure-hydrogen gas ( $X = 1, Y = Z = 0$ ),  $\mu = 1/2$ ;

for a fully ionized pure-helium gas ( $Y = 1, X = Z = 0$ ),  $\mu = 4/3$ ;

for a fully ionized gas of solar abundances ( $X = 0.71, Y = 0.27, Z = 0.02$ ),  $\mu = 0.612$ .

## 10.6 Pressure and temperature in the cores of stars

### 10.6.1 Solar values

Section 10.10 outlines how the equations of stellar structure can be used to construct a stellar model. In the context of studying the solar neutrino problem, many very detailed models of the Sun's structure have been constructed; for reference, we give the results one of these detailed models, namely Bahcall's standard model `bp2000stdmodel.dat`. This has

$$\begin{aligned} T_c &= 1.568 \times 10^7 \text{ K} \\ \rho_c &= 1.524 \times 10^5 \text{ kg m}^{-3} \\ P_c &= 2.336 \times 10^{16} \text{ N m}^{-2} \end{aligned}$$

with 50% (95%) of the solar luminosity generated in the inner 0.1 (0.2)  $R_\odot$ .

### 10.6.2 Central pressure (1)

We can use the equation of hydrostatic equilibrium to get order-of-magnitude estimates of conditions in stellar interiors; e.g., letting  $dr = R_*$  (for an *approximate* solution!) then

$$\frac{dP(r)}{dr} = \frac{-Gm(r)\rho(r)}{r^2} \quad (10.1)$$

becomes

$$\frac{P_C - P_S}{R_*} \simeq \frac{GM_*\bar{\rho}}{R_*^2}$$

where  $P_C$ ,  $P_S$  are the central and surface pressures; and since  $P_C \gg P_S$ ,

$$\begin{aligned} P_C &\simeq \frac{GM_*\bar{\rho}}{R_*} \\ &= \frac{3}{4\pi} \frac{GM_*^2}{R_*^4} \\ &\simeq 10^{15} \text{ Pa } (= \text{N m}^{-2}) \end{aligned} \tag{10.15}$$

(or about  $10^{10}$  atmospheres) for the Sun. Because of our crude approximation in integrating eqn. (10.1) we expect this to be an underestimate (more nearly an average than a central value), and reference to the detailed shows it falls short by about an order of magnitude. Nevertheless, it does serve to demonstrate high core values, and the  $\sim M^2/R^4$  dependence of  $P_C$ .

## Central pressure (2)

Another estimate can be obtained by dividing the equation of hydrostatic equilibrium (10.1) by the equation of mass continuity (10.3):

$$\frac{dP(r)}{dr} \bigg/ \frac{dm}{dr} \equiv \frac{dP(r)}{dm} = \frac{-Gm(r)}{4\pi r^4}$$

Integrating over the entire star,

$$-\int_0^{M_*} \frac{dP(r)}{dm} dm = P_C - P_S = \int_0^{M_*} \frac{Gm(r)}{4\pi r^4} dm.$$

Evidently, because  $R_* \geq r$ , it must be the case that

$$\int_0^{M_*} \frac{Gm(r)}{4\pi r^4} dm \geq \underbrace{\int_0^{M_*} \frac{Gm(r)}{4\pi R_*^4} dm}_{= \frac{GM_*^2}{8\pi R_*^4}} \tag{10.16}$$

that is,

$$\begin{aligned} P_C &> \frac{GM_*^2}{8\pi R_*^4} \quad (+P_S, \text{ but } P_S \simeq 0) \\ &> 4.5 \times 10^{13} \text{ N m}^{-2} \end{aligned}$$

for the Sun. This is a weaker estimate than, but is consistent with, eqn. (10.15), and shows the same overall scaling of  $P_C \propto M_*^2/R_*^4$ .

### 10.6.3 Central temperature

For a perfect gas,

$$P = nkT = \frac{\rho kT}{\mu m(\text{H})} \tag{10.12}$$

but

$$P_C \simeq \frac{GM_* \bar{\rho}}{R_*} \quad (10.15)$$

so

$$\begin{aligned} T_C &\simeq \frac{\mu m(\text{H})}{k} \frac{GM_*}{R_*} \frac{\bar{\rho}}{\rho_C} \\ &\simeq 1.4 \times 10^7 \text{ K} \end{aligned} \quad (10.17)$$

for the Sun – which is quite close to the results of detailed calculations. (Note that at these temperatures the gas is fully ionized and the perfect gas equation is an excellent approximation.)

#### 10.6.4 Mean temperature

We can use the Virial Theorem to obtain a limit on the *mean* temperature of a star. We have

$$\begin{aligned} U &= \int_V \frac{3}{2} kT(r) n(r) dV \\ &= \int_V \frac{3}{2} kT(r) \frac{\rho(r)}{\mu m(\text{H})} dV \\ &= \int_0^{M_*} \frac{3}{2} kT(r) \frac{\rho(r)}{\mu m(\text{H})} \frac{dm}{\rho(r)} \end{aligned} \quad (10.8)$$

and

$$\begin{aligned} -\Omega &= \int_0^{M_*} \frac{Gm(r)}{r} dm \\ &> \int_0^{M_*} \frac{Gm(r)}{R_*} dm \\ &> \frac{GM_*^2}{2R_*} \end{aligned} \quad (10.10)$$

From the Virial Theorem,  $2U = -\Omega$  (eqn. 10.11), so

$$\frac{3k}{\mu m(\text{H})} \int_0^{M_*} T dm > \frac{GM_*^2}{2R_*}$$

The integral represents the sum of the temperatures of the infinitesimal mass elements contributing to the integral; the *mass-weighted* average temperature is

$$\begin{aligned} \bar{T} &= \frac{\int_0^{M_*} T dm}{\int_0^{M_*} dm} \\ &= \frac{\int_0^{M_*} T dm}{M_*} \\ &> \frac{GM_*}{2R_*} \frac{\mu m(\text{H})}{3k} \end{aligned}$$

For the Sun, this evaluates to  $\bar{T}(\odot) > 2.3 \times 10^6$  K (using  $\mu = 0.61$ ), i.e.,  $kT \simeq 200$  eV – comfortably in excess of the ionization potentials of hydrogen and helium (and enough to substantially ionize the most abundant metals), justifying the assumption of complete ionization in evaluating  $\mu$ .

## 10.7 Mass–Luminosity Relationship

We can put together our basic stellar-structure relationships to demonstrate a scaling between stellar mass and luminosity. From hydrostatic equilibrium,

$$\frac{dP(r)}{dr} = \frac{-Gm(r)\rho(r)}{r^2} \quad \rightarrow \quad P \propto \frac{M}{R}\rho \quad (10.1)$$

but our equation of state is  $P = (\rho kT)/(\mu m(\text{H}))$ , so

$$T \propto \frac{\mu M}{R}.$$

For stars in which the dominant energy transport is radiative, we have

$$L(r) \propto \frac{r^2}{\bar{\kappa}_R} \frac{dT}{dr} T^3 \quad \propto \frac{r^2}{\bar{\kappa}_R \rho(r)} \frac{dT}{dr} T^3 \quad (3.11)$$

so that

$$L \propto \frac{RT^4}{\bar{\kappa}_R \rho}.$$

From mass continuity (or by inspection)  $\rho \propto M/R^3$ , giving

$$\begin{aligned} L &\propto \frac{R^4 T^4}{\bar{\kappa}_R M} \\ &\propto \frac{R^4}{\bar{\kappa}_R M} \left( \frac{\mu M}{R} \right)^4; \end{aligned}$$

i.e.,

$$L \propto \frac{\mu^4}{\bar{\kappa}_R} M^3.$$

This simple dimensional analysis yields a dependency which is in quite good agreement with observations; for solar-type main-sequence stars, the empirical mass–luminosity relationship is  $L \propto M^{3.5}$ .

## 10.8 The role of radiation pressure

So far we have, for the most part, considered only *gas* pressure. What about radiation pressure? From Section 1.8, the magnitude of the pressure of isotropic radiation is

$$P_{\text{R}} = \frac{4\sigma}{3c} T^4. \quad (1.31)$$

Thus the ratio of radiation pressure to gas pressure is

$$\begin{aligned} P_{\text{R}}/P_{\text{G}} &= \frac{4\sigma}{3c} T^4 \bigg/ \frac{k\rho T}{\mu m(\text{H})} \\ &\simeq 1.85 \times 10^{-20} [\text{kg m}^{-3} \text{ K}^{-3}] \times \frac{T^3}{\rho} \end{aligned} \quad (10.18)$$

For  $\bar{\rho}_{\odot} = 1.4 \times 10^3 \text{ kg m}^{-3}$  and  $T_{\text{C}}(\odot) \simeq 10^7 \text{ K}$ ,  $P_{\text{R}}/P_{\text{G}} \simeq 0.1$ . That is, radiation pressure is relatively unimportant in the Sun, even in the core.

However, radiation pressure *is* important in stars more massive than the Sun (which have hotter central temperatures). Eqtn (10.18) tells us that

$$P_{\text{R}}/P_{\text{G}} \propto \frac{T^3}{\rho} \propto \frac{T^3 R_*^3}{M_*}$$

but  $T \propto M_*/R_*$ , from eqtn. (10.17); that is,

$$P_{\text{R}}/P_{\text{G}} \propto M_*^2$$

## 10.9 The Eddington limit

Radiation pressure plays a particular role at the surfaces of luminous stars, where the radiation field is, evidently, no longer close to isotropic (the radiation is escaping from the surface). As we saw in Section 1.8, the momentum of a photon is  $h\nu/c$ .

If we consider some spherical surface at distance  $r$  from the energy-generating centre of a star, where all photons are flowing outwards (i.e., the surface of the star), the total photon momentum flux, per unit area per unit time, is

$$\frac{L}{c} \bigg/ (4\pi r^2) \quad [\text{J m}^{-3} = \text{kg m}^{-1} \text{ s}^{-2}]$$

The Thomson-scattering cross-section (for electron scattering of photons) is

$$\sigma_{\text{T}} \left[ = \frac{8\pi}{3} \left( \frac{e^2}{m_e c^2} \right)^2 \right] = 6.7 \times 10^{-29} \text{ m}^2.$$

This is a major opacity source in ionized atmospheres, so the force is exerted mostly on electrons; the radiation force per electron is

$$F_R = \frac{\sigma_T L}{4\pi r^2 c} \quad [\text{J m}^{-1} \equiv \text{N}]$$

which is then transmitted to positive ions by electrostatic interactions. For stability, this outward force must be no greater than the inward gravitational force; for equality (and assuming fully ionized hydrogen)

$$\frac{\sigma_T L}{4\pi r^2 c} = \frac{GM(m(\text{H}) + m_e)}{r^2} \simeq \frac{GMm(\text{H})}{r^2}.$$

This equality gives a limit on the maximum luminosity as a function of mass for a stable star – the *Eddington Luminosity*,

$$\begin{aligned} L_{\text{Edd}} &= \frac{4\pi GMc m(\text{H})}{\sigma_T} \\ &\simeq 1.3 \times 10^{31} \frac{M}{M_\odot} \quad [\text{J s}^{-1}], \text{ or} \\ \frac{L_{\text{Edd}}}{L_\odot} &\simeq 3.37 \times 10^4 \frac{M}{M_\odot} \end{aligned}$$

Since luminosity is proportional to mass to some power (roughly,  $L \propto M^{3-4}$  on the upper main sequence; cf. Section 10.7), it must be the case that the Eddington Luminosity imposes an upper limit to the mass of stable stars.

(In practice, instabilities cause a super-Eddington atmosphere to become clumpy, or ‘porous’, and radiation is able to escape through paths of lowered optical depth between the clumps. Nevertheless, the Eddington limit represents a good approximation to the upper limit to stellar luminosity. We see this limit as an upper bound to the Hertzsprung-Russell diagram, the so-called ‘Humphreys-Davidson limit’.)

# How to make a star (for reference only)

## 10.10 Introduction

We've assembled a set of equations that embody the basic principles governing stellar structure; renumbering for convenience, these are

$$\frac{dm(r)}{dr} = 4\pi r^2 \rho(r) \quad \text{Mass continuity} \quad (10.3=10.19)$$

$$\frac{dP(r)}{dr} = \frac{-Gm(r)\rho(r)}{r^2} \quad \text{Hydrostatic equilibrium} \quad (10.1=10.20)$$

$$\frac{dL(r)}{dr} = 4\pi r^2 \rho(r)\varepsilon(r) \quad \text{Energy continuity} \quad (10.7=10.21)$$

and radiative energy transport is described by

$$L(r) = -\frac{16\pi}{3} \frac{r^2}{\bar{k}_R(r)} \frac{dT}{dr} acT^3 \quad \text{Radiative energy transport.} \quad (3.11=10.22)$$

The quantities  $P$ ,  $\varepsilon$ , and  $\bar{k}_R$  (pressure, energy-generation rate, and Rosseland mean opacity) are each functions of density, temperature, and composition; those functionalities can be computed separately from the stellar structure problem. For analytical work we can reasonably adopt power-law dependences,

$$\bar{k}_R(r) = \kappa(r) = \kappa_0 \rho^\alpha(r) T^b(r) \quad (2.6=10.23)$$

and (anticipating Section 13)

$$\varepsilon(r) \simeq \varepsilon_0 \rho(r) T^\alpha(r), \quad (13.9=10.24)$$

together with an equation of state; for a perfect gas

$$P(r) = n(r)kT(r). \quad (10.12=10.25)$$

Mass is a more fundamental physical property than radius (the radius of a solar-mass star will change by orders of magnitude over its lifetime, while its mass remains more or less constant),

so for practical purposes it is customary to reformulate the structure equations in terms of mass as the independent variable. We do this simply by dividing the last three of the foregoing equations by the first, giving

$$\frac{dr}{dm(r)} = \frac{1}{4\pi r^2 \rho(r)} \quad (10.26)$$

$$\frac{dP(r)}{dm(r)} = \frac{-Gm(r)}{4\pi r^4} \quad (10.27)$$

$$\frac{dL(r)}{dm(r)} = \varepsilon(r) = \varepsilon_0 \rho(r) T^\alpha(r) \quad (10.28)$$

$$\frac{dT(r)}{dm(r)} = -\frac{3\bar{k}_R L(r)}{16\pi^2 r^4 a c T^3(r)} \quad (10.29)$$

(where all the radial dependences have been shown explicitly).

To solve this set of equations we require boundary conditions. At  $m = 0$  (i.e.,  $r = 0$ ),  $L(r) = 0$ ; at  $m = M_*$  ( $r = R_*$ ) we set  $P = 0$ ,  $\rho = 0$ . In practice, the modern approach is to integrate these equations numerically.<sup>3</sup> However, much progress was made before the advent of electronic computers by using simplified models, and these models still arguably provide more physical insight than simply running a computer program.

## 10.11 Homologous models

*Homologous* stellar models are defined such that their properties scale in the same way with fractional mass  $\mathbf{m} \equiv m(r)/M_*$ . That is, for some property  $X$  (which might be temperature, or density, etc.), a plot of  $X$  vs.  $\mathbf{m}$  is the same for all homologous models. Our aim in constructing such models is to formulate the stellar-structure equations so that they are independent of absolute mass, but depend only on *relative* mass.

We therefore recast the variables of interest as functions of fractional mass, with the dependency on *absolute* mass assumed to be a power law:

$$\begin{aligned} r &= M_*^{x_1} r_0(\mathbf{m}) & dr &= M_*^{x_1} dr_0 \\ \rho(r) &= M_*^{x_2} \rho_0(\mathbf{m}) & d\rho(r) &= M_*^{x_2} d\rho_0 \\ T(r) &= M_*^{x_3} T_0(\mathbf{m}) & dT(r) &= M_*^{x_3} dT_0 \\ P(r) &= M_*^{x_4} P_0(\mathbf{m}) & dP(r) &= M_*^{x_4} dP_0 \\ L(r) &= M_*^{x_5} L_0(\mathbf{m}) & dL(r) &= M_*^{x_5} dL_0 \end{aligned}$$

---

<sup>3</sup>The interested student can run his own models using the EZ ('Evolve ZAMS') code; W. Paxton, PASP, 116, 699, 2004.

where the  $x_i$  exponents are constants to be determined, and  $r_0, \rho_0$  etc. depend only on the fractional mass  $m$ . We also have

$$m(r) = m M_* \qquad dm(r) = M_* dm$$

and, from eqtns. (2.6=10.23, 13.9=10.24)

$$\begin{aligned} \kappa(r) &= \kappa_0 \rho^a(r) T^b(r)^b & &= \kappa_0 \rho_0^a(m) T_0^b(m) M_*^{ax_2} M_*^{bx_3} \\ \varepsilon(r) &\simeq \varepsilon_0 \rho(r) T^\alpha(r), & &= \varepsilon_0 \rho_0(m) T_0^\alpha(m) M_*^{x_2} M_*^{\alpha x_3}, \end{aligned}$$

### Transformed equations

We can now substitute these into our structure equations to express them in terms of dimensionless mass  $m$  in place of actual mass  $m(r)$ :

Mass continuity:

$$\frac{dr}{dm(r)} = \frac{1}{4\pi r^2 \rho(r)} \quad \text{becomes} \quad (10.26)$$

$$M_*^{(x_1-1)} \frac{dr_0(m)}{dm} = \frac{1}{4\pi r_0^2(m) \rho_0(m)} M_*^{-(2x_1+x_2)} \quad (10.30)$$

The condition of homology requires that the scaling be independent of actual mass, so we can equate the exponents of  $M_*$  on either side of the equation to find

$$3x_1 + x_2 = 1 \quad (10.31)$$

Hydrostatic equilibrium:

$$\frac{dP(r)}{dm(r)} = \frac{-Gm(r)}{4\pi r^4} \quad \text{becomes} \quad (10.27)$$

$$M_*^{(x_4-1)} \frac{dP_0(m)}{dm} = -\frac{Gm}{4\pi r_0^4} M_*^{(1-4x_1)} \quad (10.32)$$

$$\text{whence } 4x_1 + x_4 = 2 \quad (10.33)$$

Energy continuity:

$$\begin{aligned} \frac{dL(r)}{dm(r)} &= \varepsilon(r) \\ &= \varepsilon_0 \rho(r) T^\alpha(r) \quad \text{becomes} \end{aligned} \quad (10.28)$$

$$M_*^{(x_5-1)} \frac{dL_0(m)}{dm} = \varepsilon_0 \rho_0(m) T_0^\alpha(m) M_*^{x_2 + \alpha x_3} \quad (10.34)$$

$$\text{whence } x_2 + \alpha x_3 + 1 = x_5 \quad (10.35)$$

Radiative transport:

$$\frac{dT(r)}{dm(r)} = -\frac{3\bar{k}_R L(r)}{16\pi^2 r^4 a c T^3(r)} \quad \text{becomes} \quad (10.29)$$

$$M_*^{(x_3-1)} \frac{dT_0(\mathbf{m})}{dm} = -\frac{3(\kappa_0 \rho_0^a T_0^b) L_0}{16\pi^2 r_0^4 a c T_0^3(\mathbf{m})} M_*^{(x_5+(b-3)x_3+ax_2-4x_1)} \quad (10.36)$$

$$\text{whence } 4x_1 + (4-b)x_3 = ax_2 + x_5 + 1 \quad (10.37)$$

Equation of state:

$$\begin{aligned} P(r) &= n(r)kT(r) \\ &= \frac{\rho(r)kT(r)}{\mu m(\text{H})} \end{aligned} \quad (10.38)$$

(neglecting any radial dependence of  $\mu$ )

$$M_*^{x_4} P_0(\mathbf{m}) = \frac{\rho_0(\mathbf{m})kT_0(\mathbf{m})}{\mu m(\text{H})} M_*^{(x_2+x_3)} \quad (10.39)$$

$$\text{whence } x_2 + x_3 = x_4 \quad (10.40)$$

We now have five equations for the five exponents  $x_i$ , which can be solved for given values of  $a$ ,  $b$ , and  $\alpha$ , the exponents in eqtns. (2.6=10.23) and (13.9=10.24). This is quite tedious in general, but a simple solution is afforded by the (reasonable) set of parameters

$$a = 1$$

$$b = -3.5$$

$$\alpha = 4$$

(xxx see Tayler); the solutions include

$$x_1 = 1/13$$

$$x_5 = 71/13 (\simeq 5.5)$$

which we will use in the next section.

### 10.11.1 Results

Collecting the set structure equations that describe a sequence of homologous models:

$$\frac{dr_0(\mathbf{m})}{d\mathbf{m}} = \frac{1}{4\pi r_0^2(\mathbf{m})\rho_0(\mathbf{m})} \quad (10.30)$$

$$\frac{dP_0(\mathbf{m})}{d\mathbf{m}} = -\frac{G\mathbf{m}}{4\pi r_0^4} \quad (10.32)$$

$$\frac{dL_0(\mathbf{m})}{d\mathbf{m}} = \varepsilon_0\rho_0(\mathbf{m})T_0^\alpha(\mathbf{m}) \quad (10.34)$$

$$\frac{dT_0(\mathbf{m})}{d\mathbf{m}} = -\frac{3(\kappa_0\rho_0^a T_0^b)L_0}{16\pi^2 r_0^4 ac T_0^3(\mathbf{m})} \quad (10.36)$$

$$P_0(\mathbf{m}) = \frac{\rho_0(\mathbf{m})kT_0(\mathbf{m})}{\mu m(\text{H})} \quad (10.39)$$

These can be solved numerically using the boundary conditions

$$r_0 = 0L_0 = 0 \quad \text{at } \mathbf{m} = 0,$$

$$P_0 = 0\rho_0 = 0 \quad \text{at } \mathbf{m} = 1.$$

However, we can draw some useful conclusions analytically. First, it's implicit in our definition of homologous models that there must exist a mass-luminosity relation for them; since

$$L_* = M_*^{x_5} L_0(1)$$

it follows immediately that

$$L_* \propto M_*^{x_5} (\propto M_*^{5.5})$$

which is not too bad compared to the actual main-sequence mass-luminosity relationship ( $L \propto M^{3-4}$ , especially considering the crudity of the modelling).

Secondly, since

$$\begin{aligned} L_* &\propto R_*^2 T_{\text{eff}}^4 & R_* &= M_*^{x_1} r_0(1) \\ L_* &= M_*^{x_5} L_0(1), \end{aligned}$$

it follows that

$$M_*^{x_5} L_0(1) \propto M_*^{2x_1} r_0^2(1) T_{\text{eff}}^4$$

or

$$\begin{aligned} M_* &\propto T_{\text{eff}}^{4/(x_5-2x_1)} \\ &\propto T_{\text{eff}}^{52/69}. \end{aligned}$$

This is a bit off the mark for real stars, which show a slower increase in temperature with mass; but combining this with the mass-luminosity relationship gives

$$\begin{aligned} L_* &\propto T_{\text{eff}}^{4x_5/(x_5-2x_1)} \\ &\propto T_{\text{eff}}^{284/69} \end{aligned}$$

which again is not too bad for the lower main sequence – indeed, the qualitative result that there *is* a luminosity–temperature relationship is, in effect, a prediction that a main sequence exists in the HR diagram.

## 10.12 Polytropes and the Lane-Emden Equation

Another approach to simple stellar-structure models is to assume a ‘polytropic’ formalism. We can again start with hydrostatic equilibrium and mass continuity,

$$\frac{dP(r)}{dr} = \frac{-Gm(r)\rho(r)}{r^2} \tag{10.1}$$

$$\frac{dm}{dr} = 4\pi r^2 \rho(r). \tag{10.3}$$

Differentiating eqn. (10.1) gives us

$$\frac{d}{dr} \left( \frac{r^2}{\rho} \frac{dP}{dr} \right) = -G \frac{dm(r)}{dr}$$

whence, from eqn. (10.3),

$$\frac{1}{r^2} \frac{d}{dr} \left( \frac{r^2}{\rho} \frac{dP}{dr} \right) = -4\pi G \rho \tag{10.41}$$

This is, essentially, already the ‘Lane-Emden equation’ (named for the American astronomer Jonathan Lane and the Swiss Jacob Emden).

It appears that we can’t solve hydrostatic equilibrium without knowing something about the pressure, i.e., the temperature, which in turn suggests needing to know about energy generation processes, opacities, and other complexities. Surprisingly, however, we can solve for temperature  $T$  without these details, under some not-too-restrictive assumptions about the equation of state. Specifically, we adopt a *polytropic law* of adiabatic expansion,

$$P = K\rho^\gamma = K\rho^{1/n+1} \tag{10.42}$$

where  $K$  is a constant,  $\gamma$  is the ratio of specific heats,<sup>4</sup> and in this context  $n$  is the adopted *polytropic index*.

---

<sup>4</sup>This relation need not necessarily be taken to be an equation of state – it simply expresses an assumption regarding the evolution of pressure with radius, in terms of the evolution of density with radius. The Lane-Emden equation has applicability outside stellar structures.

Introducing eqtn. (10.42) into (10.41) gives

$$\frac{K}{r^2} \frac{d}{dr} \left( \frac{r^2}{\rho} \frac{d\rho^\gamma}{dr} \right) = -4\pi G\rho. \quad (10.43)$$

We now apply the so-called Emden transformation,

$$\begin{aligned} \xi &= \frac{r}{\alpha}, \\ \theta &= \frac{T}{T_c} \end{aligned} \quad (10.44)$$

(where  $\alpha$  is a constant and  $T_c$  is the core temperature), to eqtn. (10.42), giving

$$\begin{aligned} \frac{\rho}{\rho_c} &= \left( \frac{P}{P_c} \right)^{1/\gamma} = \left( \frac{\rho T}{\rho_c T_c} \right)^{1/\gamma}; \text{ i.e.,} \\ \left( \frac{\rho}{\rho_c} \right)^{1-1/\gamma} &= \left( \frac{T}{T_c} \right)^{1/\gamma} = \theta^{1/\gamma}, \text{ or} \\ \rho &= \rho_c \theta^{1/\gamma-1} \end{aligned}$$

(where we have also used  $P = nkT, \propto \rho T$ ), whence eqtn. (10.43) becomes

$$\frac{K}{(\alpha\xi)^2} \frac{d}{d(\alpha\xi)} \left[ \frac{(\alpha\xi)^2}{\rho_c \theta^n} \frac{d \left( \{\rho_c \theta^n\}^{(n+1)/n} \right)}{d(\alpha\xi)} \right] = -4\pi G\rho_c \theta^n.$$

Since

$$\frac{d}{d\xi} (\theta^{n+1}) = (n+1)\theta^n \frac{d\theta}{d\xi}$$

we have

$$\frac{(n+1)K\rho_c^{1/n-1}}{4\pi G\alpha^2} \frac{1}{\xi^2} \frac{d}{d\xi} \left( \xi^2 \frac{d\theta}{d\xi} \right) = -\theta^n.$$

Finally, letting the constant  $\alpha$  (which is freely selectable, provided its dimensionality – length – is preserved) be

$$\alpha \equiv \left[ \frac{(n+1)K\rho_c^{1/n-1}}{4\pi G} \right]^{1/2},$$

we obtain the Lane-Emden equation, relating (scaled) radius to (scaled) temperature:

$$\frac{1}{\xi^2} \frac{d}{d\xi} \left( \xi^2 \frac{d\theta}{d\xi} \right) = -\theta^n,$$

or, equivalently,

$$\frac{1}{\xi^2} \left( 2\xi \frac{d\theta}{d\xi} + \xi^2 \frac{d^2\theta}{d\xi^2} \right) + \theta^n = \frac{d^2\theta}{d\xi^2} + \frac{2}{\xi} \frac{d\theta}{d\xi} + \theta^n = 0.$$

We can solve this equation with the boundary conditions

$$\begin{aligned}\theta &= 1, \\ \frac{d\theta}{d\xi} &= 0\end{aligned}$$

at  $\xi = 0$  (recalling that  $\xi$  and  $\theta$  are linear functions of  $r$  and  $T$ ).

Numerical solutions are fairly straightforward to compute; analytical solutions are possible for polytropic indexes  $n = 0, 1$  and  $5$  (i.e., ratios of specific heats  $\gamma = \infty, 2$ , and  $1.2$ ); these are, respectively,

$$\begin{aligned}\theta(\xi) &= 1 - \xi^2/6 & \zeta &= \sqrt{6}, \\ &= \sin \xi/\xi & &= \pi, \text{ and} \\ &= (1 + \xi^2/3)^{-1/2} & &= \infty\end{aligned}$$

A polytrope with index  $n = 0$  has a uniform density, while a polytrope with index  $n = 5$  has an infinite radius. A polytrope with index  $n = \infty$  corresponds to a so-called ‘isothermal sphere’, a self-gravitating, isothermal gas sphere, used to analyse collisionless systems of stars (in particular, globular clusters). In general, the larger the polytropic index, the more centrally condensed the density distribution.

We’ve done a lot of algebra; what about the physical interpretation of all this?

What about stars? Neutron stars are well modeled by polytropes with index about in the range  $n = 0.5$ – $1$ .

A polytrope with index  $n = 3/2$  provides a reasonable model for degenerate stellar cores (like those of red giants), white dwarfs, brown dwarfs, gas giants, and even rocky planets.

Main-sequence stars like our Sun are usually modelled by a polytrope with index  $n = 3$ , corresponding to the *Eddington standard model* of stellar structure.

# Section 11

## LTE

Basic treatments of stellar atmospheres adopt, as a starting point, the assumptions of Local Thermodynamic Equilibrium (LTE), and hydrostatic equilibrium. The former deals with the microscopic properties of the atoms, and we will discuss it here; the latter addresses the large-scale conditions (and applies throughout a normal star), and is discussed in Section 10.1.

### 11.1 Local Thermodynamic Equilibrium

Fairly obviously, in Local Thermodynamic Equilibrium (LTE) it is assumed that all thermodynamic properties in a small volume have the thermodynamic equilibrium values at the *local* values of temperature and pressure.

Specifically, this applies to quantities such as the occupation numbers of atoms, the opacity, emissivity, etc. The LTE assumption is equivalent to stating that

1. the electron and ion velocity distributions are Maxwellian,

$$\frac{dn(v)}{dv} = n \left( \frac{m}{2\pi k T_k} \right)^{3/2} \exp \left\{ \frac{-mv^2}{2k T_k} \right\}$$

for number density  $n$  of particles of mass  $m$  at kinetic temperature  $T_k$ ;

2. the photon source function is given by the Planck function at the local temperature (i.e.,  $S_\nu = B_\nu$ , and  $j_\nu = k_\nu B_\nu$ ).
3. the excitation equilibrium is given by the Boltzmann equation

$$\frac{n_j}{n_i} = \frac{g_j}{g_i} \exp \left\{ \frac{-(E_j - E_i)}{kT} \right\} \tag{11.1}$$

4. the ionization equilibrium is given by the Saha equation

$$\frac{n_e n_{2,1}}{n_{1,i}} = \frac{2g_{2,1}}{g_{1,i}} \exp\left\{\frac{-\chi_{1,i}}{kT}\right\} \frac{(2\pi m_e kT)^{3/2}}{h^3} \quad (11.2)$$

where  $1, i, 2, 1$  denote levels  $i, 1$  in ionization stages 1, 2.

One might augment this list with the perfect-gas equation of state,  $P = nkT$ , but since this applies under many circumstances where LTE doesn't hold, it's not usually mentioned in this context.

If a process is purely collisional, conditions are, naturally, determined on a purely local basis locally, and LTE applies. We have already encountered one such situation where LTE is a good approximation: free-free emission results from a purely collisional process, justifying our adoption of  $S_\nu = B_\nu$  (Section 6).

If radiation plays a role, then provided the photon and particle mean free paths are short compared to the length scales over which conditions change significantly (i.e., if the opacity is high), then we can again expect LTE to be a reasonable assumption; this is a good approximation in stellar interiors.

In stellar atmospheres the LTE approximation may be a poor one, as photon mean free paths are typically larger than those of particles. Thus one region can be affected by the radiation field in another part of the atmosphere (e.g., a deeper, hotter region). As a rule of thumb, therefore, LTE is a poor approximation if the radiation field is important in establishing the ionization and excitation equilibria (as in hot stars, for example). It's more likely to be acceptable when particle densities are high and the radiation field is relatively weak; for stars, this means higher gravities (i.e., main-sequence stars rather than supergiants) and cooler effective temperatures. When LTE breaks down, we have a 'non-LTE' (nLTE) situation, and level populations must be calculated assuming statistical equilibrium (section 2.3.2).

## 11.2 The Saha Equation

The Boltzmann Equation gives the relative populations of two bound levels  $i$  and  $j$ , in some initial (or 'parent') ionization stage '1':

$$\frac{n_{1,j}}{n_{1,i}} = \frac{g_{1,j}}{g_{1,i}} \exp\left\{\frac{-(E_{1,j} - E_{1,i})}{kT}\right\} \quad (11.1)$$

where  $E_{1,i}$  &  $E_{1,j}$  are the level energies (measured from the ground state,  $E_{1,1} = 0$ ), and  $g_{1,i}$  &  $g_{1,j}$  are their statistical weights ( $2J + 1$ , where  $J$  is the total angular-momentum quantum number).

To generalize the Boltzmann eqtn. to deal with collisional ionization to the next higher (or ‘daughter’) ionization stage ‘2’, we identify the upper level  $j$  with a *continuum* state;  $n_{1,j}$ , the number of parent ions in excitation state  $j$ , then equates with  $n_{2,1}(v)$ , the number of ionized atoms where the *detached* electron has velocity  $v$ .

(Note that ionization stages ‘1’ and ‘2’ always represent any two *consecutive* stages – for example,  $H^0$  and  $H^+$ , or  $C^{2+}$  and  $C^{3+}$ .)

The total statistical weight of the ionized system is given by the combined statistical weights<sup>1</sup> of the newly created ion *and* the electron, i.e.,  $g_2 g_e(v)$ ; while the relevant energy is the sum of the ionization energy and the kinetic energy of the free electron. Thus we have

$$\frac{n_{2,1}(v)}{n_{1,i}} = \frac{g_2 g_e(v)}{g_{1,i}} \exp \left\{ \frac{-(\chi_{1,i} + \frac{1}{2} m_e v^2)}{kT} \right\} \quad (11.3)$$

where  $\chi_{1,i} = E_\infty - E_{1,i}$  is the ionization potential for level  $i$  in the parent species.

**An aside: The statistical weight of a free electron.** The statistical weight of a free electron is just the probability of finding it in a specific cell of ‘phase space’. Since the state of a free particle is specified by three spatial coördinates  $x, y, z$  and three momentum coördinates  $p(x), p(y), p(z)$ , the number of quantum states (for which the statistical weights are each 1) in an element of phase space,

$$dx dy dz \cdot dp(x) dp(y) dp(z) = dN$$

is given by

$$g_e(v) = \frac{2 dN}{h^3} = \frac{2}{h^3} dx dy dz \cdot dp(x) dp(y) dp(z)$$

where  $h$  is Planck’s constant and the factor 2 arises because the electron has two possible spin states. The statistical weight *per unit volume* is thus

$$\frac{2}{h^3} dp(x) dp(y) dp(z)$$

for a *single* electron. However, there may be other free electrons, from other ions, which occupy some of the available states in the element of phase space  $dN$ . If the number density of electrons is  $n_e$  then the effective volume available to a collisionally ejected electron is reduced by a factor  $1/n_e$ . Thus the statistical weight available to a single free electron is

$$g_e(v) = \frac{2 dp(x) dp(y) dp(z)}{n_e h^3}.$$

Furthermore, if the velocity field is isotropic, the ‘momentum volume’ can be replaced simply by its counterpart in spherical coördinates,

$$dp(x) dp(y) dp(z) = 4\pi p^2 dp$$

Using these results we can write eqtn. (11.3) as

$$\frac{n_e n_{2,1}(v)}{n_{1,i}} = \frac{2g_i}{h^3 g_{1,i}} \exp \left\{ \frac{-(\chi_{1,i} + \frac{1}{2} m_e v^2)}{kT} \right\} 4\pi p^2 dp$$

---

<sup>1</sup>The statistical weight is a form of probability, and the probability of ‘A and B’,  $P(A+B)$ , is the product  $P(A)P(B)$ .

but the momentum  $p = m_e v$ ; i.e.,  $\frac{1}{2} m_e v^2 = p^2 / (2m_e)$ , whence

$$\frac{n_e n_{2,1}(v)}{n_{1,i}} = \frac{2g_2}{h^3 g_{1,i}} \exp\left\{\frac{-\chi_{1,i}}{kT}\right\} \exp\left\{\frac{-p^2}{2m_e kT}\right\} 4\pi p^2 dp.$$

Since we're interested in the ionization balance (not the velocity distribution of the ionized electrons), we integrate over velocity to obtain the total number of daughter ions:

$$\frac{n_e n_{2,1}}{n_{1,i}} = \frac{2g_2}{h^3 g_{1,i}} \exp\left\{\frac{-\chi_{1,i}}{kT}\right\} 4\pi \int_0^\infty p^2 \exp\left\{\frac{-p^2}{2m_e kT}\right\} dp.$$

We can then use result of a standard integral,

$$\int_0^\infty x^2 \exp(-a^2 x^2) dx = \sqrt{\pi} / (4a^3)$$

to obtain

$$\frac{n_e n_{2,1}}{n_{1,i}} = \frac{2g_2}{g_{1,i}} \exp\left\{\frac{-\chi_{1,i}}{kT}\right\} \frac{(2\pi m_e kT)^{3/2}}{h^3} \quad (11.2)$$

This is one common form of the *Saha Equation* (often expressed in terms of the ground state of the parent ion,  $n_{1,1}$ ).

### 11.3 Partition functions

The version of the Saha equation given in eqtn. (11.2) relates populations in single states of excitation for each ion. Generally, we are more interested in the ratios of number densities of different ions summed over all states of excitation – i.e., the overall ionization balance. We determine this by defining the *partition function* as

$$U = \sum_n g_n \exp(-E_n/kT)$$

(an easily evaluated function of  $T$ ), whence

$$\frac{n_e n_2}{n_1} = \frac{2U_2}{U_1} \frac{(2\pi m_e kT)^{3/2}}{h^3} \exp\left\{\frac{-\chi_1}{kT}\right\} \quad (11.4)$$

where we use  $\chi_1$ , the ground-state ionization potential of the parent atom, as it is to this that the partition function is referred (i.e.,  $E_{1,1} \equiv 0$ ).

Since the electron pressure is  $P_e = n_e kT$  we can also express the Saha equation in the form

$$\frac{n_2}{n_1} = \frac{2U_2}{U_1} \frac{(2\pi m_e)^{3/2}}{h^3} \frac{(kT)^{5/2}}{P_e} \exp\left\{\frac{-\chi_1}{kT}\right\} \quad (11.5)$$

### 11.3.1 An illustration: hydrogen

The Balmer lines of hydrogen, widely observed as absorption lines in stellar spectra, arise through photoexcitation from the  $n = 2$  level of neutral hydrogen. To populate the  $n = 2$  level, we might suppose that we need temperatures such that  $kT \simeq E_{1,2} = 10.2\text{eV}$ ; i.e.,  $T \simeq 10^5\text{K}$ . However, the  $\text{H}\alpha$  line strength peaks in A0 stars, which are much cooler than this ( $T \sim 10^4\text{K}$ ). Why? Because we need to consider *ionization* as well as excitation. We therefore need to combine the Saha and Boltzmann equations to obtain the density of atoms in a given state of excitation, for a given state of ionization.

We express the Boltzmann equation, eqtn. (11.1), in terms of the partition function  $U$ :

$$\frac{n_{1,2}}{n_1} = \frac{g_{1,2}}{U_1} \exp\left(\frac{-E_{1,2}}{kT}\right)$$

where  $n_1$  is the number density of  $\text{H}^0$  atoms in *all* excitation states and  $E_{1,2}$  is the excitation energy of the  $n = 2$  level (10.2 eV); that is,

$$n_{1,2} = \frac{g_{1,2}}{U_1} \exp\left(\frac{-E_{1,2}}{kT}\right) n_1.$$

However, the *total* number of hydrogen nuclei is  $n(\text{H}) = n_1 + n_2 = n_1(1 + n_2/n_1)$ ; that is,  $n_1 = n(\text{H})(1 + n_2/n_1)^{-1}$ . Using this, and  $n_2/n_1$  from eqtn. (11.4), we find

$$\begin{aligned} n_{1,2} &= \frac{g_{1,2}}{U_1} \exp\left(\frac{-E_{1,2}}{kT}\right) \left(1 + \left[\frac{2U_2}{n_1U_1} \frac{(2\pi m_e kT)^{3/2}}{h^3} \exp\left\{\frac{-\chi_1}{kT}\right\}\right]\right)^{-1} n(\text{H}) \\ &= \frac{g_{1,2}}{U_1} \exp\left(\frac{-E_{1,2}}{kT}\right) \left(1 + \left[\frac{2U_2}{n_1U_1} \frac{(2\pi m_e)^{3/2}}{h^3} \frac{(kT)^{5/2}}{P_e} \exp\left\{\frac{-\chi_1}{kT}\right\}\right]\right)^{-1} n(\text{H}) \end{aligned}$$

We can now see why the Balmer lines peak around  $10^4\text{K}$ : while higher temperatures give larger populations  $n_{1,2}/n(\text{H}^0)$ , they give smaller populations  $n(\text{H}^0)/n(\text{H})$ . The overall result is that  $n_{1,2}/n(\text{H})$  peaks around  $10\text{kK}$ .

The Saha equation also gives an explanation of why supergiant stars are cooler than main-sequence stars of the same spectral type. Spectral characteristics are defined by ratios of lines strengths; e.g., O-star subtypes are defined by the ratio  $(\text{He II } \lambda 4542)/(\text{He I } \lambda 4471)$ , which in turn traces the ratio  $\text{He}^+/\text{He}^0$ . Of course, higher temperatures increase the latter ratio. However, a supergiant star has a lower surface gravity (and atmospheric pressure) than a main-sequence star. From eqtn. (11.5) we see that a lower pressure at the same temperature gives rise to a larger ratio  $n_2/n_1$ , so for two stars of the same temperature, the supergiant has an earlier spectral type (or, equivalently, at the same spectral type the supergiant is cooler).



## Section 12

# Stellar Timescales

### 12.1 Dynamical timescale

#### 12.1.1 ‘Hydrostatic equilibrium’ approach

If we look at the Sun in detail, we see that there is vigorous convection in the envelope. With gas moving around, is the assumption of hydrostatic equilibrium justified? To address this question, we need to know how quickly displacements are restored; if this happens quickly (compared to the displacement timescales), then hydrostatic equilibrium remains a reasonable approximation even under dynamical conditions.

We have written an appropriate equation of motion,

$$\rho a = \rho g + \frac{dP}{dr} \tag{10.2}$$

where  $g$  is the acceleration due to gravity and

$$a = \frac{d^2r}{dt^2}$$

is the nett acceleration. As the limiting case we can ‘take away’ gas-pressure support (i.e., set  $dP/dr = 0$ ), so our equation of motion for collapse under gravity is just

$$\frac{d^2r}{dt^2} = -\frac{Gm(r)}{r^2}.$$

Integrating (and taking  $r$  from the surface inwards),

$$r = \frac{Gm(r)}{r^2} \frac{t^2}{2} = \frac{1}{2}gt^2 \quad (\text{for initial velocity } v_0 = 0). \tag{12.1}$$

Identifying the time  $t$  in eqn. (12.1) with a *dynamical timescale*, we have

$$t_{\text{dyn}} = \sqrt{\frac{2r^3}{Gm(r)}}. \quad (12.2)$$

Departures from hydrostatic equilibrium are restored on this timescale (by gravity in the case of expansion, or pressure in the case of contraction). In the case of the Sun,

$$t_{\text{dyn}} = \sqrt{\frac{2R_{\odot}^3}{GM_{\odot}}} \simeq 37 \text{ min.}$$

If you removed gas-pressure support from the Sun, this is how long it would take a particle at the surface to free-fall to the centre. Since the geological record shows that the Sun hasn't changed substantially for at least  $10^9$  yr, it is clear that any departures from hydrostatic equilibrium must be extremely small on a global scale.

We might expect departures from spherical symmetry to be restored on a dynamical timescale (in the absence of significant centrifugal forces), and by indeed comparing eqtns. (10.6) and (12.2) we see that spherical symmetry is appropriate if

$$\omega \ll \frac{\sqrt{2}}{t_{\text{dyn}}}$$

### 12.1.2 'Virial' approach

The 'hydrostatic equilibrium' approach establishes a collapse timescale for a particle to fall from the surface to the centre. As an alternative, we can consider a timescale for gas pressure to fill a void – a pressure-support timescale. Noting that a pressure wave propagates at the sound speed, this dynamical timescale can be equated to a sound-crossing time for transmitting a signal from the centre to the surface.

The sound speed is given by

$$c_{\text{S}}^2 = \gamma \left( \frac{kT}{\mu m(\text{H})} \right) \quad (12.3)$$

(where  $\gamma = C_p/C_v$ , the ratio of specific heats at constant pressure and constant volume).

From the virial theorem,

$$2U + \Omega = 0 \quad (10.11)$$

with

$$U = \int_V \frac{3}{2} kT n(r) dV = \int_V \frac{3}{2} kT \frac{\rho(r)}{\mu m(\text{H})} dV \quad (10.8)$$

and

$$\Omega = - \int_0^M \frac{Gm(r)}{r} dm = - \int_V \frac{Gm(r)}{r} \rho(r) dV \quad (10.10)$$

so that

$$\frac{3kT}{\mu m(\text{H})} = \frac{Gm(r)}{r}; \quad (12.4)$$

that is, from eqtn. (12.3),

$$\frac{3}{\gamma} c_S^2 = \frac{Gm(r)}{r} \quad (12.5)$$

For a monatomic gas we have  $\gamma = 5/3$ , giving, from eqtns. (12.3) and (12.4),

$$c_S^2 = \frac{5}{9} \frac{Gm(r)}{r}$$

so that the (centre-to-surface) sound crossing time is

$$t = \frac{r}{c_S} = \sqrt{\frac{9/5 r^3}{Gm(r)}} \quad (12.6)$$

(which is within  $\sim 10\%$  of eqtn. (12.2)).

## 12.2 Kelvin-Helmholtz and Thermal Timescales

Before nuclear fusion was understood, the conversion of potential to radiant energy, through gravitational contraction, was considered as a possible source of the Sun's luminosity.<sup>1</sup> The time over which the Sun's luminosity can be powered by this mechanism is the *Kelvin-Helmholtz* timescale.

The available gravitational potential energy is

$$\Omega = \int_0^M \frac{-Gm(r)}{r} dm \quad (10.10)$$

but

$$m(r) = \frac{4}{3} \pi r^3 \bar{\rho} \quad \text{so} \quad dm = 4\pi r^2 \bar{\rho} dr$$

---

<sup>1</sup>Recall from Section 10.4 that half the gravitational potential energy lost in contraction is radiated away, with the remainder going into heating the star.

and

$$\begin{aligned}\Omega &= \int_0^R -G \frac{16\pi^2}{3} r^4 \bar{\rho}^2(r) dr \\ &\simeq -\frac{16}{15} \pi^2 G \bar{\rho}^2 R^5\end{aligned}\tag{12.7}$$

(assuming  $\bar{\rho}(r) = \bar{\rho}(R)$ ).

The Kelvin-Helmholtz timescale for the Sun is therefore

$$t_{\text{KH}} = \frac{|\Omega(\odot)|}{L_{\odot}}.\tag{12.8}$$

which for  $\bar{\rho} = 1.4 \times 10^3 \text{ kg m}^{-3}$ ,  $\Omega = 2.2 \times 10^{41} \text{ J}$  is  $t_{\text{KH}} \simeq 10^7 \text{ yr}$ .<sup>2</sup>

The Kelvin-Helmholtz timescale is often identified with the *thermal timescale*, but the latter is more properly defined as

$$t_{\text{th}} = \frac{U(\odot)}{L_{\odot}},\tag{12.9}$$

which (from the virial theorem) is  $\sim 1/2 t_{\text{KH}}$ . In practice, the factor 2 difference is of little importance for these order-of-magnitude timescales.

## 12.3 Nuclear timescale

We now know that the source of the Sun's energy is nuclear fusion, and we can calculate a corresponding nuclear timescale,

$$t_{\text{N}} = \frac{f M c^2}{L}\tag{12.10}$$

where  $f$  is just the fraction of the rest mass available to the relevant nuclear process. In the case of hydrogen burning this fractional 'mass defect' is 0.007, so we might expect

$$t_{\text{N}} = \frac{0.007 M_{\odot} c^2}{L_{\odot}} (\simeq 10^{11} \text{ yr for the Sun}).$$

However, in practice, only the core of the Sun – about  $\sim 10\%$  of its mass – takes part in hydrogen burning, so its nuclear timescale for hydrogen burning is  $\sim 10^{10} \text{ yr}$ . Other evolutionary stages have their respective (shorter) timescales.

---

<sup>2</sup>At the time that this estimate was made, the fossil record already indicated a much older Earth ( $\sim 10^9 \text{ yr}$ ). Kelvin noted this discrepancy, but instead of rejecting contraction as the source of the Sun's energy, he instead chose to reject the fossil record as an indicator of age.

## 12.4 Diffusion timescale for radiative transport

Deep inside stars the radiation field is very close to black body. For a black-body distribution the average photon energy is

$$\bar{E} = U/n \simeq 4 \times 10^{-23} T \quad [\text{J photon}^{-1}]. \quad (1.28)$$

The core temperature of the Sun is  $T_c \simeq 1^{1/2} \times 10^7$  K (cf. eqtn. 10.17), whence  $\bar{E} = 3.5$  keV – i.e., photon energies are in the X-ray regime.

Light escaping the surface of the Sun ( $T_{\text{eff}} \simeq 5770\text{K}$ ) has a mean photon energy  $\sim 3 \times 10^3$  smaller, in the optical.

The source of this degradation in the mean energy is the coupling between radiation and matter. Photons obviously don't flow directly out from the core, but rather they *diffuse* through the star, travelling a distance of order the local mean free path,  $\ell$ , before being absorbed and re-emitted in some other direction (a 'random walk'). The mean free path depends on the opacity of the gas:

$$\ell = 1/k_\nu = 1/(\kappa_\nu \rho) \quad (2.4)$$

where  $k_\nu$  is the volume opacity (units of area per unit volume, or  $\text{m}^{-1}$ ) and  $\kappa_\nu$  is the mass opacity (units of  $\text{m}^2 \text{kg}^{-1}$ ).

After  $n_{\text{sc}}$  scatterings the *radial* distance travelled is, on average,  $\sqrt{n_{\text{sc}}}\ell$  (it's a statistical, random-walk process). Thus to travel a distance  $R_\odot$  we require

$$n_{\text{sc}} = \left( \frac{R_\odot}{\ell} \right)^2. \quad (12.11)$$

Solar-structure models give an average mean free path  $\ell \simeq 1$  mm (incidentally, justifying the LTE approximation in stellar interiors); with  $R_\odot \simeq 7 \times 10^8$  m,

$$n_{\text{sc}} \simeq 5 \times 10^{23}$$

The total distance travelled by a (fictitious!) photon travelling from the centre to the surface is  $n_{\text{sc}} \times \ell \simeq 5 \times 10^{20}$  m ( $\sim 10^{12} R_\odot!$ ), and the time to diffuse to the surface is  $(n_{\text{sc}} \times \ell)/c \simeq 5 \times 10^4$  yr.

[More detailed calculations give  $17 \times 10^4$  yr; why? Naturally, there are regions within the Sun that have greater or lesser opacity than the average value, with the largest opacities in the central  $\sim 0.4 R_\odot$  and in the region immediately below the photosphere. Because of the 'square root' nature of the diffusion, a region with twice the opacity takes four times longer to pass through, while a region with half the opacity takes only 1.414 times shorter; so any non-uniformity in the opacity inevitably leads to a longer total diffusion time.]

## PART V: STARS – II



## Section 13

# Nuclear reactions in stars

### 13.1 Introduction

In general, nuclear processes in stars involve fission of a nucleus, or (more usually in ‘normal’ evolutionary phases), the fusion of two nuclei. Through all these processes, key physical quantities are conserved:

- the baryon number (the number of protons, neutrons, and their antiparticles);
- the lepton number (electrons, neutrinos, related light particles, and their antiparticles);
- charge; and
- total mass–energy.

Consider two types of nuclei,  $A$  and  $B$ , number densities  $n(A)$ ,  $n(B)$ . The rate at which a particular (nuclear) reaction occurs between particles moving with relative velocity  $v$  is

$$r(v) = n(A) n(B) v \sigma(v) \tag{13.1}$$

(per unit volume per unit time) where  $\sigma(v)$  is the cross-section for the reaction. Of course, we need to integrate over velocity to get the total reaction rate:

$$\begin{aligned} r &= n(A) n(B) \int v \sigma(v) f(v) dv \\ &\equiv n(A) n(B) \langle \sigma(v) v \rangle \quad [ \text{m}^{-3} \text{s}^{-1} ] \end{aligned} \tag{13.2}$$

where  $f(v)$  is the (Maxwellian) velocity distribution, and the angle brackets denote a weighted average (i.e., the integral in the first part of eqtn. 13.2).

Since the reaction destroys  $A$  (and  $B$ ), we have

$$\frac{\partial n(A)}{\partial t} = -n(A) n(B) \langle \sigma(v) v \rangle; \quad (13.3)$$

and the number density of species  $A$  falls with time as

$$n(A, t) = n_0(A) \exp \{-n(B) \langle \sigma(v) v \rangle t\} \quad (13.4)$$

which defines a characteristic ( $e$ -folding) timescale

$$\tau = \frac{1}{n(B) \langle \sigma(v) v \rangle}. \quad (13.5)$$

Finally, the total energy generated through this reaction, per unit mass per unit time, is

$$\begin{aligned} \varepsilon &= \frac{Q r}{\rho} \\ &= \frac{n(A) n(B)}{\rho} Q \langle \sigma(v) v \rangle \quad [\text{J kg}^{-1} \text{ s}^{-1}] \end{aligned} \quad (13.6)$$

where  $Q$  is the energy produced per reaction and  $\rho$  is the mass density.

## 13.2 Tunnelling

Charged nuclei experience Coulomb repulsion at intermediate separations, and nuclear attraction at small separations. In stellar cores the high temperatures give rise to high velocities, and increased probability of overcoming the Coulomb barrier. For nuclear charge  $Z$  (the atomic number), the energy needed to overcome the Coulomb barrier is

$$E_C \simeq \frac{Z_1 Z_2 e^2}{r_0} \quad (13.7)$$

$$(\simeq 2 \times 10^{-13} \text{ J}, \quad \simeq 1 \text{ MeV, for } Z_1 = Z_2 = 1) \quad (13.8)$$

where  $r_0 \simeq 10^{-15} \text{ m}$  is the radius at which nuclear attraction overcomes Coulomb repulsion for proton pairs.

In the solar core,  $T_c \sim 1.5 \times 10^7 \text{ K}$ ; that is,  $E (= 3/2 kT) \simeq \text{keV}$ , or  $\sim 10^{-3} E_C$ . This energy is only sufficient to bring protons to within  $\sim 10^3 r_0$  of each other; this is much too small to be effective, so reactions only occur through a process of “quantum tunneling” (barrier penetration). In this temperature regime the rate of nuclear energy generation is well approximated by a power-law dependence on temperature,

$$\varepsilon \simeq \varepsilon_0 \rho T^\alpha \quad (13.9)$$

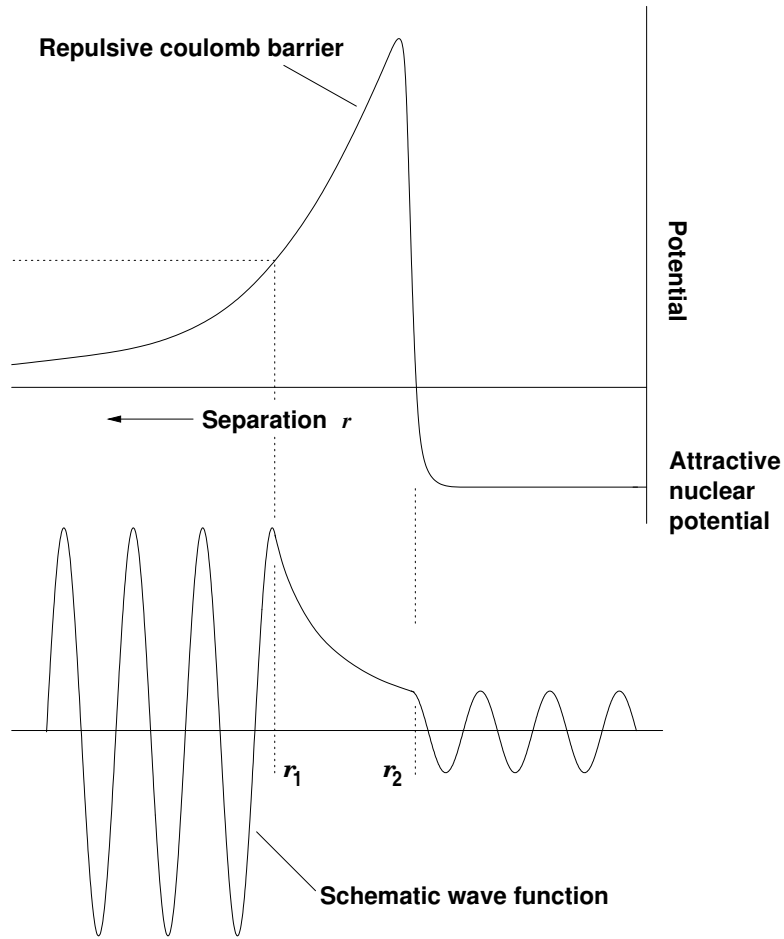


Figure 13.1: Upper section: a schematic plot of the potential between two charged nucleons as a function of separation. At ‘large’ separations ( $\gtrsim 10^{-15}$  m), the repulsive Coulomb force is given by eqtn. (13.8); classically, particles cannot come closer than the point  $r_1$  at which the relative kinetic energy corresponds to the repulsive potential. Quantum-mechanical tunneling allows the nucleons to approach closer, to separation  $r_2$ , at which point the strong nuclear force dominates.

The lower panel expresses this tunnelling schematically. The (square of the) amplitude of the wave function is a measure of the probability of a particle being in a particular location; the amplitude of the wave function decreases exponentially between  $r_1$  and  $r_2$ , but does not fall to zero. (See Aside 13.1 for further details.)

where  $\alpha \simeq 4.5$  for proton-proton reactions in the Sun [Section 13.4;  $\varepsilon_0 \propto n^2(\text{H})$ ], and  $\alpha \simeq 18$  for CN processing [Section 13.5;  $\varepsilon_0 \propto n(\text{H})n(\text{C, N})$ ].

[Note that eqtn. (13.9) characterizes the rate of energy generation per unit *mass* (or, if you like, per nucleon). Although density appears here as a simple linear multiplier, reference to eqtn. 13.6 reminds us that, like nearly all ‘collisional’ processes, the energy generation rate per unit *volume* – or the probability of a given nucleus undergoing fusion – depends on density *squared*.]

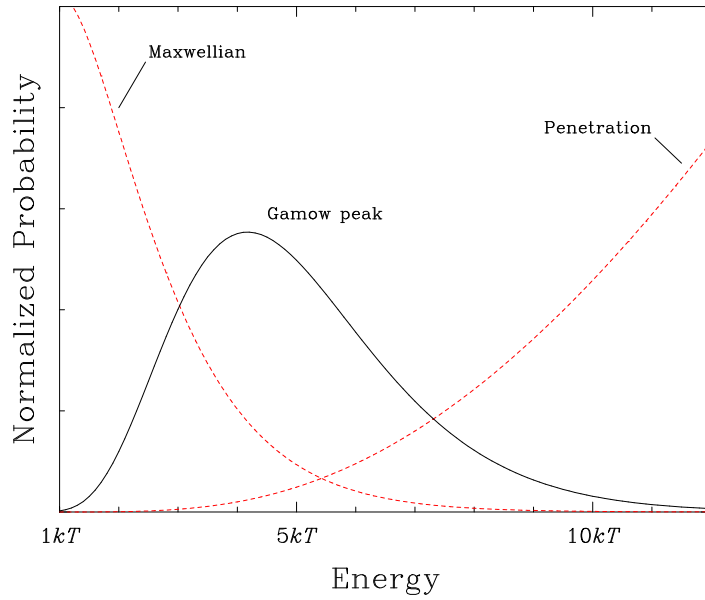


Figure 13.2: The main energy-dependent factors determining two-body reaction rates are the numbers of reagents as a function of energy (the Maxwellian velocity distribution) and the tunnelling probability of penetration. The product of these two terms gives the energy distribution of particles participating in fusion. These factors are illustrated here, on arbitrary vertical scales, for the fusion of two protons in the solar core (Gamow energy  $E_G = 290kT$  for  $T = 2 \times 10^7$  K;  $E_0 = 4.2kT$ ,  $1/e$  width  $\Delta = 4.8kT$ ). See Aside 13.1.

### Aside 13.1: The Gamow Peak

As illustrated in Fig. 13.1, ‘tunnelling’ can occur to allow fusion to occur at particle energies which classical mechanics would indicate to be too low to overcome the Coulomb barrier. For higher temperatures (and larger kinetic energies), particles will come closer together ( $r_1$  approaches  $r_2$ ), the decay of the wave function is reduced, and so the amplitude of the wave function in the region  $r < r_2$  becomes larger – that is, the tunnelling probability increases as the kinetic energy of the incoming nucleus increases.

Obtaining the probability of barrier penetration,  $p_p$ , for given energy, is a standard problem in wave mechanics. We simply quote the result that the probability of penetration varies exponentially with the ratio of kinetic energy to barrier size,

$$p_p \propto \exp \left\{ - \left( \frac{E_G}{E} \right)^{1/2} \right\} \quad (\text{A-13.1})$$

with the ‘Gamow energy’  $E_G$  (unnamed and written as  $b^2$  in some sources) given by

$$E_G = 2m_R c^2 (\pi\alpha Z_1 Z_2)^2 \quad (= 493 \text{ keV for proton-proton fusion}), \quad (\text{A-13.2})$$

where  $\alpha$  is the fine structure constant,

$$\alpha = \frac{e^2}{4\pi\epsilon_0\hbar c} \simeq \frac{1}{137}. \quad (\text{A-13.3})$$

and  $m_R$  is the ‘reduced mass’,

$$m_R = \frac{m_1 m_2}{m_1 + m_2}$$

for particles of mass  $m_1, m_2$  ( $\simeq A_1 m(\text{H}), A_2 m(\text{H})$ ) of charge  $Z_1, Z_2$ . (Using the reduced mass means that velocities and kinetic energies are measured with reference to the centre of mass of the particles involved.)

The fusion cross-section  $\sigma(v)$  (eqtn 13.1) is evidently dependent on this penetration probability. We also expect it to depend on the effective size, or ‘target area’, of the particles; this geometrical factor is proportional to  $\pi\lambda^2$ , where  $\lambda$  is the de Broglie wavelength,  $\lambda^2 \propto 1/E$ . The intrinsic properties of the nuclei must also be involved; these will be constant, or slowly varying functions of energy, in most circumstances (although resonances may occur). We therefore write the total reaction cross-section in the form

$$\sigma(E) = \frac{S(E)}{E} \exp \left\{ - \left( \frac{E_G}{E} \right)^{1/2} \right\} \quad (\text{A-13.4})$$

where  $S(E)$  encapsulates the nuclear physics of the actual fusion process.

At any given temperature, the number of particles in a Maxwellian velocity distribution falls off exponentially with increasing energy (eqtn. 8.15); that is, the probability of encountering a particle with energy  $E$  at kinetic temperature  $T$  is

$$f(E) dE = \frac{2}{\sqrt{\pi}} \frac{E}{kT} \exp \left\{ - \frac{E}{kT} \right\} \frac{dE}{(kTE)^{1/2}} \quad (\text{A-13.5})$$

These two competing factors – the increasing probability of penetration with increasing energy (eqtn. A-13.1) and the decreasing number of particles with increasing energy (eqtn. A-13.5) – mean that there is a limited range of energies at which most reactions occur. This is illustrated in Fig. 13.2; the product of the two exponential terms leads to the ‘Gamow peak’, where the probability of fusion occurring is at a maximum.<sup>1</sup>

To explore this in greater detail, we write the reaction rate per particle pair, eqtn. 13.2, as

$$\langle \sigma(v) v \rangle = \int_0^\infty \sigma(E) v f(E) dE$$

where  $\sigma(E), v$  are particle cross-sections and velocities at energy  $E$ ; from eqtns. (A-13.4) and (A-13.5), and using  $E = \frac{1}{2} m_R v^2$ ,

$$\langle \sigma(v) v \rangle = \int_0^\infty \frac{S(E)}{E} \exp \left\{ - \left( \frac{E_G}{E} \right)^{1/2} \right\} \sqrt{\frac{2E}{m_R}} \frac{2}{\sqrt{\pi}} \frac{E}{kT} \exp \left\{ - \frac{E}{kT} \right\} \frac{dE}{(kTE)^{1/2}} \quad (\text{A-13.6})$$

$$= \left( \frac{8}{\pi m_R} \right)^{1/2} \frac{1}{(kT)^{3/2}} \int_0^\infty S(E) \exp \left\{ - \frac{E}{kT} - \left( \frac{E_G}{E} \right)^{1/2} \right\} dE \quad (\text{A-13.7})$$

at some fixed temperature  $T$ . Eqtn. (A-13.7) is the integral over the Gamow peak; the larger the area, the greater the reaction rate.

The Gamow peak is appropriately named in that it is indeed quite strongly peaked; it is therefore a reasonable approximation to take the  $S(E)$  term as locally constant. In that case, the integrand peaks at energy  $E_0$ , when

$$\frac{d}{dE} \left\{ \frac{E}{kT} + \left( \frac{E_G}{E} \right)^{1/2} \right\} = \frac{1}{kT} - \frac{1}{2} \left( \frac{E_G}{E_0^3} \right)^{1/2} = 0;$$

i.e.,

$$E_0 = \left( \frac{kT\sqrt{E_G}}{2} \right)^{2/3} \quad (\text{A-13.8})$$

$$= \left[ \sqrt{2} (\pi \alpha k c)^2 m_R (Z_1 Z_2 T)^2 \right]^{1/3}$$

---

<sup>1</sup>Clearly, the area under the Gamow peak determines the total reaction rate.

$E_0$ , the location of the Gamow peak, is the most effective energy for thermonuclear reactions; it greatly exceeds  $kT$ , the typical thermal energy, but falls well below the Gamow energy of the Coulomb barrier.

There is no simple analytical solution for the width of the peak, but one common (and reasonable) approach is to approximate the exponential term in the integral (eqn. A-13.7) with a gaussian centred on  $E_0$ . Conventionally, in this context 'the' width is not characterized by the gaussian ' $\sigma$ ' parameter, but rather by  $\Delta$ , the full width at  $1/e$  of the peak value (so  $\Delta \equiv 2\sqrt{2}\sigma$ ); thus we need to solve for

$$\exp\left\{-\frac{E}{kT} - \left(\frac{E_G}{E}\right)^{1/2}\right\} \simeq C \exp\left\{-\left(\frac{E - E_0}{\Delta/2}\right)^2\right\}. \quad (\text{A-13.9})$$

Requiring the two sides to be equal at  $E = E_0$  we immediately find

$$\begin{aligned} C &= \exp\left\{-\frac{E_0}{kT} - \left(\frac{E_G}{E_0}\right)\right\}, \\ &= \exp\left\{-\frac{3E_0}{kT}\right\} \end{aligned} \quad (\text{from eqn. A-13.8})$$

while requiring the curvatures (second derivatives) on either side of eqn. A-13.9 to be equal gives, after some algebra,

$$\Delta = \sqrt{\frac{16}{3}E_0kT}.$$

The total reaction rate depends on the integrated area under the Gamow peak; again using a gaussian approximation to the peak, and constant  $S(E)$  across the peak, then from eqn. (A-13.7), we have

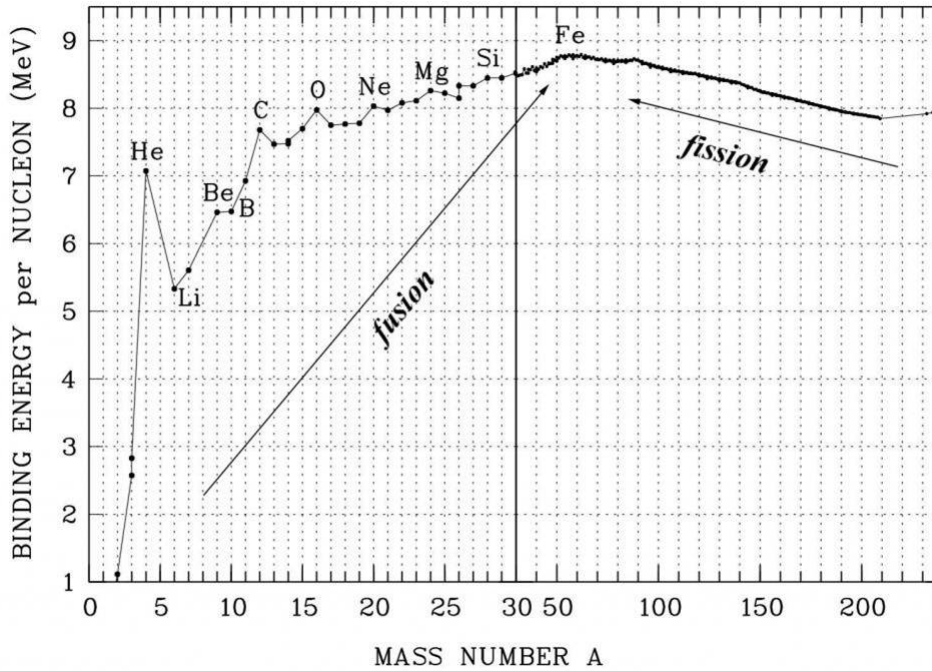
$$\begin{aligned} \langle \sigma(v) v \rangle &= \left(\frac{8}{\pi m_R}\right)^{1/2} \frac{S(E_0)}{(kT)^{3/2}} \exp\left\{-\frac{3E_0}{kT}\right\} \int_0^\infty \exp\left\{-\left(\frac{E - E_0}{\Delta/2}\right)^2\right\} dE, \\ &\simeq \left(\frac{8}{\pi m_R}\right)^{1/2} \frac{S(E_0)}{(kT)^{3/2}} \exp\left\{-\frac{3E_0}{kT}\right\} \frac{\Delta\sqrt{\pi}}{2} \end{aligned} \quad (\text{A-13.10})$$

(where, in order to perform the integration analytically, the limits have been extended from  $0/+ \infty$  to  $-\infty/+ \infty$ ; the error thus introduced is negligible provided that  $E_0 > \Delta/2$ ). Bowers & Deeming give a mathematical development from this point which leads to a demonstration that  $\varepsilon \simeq \varepsilon_0 \rho T^\alpha$  (eqn. 13.9).

Furthermore, substituting eqn. (A-13.8) into eqn. (A-13.7) we obtain

$$\langle \sigma v \rangle \propto \exp[-(E_G/kT)^{1/3}].$$

### 13.3 The mass defect and nuclear binding energy



The mass of any nucleus is less than the sum of the separate masses of its protons and neutrons. The *binding energy* of a particular isotope is the energy corresponding to the ‘missing’ mass (or *mass defect*), and is the energy produced in forming that isotope from its raw ingredients; equivalently, it is the amount of energy needed to break it up into protons and neutrons.<sup>2</sup> The binding energy peaks in the iron group, with <sup>62</sup>Ni the most tightly-bound nucleus, followed by <sup>58</sup>Fe and <sup>56</sup>Fe;<sup>3</sup> this is the basic reason why iron and nickel are very common metals in planetary cores, since they are produced as end products in supernovae.

For atomic masses  $A \gtrsim 60$ , energy release is through *fission* (generally involving much less energy).

For a nucleus with  $Z$  protons,  $N (= A - Z)$  neutrons, and mass  $m(Z, N)$  the binding energy is therefore

$$Q(Z, N) = [Zm_p + Nm_n - m(Z, N)] c^2 \quad (13.10)$$

<sup>2</sup>The binding energy explains why the masses of the proton and neutron are both larger than the ‘atomic mass unit’, or amu; the amu is defined to be  $1/12$  the mass of <sup>12</sup>C, but each nucleon in that isotope has given up almost 1% of its mass in binding energy.

<sup>3</sup>Many sources cite <sup>56</sup>Fe as the most tightly bound nucleus; see M.P. Fewell, Am.J.Phys., 63, 653, 1995 for a discussion which lays the blame for this misconception squarely at the door of astrophysicists!

(where  $m_p$ ,  $m_n$  are the proton, neutron masses), and the binding energy per baryon is

$$Q(Z, N)/(Z + N).$$

Converting ‘MeV per baryon’ to ‘J kg<sup>-1</sup>’, we find that burning protons into helium yields

$$\text{H} \rightarrow \text{He}: \quad 6.3 \times 10^{14} \text{ J kg}^{-1}$$

but

$$\text{H} \rightarrow \text{Fe}: \quad 7.6 \times 10^{14} \text{ J kg}^{-1};$$

that is, burning H to He alone releases 83% of the total nuclear energy available per nucleon.

## Physical processes

To do –

Nuclear models (liquid-drop, shell)

Line of stability (neutron, proton drip lines)

## 13.4 Hydrogen burning – I: the proton–proton (PP) chain

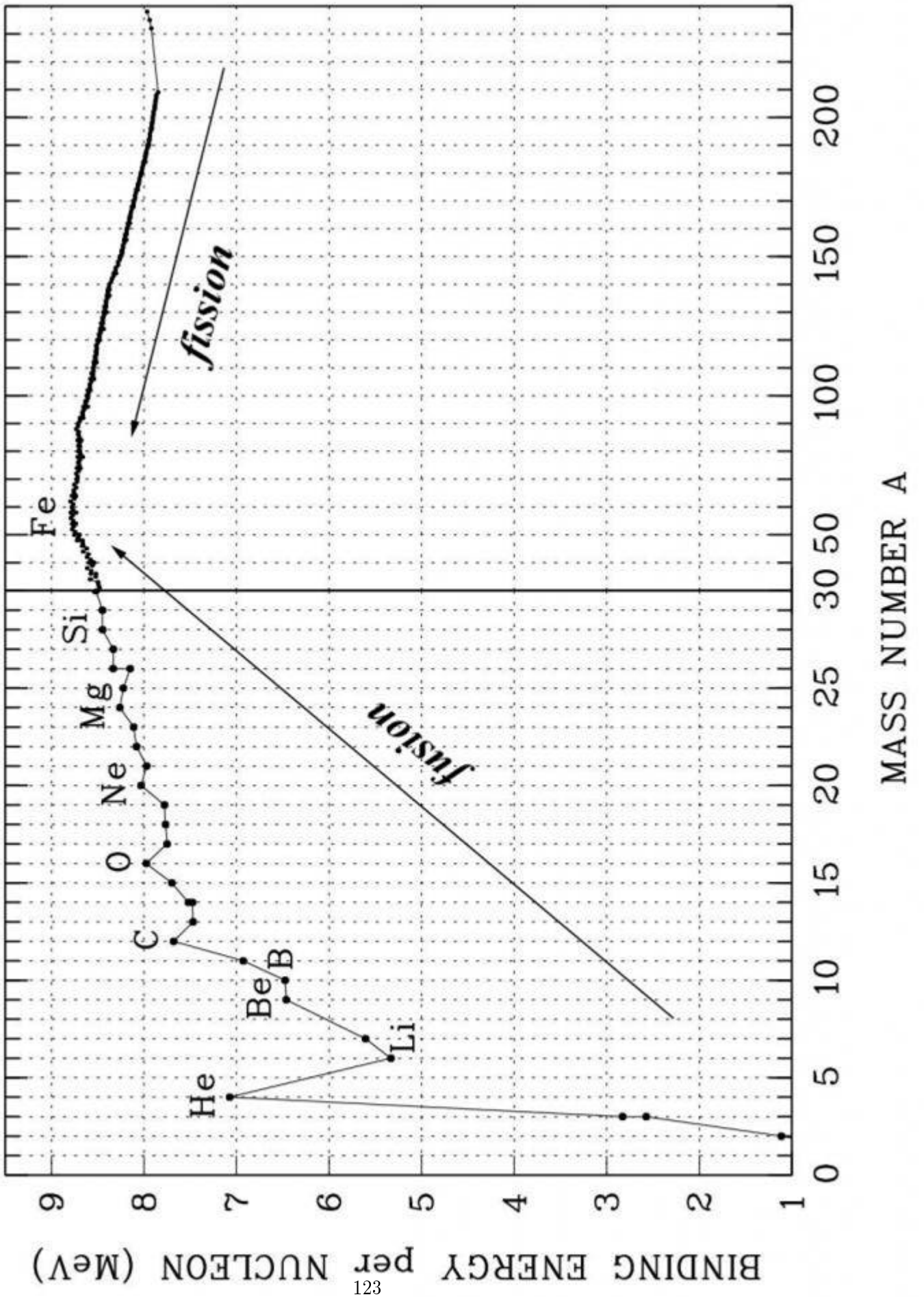
### 13.4.1 PP–I

Step	Process	Energy Release	Solar Timescale
(1)	$p + p \rightarrow {}^2\text{D} + e^+ + \nu_e$	1.44 MeV †	$7.9 \times 10^9$ yr
(2)	${}^2\text{D} + p \rightarrow {}^3\text{He}$	5.49 MeV	1.4s
		<u>6.92 MeV</u> ×2	
(3a)	${}^3\text{He} + {}^3\text{He} \rightarrow {}^4\text{He} + p + p$	12.86 MeV	$2.4 \times 10^5$ yr
		<u>26.72 MeV</u>	

†Includes 1.02 MeV from  $e^+ + e^- \rightarrow 2\gamma$

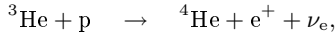
Reaction (1) is very slow because it involves the *weak interaction*,<sup>4</sup> which is required to operate during the short period when protons are close together.

<sup>4</sup>i.e., involves  $\beta$  decay; in this case  $\beta^+$  decay,  $p^+ \rightarrow n^0 + e^+ + \nu_e$  (cp.  $\beta^-$  decay,  $n^0 \rightarrow p^+ + e^- + \bar{\nu}_e$ ).



Reactions (2) and (3a) involve the *strong interaction* and in consequence are much faster.

[Note that reaction (3a) is preferred to



even though protons vastly outnumber  ${}^3\text{He}$  particles, because this again involves the weak interaction (the  $\nu_e$  is the giveaway).]

Reaction (1) occurs twice for each  ${}^4\text{He}$  production, each time generating an electron neutrino with energy 0.26 MeV. These leave the Sun without further interaction, so the energy available for heating is 26.2 MeV ( $26.72 - 2 \times 0.26$  MeV).

### 13.4.2 PP-II, PP-III

There are two principal secondary channels in the proton-proton chain, each catalysed by a pre-existing  $\alpha$  particle ( ${}^4\text{He}$  nucleus):

PP-II (follows steps 1 & 2, which yield 6.92 MeV):

Step	Process	Energy Release	Solar Timescale
(1)	$\text{p} + \text{p} \rightarrow {}^2\text{D} + \text{e}^+ + \nu_e$	1.44 MeV †	$7.9 \times 10^9$ yr
(2)	${}^2\text{D} + \text{p} \rightarrow {}^3\text{He}$	5.49 MeV	1.4s
(3b)	${}^3\text{He} + {}^4\text{He} \rightarrow {}^7\text{Be}$	1.59 MeV	$9.2 \times 10^5$ yr
(4b)	${}^7\text{Be} + \text{e}^- \rightarrow {}^7\text{Li} + \nu_e$	0.86 MeV	0.39 yr
(5b)	${}^7\text{Li} + \text{p} \rightarrow {}^4\text{He} + {}^4\text{He}$	<u>17.35 MeV</u>	570s
		<u>26.72 MeV</u>	

†Includes 1.02 MeV from  $\text{e}^+ + \text{e}^- \rightarrow 2\gamma$

In this case, neutrino losses average 0.80 MeV.

PP-III (follows steps 1, 2, and 3b):

Step	Process	Energy Release	Solar Timescale
(1)	$\text{p} + \text{p} \rightarrow {}^2\text{D} + \text{e}^+ + \nu_e$	1.44 MeV †	$7.9 \times 10^9$ yr
(2)	${}^2\text{D} + \text{p} \rightarrow {}^3\text{He}$	5.49 MeV	1.4s
(3b)	${}^3\text{He} + {}^4\text{He} \rightarrow {}^7\text{Be}$	1.59 MeV	$9.2 \times 10^5$ yr
(4c)	${}^7\text{Be} + \text{p} \rightarrow {}^8\text{B}$	0.14 MeV	66 yr
(5c)	${}^8\text{B} \rightarrow {}^8\text{Be}^* + \text{e}^+ + \nu_e$	16.04 MeV †	1 s
(6c)	${}^8\text{Be}^* \rightarrow {}^4\text{He} + {}^4\text{He}$	<u>3.30 MeV</u>	$10^{-16}$ s
		<u>26.72 MeV</u>	

†Includes 1.02 MeV from  $\text{e}^+ + \text{e}^- \rightarrow 2\gamma$

Neutrino losses here are 7.2 MeV on average, predominantly through step (5c).<sup>5</sup>

In the Sun, ~91% of reactions go through (3a); ~9% end at (5b); and ~0.1% end at (6c).

## 13.5 Hydrogen burning – II: the CNO cycle

Because the first reaction in the PP chain is so slow ( $7.9 \times 10^9$  yr), under certain circumstances it is possible for reactions involving (much less abundant) heavier nuclei, acting as catalysts, to proceed faster than PP. The larger charges (and masses) of these heavier particles imply that higher temperatures are required. Of these processes, the CNO, or CNO-I, cycle<sup>6</sup> is the most important:

Step	Process	Energy Release	Solar Timescale
(1)	${}^{12}_6\text{C} + \text{p} \rightarrow {}^{13}_7\text{N}$	1.94 MeV	$1.3 \times 10^7$ yr
(2)	${}^{13}_7\text{N} \rightarrow {}^{13}_6\text{C} + \text{e}^+ + \nu_e$	2.22 MeV †	7 m
(3)	${}^{13}_6\text{C} + \text{p} \rightarrow {}^{14}_7\text{N}$	7.55 MeV	$2.7 \times 10^6$ yr
(4)	${}^{14}_7\text{N} + \text{p} \rightarrow {}^{15}_8\text{O}$	7.29 MeV	$3.2 \times 10^8$ yr
(5)	${}^{15}_8\text{O} \rightarrow {}^{15}_7\text{N} + \text{e}^+ + \nu_e$	2.76 MeV †	82 s
(6a)	${}^{15}_7\text{N} + \text{p} \rightarrow {}^{12}_6\text{C} + {}^4_2\text{He}$	4.96 MeV	$1.1 \times 10^5$ yr
		<u>26.72 MeV</u>	

†Includes 1.02 MeV from  $\text{e}^+ + \text{e}^- \rightarrow 2\gamma$

As in PP, we have created one  ${}^4\text{He}$  from four protons, with release of some 26.7 MeV in the process; the neutrinos carry off 1.71 MeV for every  $\alpha$  particle created, so 25 MeV is available to heat the gas. Although steps (2) and (5) both involve the weak interaction, they proceed faster than reaction (1) of the PP chain, since the nucleons involved are already bound to each other (which allows more time for the weak interaction to occur).

---

<sup>5</sup>It is the high-energy neutrinos from this reaction that were famously searched for by experimentalist Raymond Davis and his partner theoretician John Bahcall; the failure to detect them in the expected numbers became known as the ‘Solar Neutrino Problem’. The ‘problem’ is now resolved through better understanding of neutrino physics – the electron neutrinos (the only type of neutrino detectable in the 1960s, ’70s, and ’80s) ‘oscillate’ to other neutrino flavours.

<sup>6</sup>Sometimes called the ‘carbon cycle’, although this risks confusion with cycling of carbon between the Earth’s atmosphere, biosphere, hydrosphere, which also goes by that name. The CNO-I and CNO-II cycles together constitute the ‘CNO bi-cycle’. Where do the CNO nuclei come from? The answer is that they were created in previous generations of stars, in processes shortly to be described.

The cycle starts *and finishes* with  $^{12}\text{C}$ , which acts as a catalyst.<sup>7</sup> However, during CNO cycling, the overall abundances nonetheless change – why is this?

Step (4),  $^{14}\text{N} + \text{p}$ , is more than  $10\times$  slower than the next-slowest reaction (step (1),  $^{12}\text{C} + \text{p}$ ). It therefore acts as a ‘bottleneck’, with a build-up of  $^{14}\text{N}$  at the expense of  $^{12}\text{C}$  until the reaction rates<sup>8</sup> of steps (1) and (4) are equal (these depending on the number densities of reagents; eqn. (13.2)). The equilibrium condition that reaction rates are equal determines the abundances, which can be compared to ‘solar’ abundances:

	CN cycle	Solar	
$n(^{12}\text{C})/n(^{13}\text{C})$	4	89	
$n(^{14}\text{N})/n(^{15}\text{N})$	2800	250	[ $^{15}\text{N}$ reduced by step (6a)]
$n(^{14}\text{N} + ^{15}\text{N})/n(^{12}\text{C} + ^{13}\text{C})$	21	0.3	[ $^{14}\text{N}$ increased by step (3)]

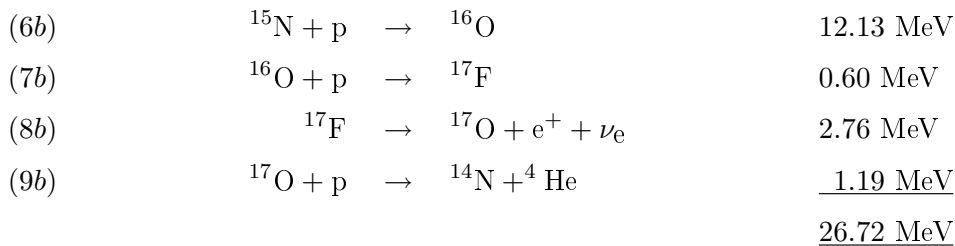
at  $T \sim 1.3 \times 10^7 \text{K}$  (the solar-core temperature; the timescale required to establish equilibrium is set by the slowest reaction, and so is  $\sim 10^8$  yr at this temperature). These anomalous abundance patterns are a clear signature of CN processing if the products are brought to the stellar surface.

We can similarly evaluate equilibrium abundances for PP processing; for  $T \simeq 1.3 \times 10^7 \text{K}$ ,

$$\begin{aligned} n(^2\text{D})/n(^1\text{H}) &= 3 \times 10^{-17} \\ n(^3\text{He})/n(^1\text{H}) &= 10^{-4} \\ & (= 10^{-2} \text{ at } 8 \times 10^6 \text{K}) \end{aligned}$$

### 13.5.1 CNO-II

There are a number of subsidiary reactions to the main CNO cycle, particularly involving oxygen. The CNO-II bi-cycle accounts for about 1 in 2500  $^4\text{He}$  productions in the Sun:



which returns to step (4) in CNO-I

---

<sup>7</sup>Note that given ordering is arbitrary – the cycle can be considered as beginning at any point [e.g., starting at step (4), ending at (3)].

<sup>8</sup>Recall that reaction rates depend on both timescales and reagent abundances – cf. eqn13.1

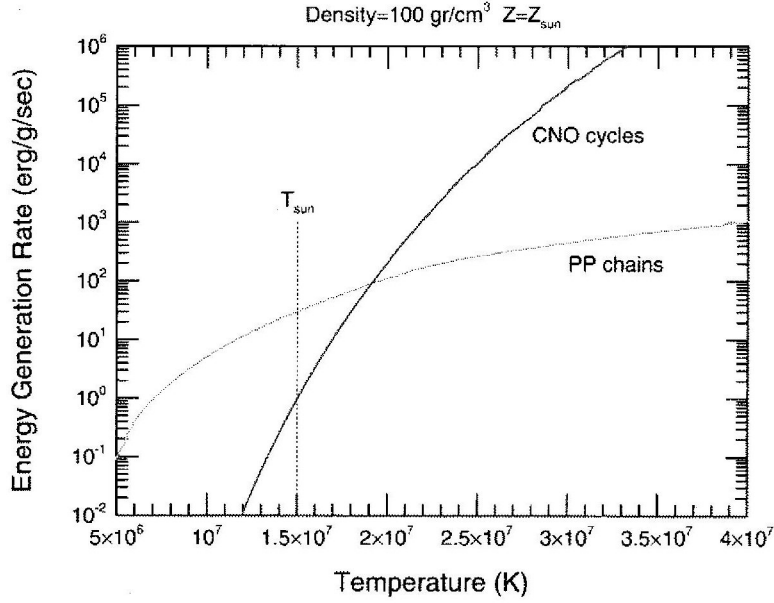
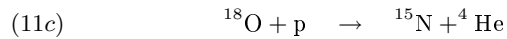
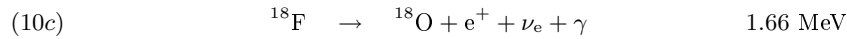
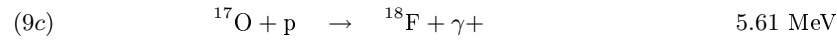


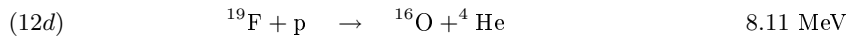
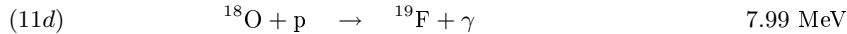
Figure 13.3: Energy generation rates: CNO vs. PP processing

### CNO-III, IV

The ‘OF cycle’ (which with CNO-I and CNO-II makes up the ‘CNO tri-cycle’) occurs in massive stars, and can be divided into CNO-III and CNO-IV; each branch starts from a  $^{17}\text{O}$  produced in CNO-II:

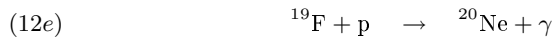


which returns to step (6b) in CNO-II; or, proceeding to CNO-IV:



which returns to step (7b) in CNO-II

The only possible breakout from a closed cycle at temperatures relevant for quiescent hydrogen burning would be an alternative to step (12d),



but the rate is negligibly small, ensuring that the CNO cycles are completely closed.

We have seen that

$$\varepsilon \simeq \varepsilon_0 \rho T^\alpha \tag{13.9}$$

where  $\alpha \simeq 4.5$  for proton-proton reactions in the Sun and  $\alpha \simeq 18$  for CN processing. Because core temperature scales with mass (Section 10.6.3), PP dominates for lower-mass stars, while CN cycling dominates for higher-mass stars. The Sun lies just below the crossover point (fig. 13.5.1), and although the PP chain dominates, the CN cycle is not negligible.

## 13.6 Helium burning

### 13.6.1 $3\alpha$ burning

Hydrogen burning dominates the stellar lifetime (the main-sequence phase), but the core pressure,

$$P = \frac{\rho k T}{\mu m(\text{H})},$$

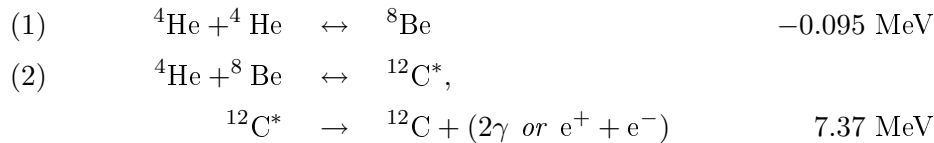
reduces as the mean molecular weight  $\mu$  changes from 0.5 (for fully-ionized pure hydrogen) to  $4/3$  (for fully-ionized pure helium). As a consequence the core contracts, and heats. If the star is more massive than about  $0.5M_\odot$  the resulting core temperature and pressure are high enough to ignite helium burning ( $\sim 10^8\text{K}$ ,  $10^8 \text{ kg m}^{-3}$ ; lower-mass stars don't have enough gravitational potential energy); the reactions have a nett effect of



However, the process is hindered by the absence of stable mass-5 ( ${}^4\text{He} + \text{p}$ ) and mass-8 ( ${}^4\text{He} + {}^4\text{He}$ ) nuclei; in particular, the  ${}^8\text{Be}$  is unstable, and decays back to a pair of alpha particles in only about  $10^{-16}\text{s}$ . Nonetheless, in equilibrium a small population of  ${}^8\text{Be}$  particles exists (at a level of 1 for every  $\sim 10^9$   $\alpha$  particles) and these can interact with  ${}^4\text{He}$  under stellar-core conditions. Exceptionally, because the lifetimes are so short, the production of  ${}^{12}\text{C}$  is, essentially, a *3-body* process, with an energy-generation rate:

$$\varepsilon_{3\alpha} \simeq \varepsilon_0 \rho^2 T^{30}$$

(where  $\varepsilon_0 \propto n({}^4\text{He})$  and the density-*squared* dependence is because of the three-body nature of the reaction).

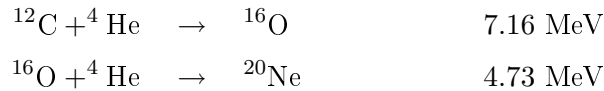


The first stage is endothermic;  ${}^8\text{Be}$  is more massive than two  ${}^4\text{He}$  nuclei, so the relative binding energy is *negative*.

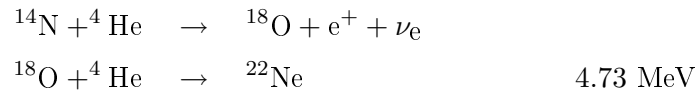
Reaction (2) is favoured by the existence of a resonance at 287 keV, which results in a  ${}^{12}\text{C}$  nucleus excited 7.65 MeV above the ground state.<sup>9</sup> The lifetime of this excited state is very small (about  $5 \times 10^{-17}$  s!), and normally decays straight back to  ${}^4\text{He} + {}^8\text{Be}$ , but 1 in  $\sim 2400$  decays is to a ground-state  ${}^{12}\text{C}$  nucleus, with the emission of two photons. These decays are irreversible, and so a population of  ${}^{12}\text{C}$  nuclei slowly builds up.

### 13.6.2 Further helium-burning stages

Once carbon has been created, still heavier nuclei can be built up:



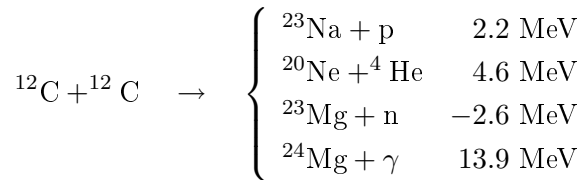
These processes therefore generate C, O, and Ne.  ${}^{12}\text{C}$  and  ${}^{16}\text{O}$  are the most abundant nuclei at the end of He burning (and the most cosmically abundant elements after H and He, with about 1 C or O for every  $10^3$  hydrogens, or every 100 heliums) The situation is more complicated for  ${}^{14}\text{N}$ , which is enhanced during CNO processing<sup>10</sup> but which is destroyed during He burning by the reactions



## 13.7 Advanced burning

### 13.7.1 Carbon burning

After exhaustion of  ${}^4\text{He}$ , the core of a high-mass star contracts further, and at  $T \sim 10^8\text{--}10^9\text{K}$  *carbon burning* can take place:




---

<sup>9</sup>Hoyle (1954) deduced that such a resonance in a previously unknown excited state of carbon must exist to allow an  $\alpha$  particle to combine with an  ${}^8\text{Be}$  with sufficient probability for the triple-alpha process to proceed.

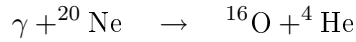
<sup>10</sup>All the initial  ${}^{12}\text{C}$  and  ${}^{16}\text{O}$  ends up as  ${}^{14}\text{N}$ .

with a temperature dependence of

$$\varepsilon_C \simeq \varepsilon_0 \rho T^{32}$$

### 13.7.2 Neon burning

Neon burning takes place after carbon burning if the core temperature reaches  $\sim 10^9\text{K}$ , but at these temperatures photodisintegration also occurs:

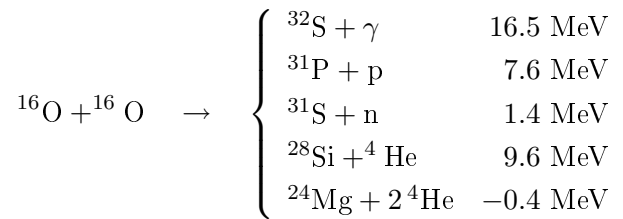


These ‘new’ alpha particles can then react with undissociated neons:



### 13.7.3 Oxygen burning

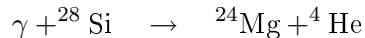
After neon burning the core consists mainly of  ${}^{16}\text{O}$  and  ${}^{24}\text{Mg}$ . Oxygen burning occurs at  $\sim 2 \times 10^9\text{K}$ :



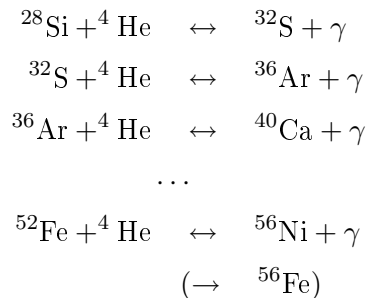
with silicon being the most important product.

### 13.7.4 Silicon burning

At  $\sim 3 \times 10^9\text{K}$ , silicon burning can occur; the Si is slowly photodisintegrated, releasing protons, neutrons, and alpha particles (a process sometimes called ‘silicon melting’ as opposed to ‘silicon burning’). Of particular interest is the reaction



These alpha particles then combine with undissociated nuclei to build more massive nuclei; for example, by way of illustration,

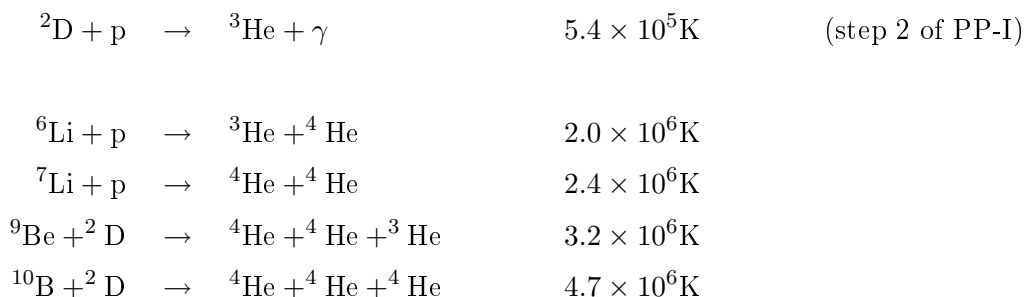


The overall timescale is set by the slowest step, which is the initial photodisintegration of Si.

Because the binding energy per nucleon peaks around mass  $A = 56$  (the ‘iron-peak’ elements Cr, Mn, Fe, Co, Ni) energy is *absorbed* to form heavier nuclei. Elements beyond the iron peak are therefore not formed during silicon burning.

## 13.8 Pre-main-sequence burning

Although not as important as energy-generating sources, some reactions involving light nuclei can occur at  $\sim 10^6\text{K}$  – i.e., lower temperatures than those discussed so far:



These reactions generally *destroy* light elements such as lithium (produced, e.g., primordially) at relatively low temperatures.

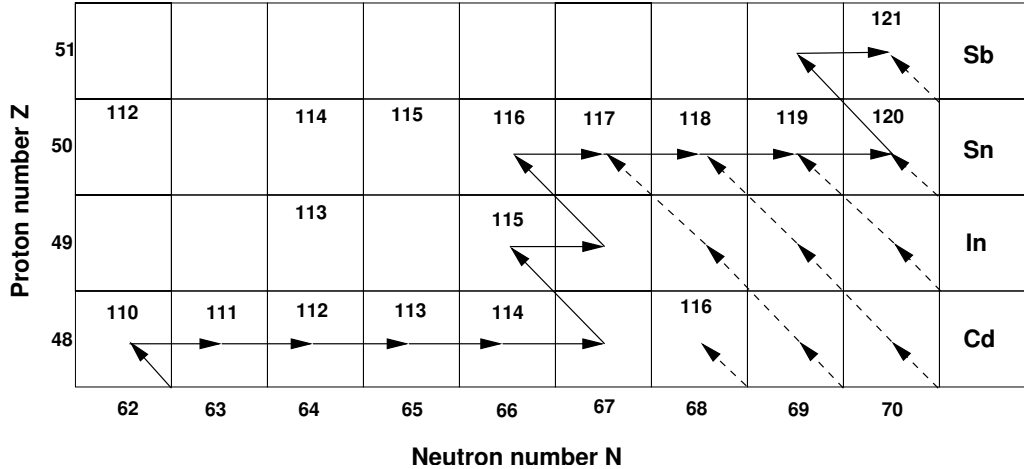
Note that the first step, burning of *pre-existing* deuterium, defines brown dwarfs – objects with cores too cool to produce deuterium by proton-proton reactions.

## 13.9 Synthesis of heavy elements

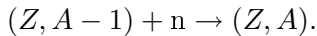
### 13.9.1 Neutron capture: *r* and *s* processes

Carbon burning, oxygen burning etc. can generate heavy elements in the cores of very massive stars, but only as far as the iron peak. However, a quite different set of reactions can occur at lower temperatures ( $\sim 10^8\text{K}$ , comparable to that need for  $3\alpha$  burning).

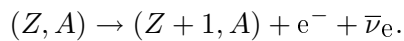
Since neutrons are electrically neutral, they see no Coulomb barrier, and can be absorbed into nuclei even at quite low energies (in fact, heavy nuclei have relatively large neutron-capture cross-sections). Neutron absorption produces a heavier isotope (increases  $A$  but not  $Z$ ); a change in element may then result if the nucleus is unstable to  $\beta$  decay ( $n \rightarrow p + e^- + \bar{\nu}_e$ ).



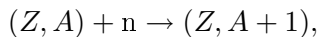
Following the pioneering work of Burbidge, Burbidge, Fowler & Hoyle (Rev. Mod. Phys., 29, 547, 1955), it is conventional to distinguish between *r* and *s* processes, depending on whether neutron capture is *r*apid or *s*low compared to the  $\beta$ -decay timescale. If it is rapid, then more and more massive isotopes accumulate; if it is slow, then decay to a higher- $Z$  element takes place. Suppose we start off with a neutron capture to produce some new isotope:



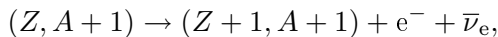
Then if neutron capture happens slowly compared to decay for this new isotope,  $\beta$  decay precedes any further neutron capture, and a new element is formed:



However, if neutron capture is *r*apid then a further isotope is produced,



which will in turn  $\beta$ -decay,



or assimilate a further neutron.

The timescales involved for the *r* and *s* processes are largely set by the relevant nuclear timescales.<sup>11</sup> The *s* process occurs during non-catastrophic evolutionary phases (principally the AGB phase); we *know* this from the observation that technetium occurs in S-type stars (moderately carbon rich M stars). Even the longest-lived technetium isotope, <sup>99</sup>Tc, has a

<sup>11</sup>Just to have some sense of the numbers, the *s* process typically operates on timescales of  $\sim 10^4$  yr at neutron densities of  $\sim 10^{11} \text{ m}^{-3}$ ; corresponding numbers for the *r* process are a few seconds at  $\sim 10^{25} \text{ m}^{-3}$ .

half-life only of order  $10^4$  yr, and so it must be produced within stars during normal evolutionary processes.

Where do the free neutrons come from? For the  $s$  process, the CNO cycle establishes an appreciable abundance of  $^{13}\text{C}$  (step 2 in the sequence set out in Section 13.5), which can react with  $^4\text{He}$ :



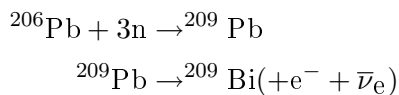
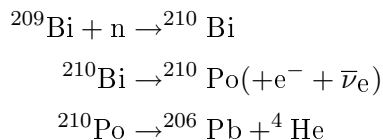
This is the main source of neutrons in AGB stars; at higher temperatures,



is significant.

Neutron-capture cross-sections are exceptionally small for certain nuclear neutron numbers. Because it's harder for the corresponding isotopes to increase in mass through neutron capture, they build up in abundance. We see this effect as peaks in the element-abundance distribution for elements such as  $^{88}_{38}\text{Sr}$ ,  $^{138}_{56}\text{Ba}$ , and  $^{208}_{82}\text{Pb}$ .

Elements beyond bismuth ( $Z = 83$ ) cannot be produced through the  $s$  process, the terminating cycle being



(involving  $Z = 84$  polonium and  $Z = 82$  lead in addition to bismuth).

Many, but not all, elements at lower atomic masses can be produced by both  $r$  and  $s$  processes;  $s$ -only products include  $^{87}_{38}\text{Sr}$  and  $^{187}_{76}\text{Os}$ .

The  $r$  process requires very high neutron fluxes, so that neutron capture rates exceed or compete with  $\beta$ -decay rates. These conditions can only occur during catastrophic, short-timescale phases – supernova explosions. Although some isotopes can be produced by both processes, in general there are significant differences between their products.

	115	116	117	118	119	120	121	122	123	124	125	126	127	128
$_{83}\text{Bi}$									$\epsilon$	$\epsilon$	$\epsilon$	100	$\beta$	$\alpha$
$_{82}\text{Pb}$					$\epsilon$	$\epsilon$	$\epsilon$	1.42	$\epsilon$	24.1	22.1	52.3	$\beta$	$\beta$
$_{81}\text{Tl}$					$\epsilon$	$\epsilon$	$\epsilon$	29.5	$\beta$	70.5	$\beta$	$\beta$		
$_{80}\text{Hg}$	$\epsilon$	0.15	$\epsilon$	10.0	16.8	23.1	13.3	29.8	$\beta$	6.9	$\beta$			
$_{79}\text{Au}$	$\epsilon$	$\epsilon$	$\epsilon$	100	$\beta$	$\beta$								

Figure 13.4: Isotopes of gold–bismuth. The top row lists the number of neutrons in the isotope, while the atomic number (number of protons) is given by the element name. Unstable isotopes decay by conversion of a proton to a neutron (electron capture,  $\epsilon$ ), conversion of a neutron to a proton ( $\beta$  decay), or emission of a helium nucleus ( $\alpha$  decay,  $\text{Bi}^{211}$  only). Numbers give natural percentage abundances of stable isotopes (blanks are for isotopes that do not occur in nature).

The dashed line shows the  $s$ -process path from the only stable isotope of gold ( $\text{Au}^{197}$ ) to the only stable isotope of bismuth ( $\text{Bi}^{209}$ ).  $\text{Hg}^{204}$  is an example of an isotope that can be made only by the  $r$  process.

### 13.9.2 The $p$ process (for reference only)

In their seminal paper, Burbidge, Burbidge, Fowler & Hoyle ( $\text{B}^2\text{FH}$ ) identified the need for a process to create certain relatively proton-rich nuclei, heavier than iron, that cannot be produced by either of the  $r$  or  $s$  processes (e.g.,  $^{190}\text{Pt}$ ,  $^{168}\text{Yb}$ ).

They originally envisaged a proton-capture process, but we now believe that these proton-rich nuclei are not produced by addition of protons, but by removal of neutrons by photodisintegration (i.e., impact by high-energy photons).<sup>12</sup> This occurs through neutron photodisintegration (ejection of a neutron) or  $\alpha$  photodisintegration (emission of an  $\alpha$  particle). These processes require high temperatures (i.e., high-energy photons), and is believed to occur during core collapse of supernovae.

## 13.10 Summary

Hydrogen and helium were produced primordially. After these, CNO are the most abundant elements, with CO produced through helium burning,<sup>13</sup> with nitrogen generated in CNO processing.

Stars more massive than  $\sim 8M_{\odot}$  go on to produce elements such as neon, sodium, and magnesium, with stars more massive than  $\sim 11M_{\odot}$  proceeding to silicon burning, thereby generating nuclei all the way up to the iron peak.

<sup>12</sup>Luckily, ‘photodisintegration’ fits the description ‘ $p$  process’ as well as ‘proton capture’ does! There *is* a proton-capture mechanism, now called the  $rp$  process, but it is generally less important than the  $p$  process.

<sup>13</sup>The balance between C and O is determined by the balance between the rate of production of C and the rate of destruction (in O formation). If the ratio favoured O only a little more, then we wouldn’t be here.

Subsequent processing primarily involves neutron capture (although other processes, such as spallation and proton capture, have a small role).

The timescales for various burning stages are progressively shorter, as energy production rates increase to compensate increasing energy losses (e.g., by increasing neutrino losses). Only massive stars have enough gravitational potential energy to power the most advanced burning stages, so we review the timescales for a 25- $M_{\odot}$  star:

Burning stage	Timescale	$T_c/10^9\text{K}$	$\rho_c$ (kg m <sup>-3</sup> )	Products
H	$7 \times 10^6$ yr	0.06	$5 \times 10^4$	He; N (CNO process)
He	$5 \times 10^5$ yr	0.1	$7 \times 10^5$	C, O
C	$6 \times 10^2$ yr	0.6	$2 \times 10^8$	Ne, Na, Mg, etc.
Ne	$1 \times 10^0$ yr	1	$4 \times 10^9$	O, Na, Mg, etc.
O	$5 \times 10^{-1}$ yr	2	$1 \times 10^{10}$	Si, S, P, etc.
Si	1 d	3	$3 \times 10^{10}$	Mn, Cr, Fe, Co, Ni etc.



## Section 14

# Supernovae

### 14.1 Observational characteristics

Supernovae (SNe) are classified principally on the basis of their spectral morphology at maximum light:

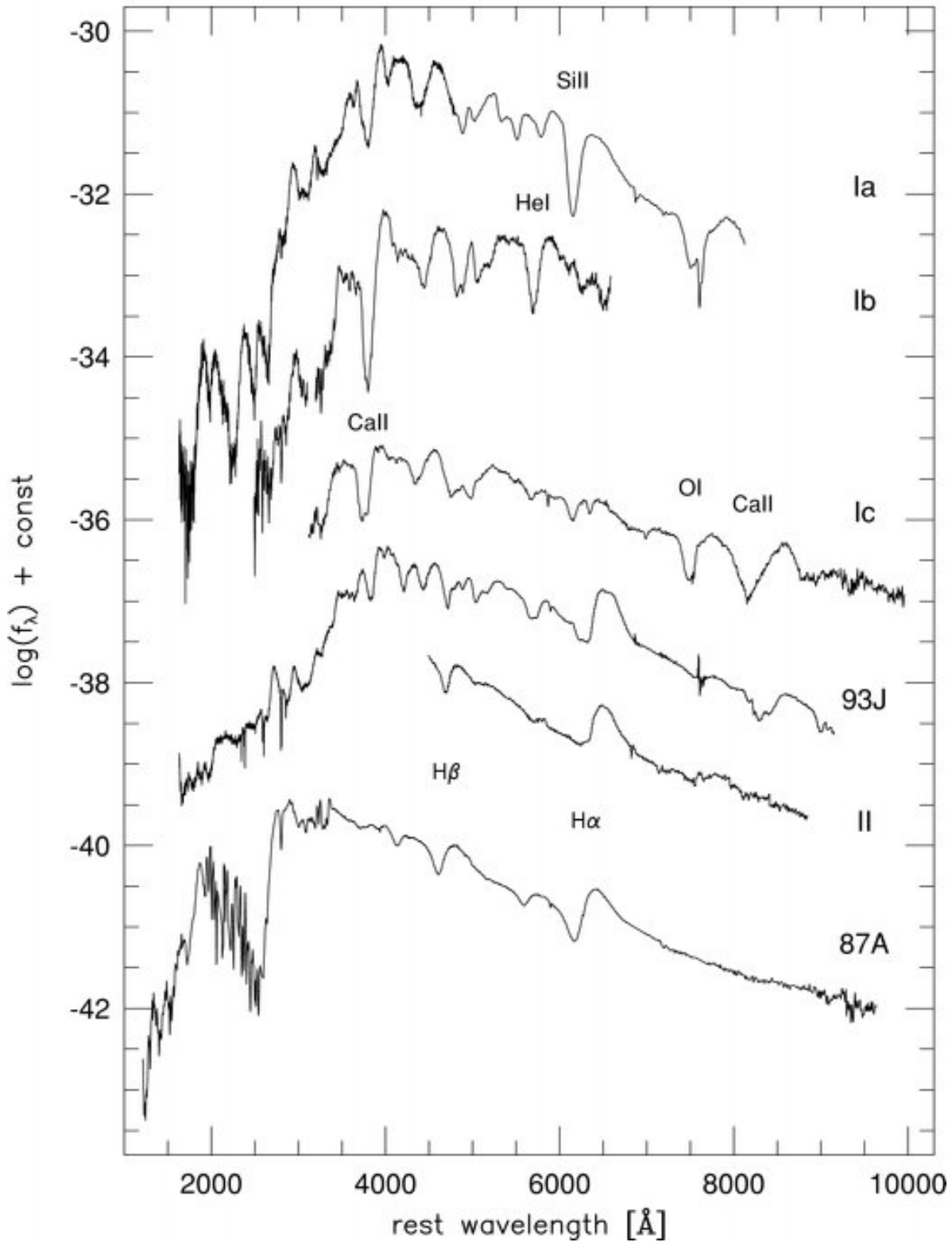
Hydrogen present?	No:	Type I
		Silicon? Yes: Ia
		No: Helium? Yes: Ib
		No: Ic
	Yes:	Type II (II-L, II-P, IIn, Peculiar)

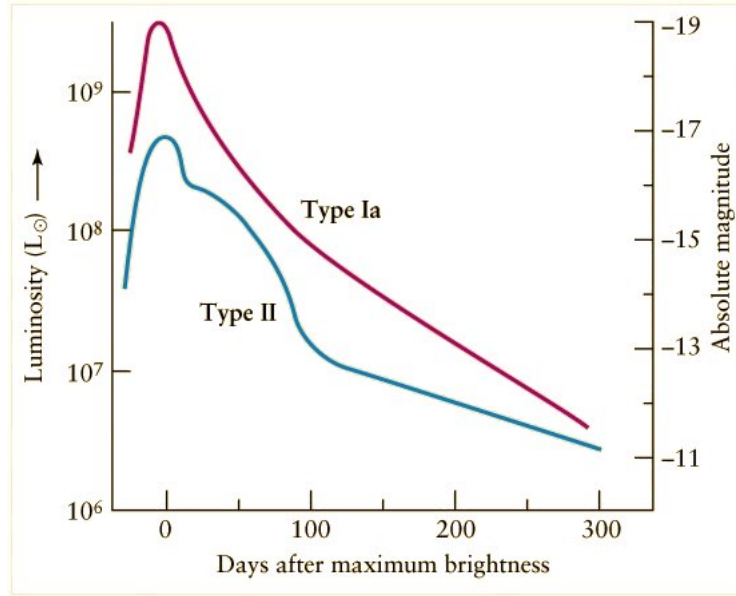
[Our discussion of nucleosynthesis should now inform this empirical classification: e.g., abundant silicon can only result from exposure of material that has undergone advanced burning stages.]

Type II is subclassified according to light-curve morphology; II-L shows a *Linear* decrease in magnitude with time, while II-P supernovae show a *Plateau*. While type II SNe generally show broad lines (corresponding to ejection velocities of thousands of  $\text{km s}^{-1}$ ), some show relatively *narrow* lines (few hundred  $\text{km s}^{-1}$ ); these are classified IIn.

Note that the classification originated in low-resolution photographic spectra, and in the light of modern data is seen to be fairly rough; some spectra are intermediate between these types, and some supernovae may appear as different types at different times. As we shall see, the most important *physical* difference is between Type Ia SNe and ‘the rest’ (that is, between ‘thermonuclear’ & ‘core-collapse supernovae’) – and we will begin with ‘the rest’.

Spectra of SN at maximum





## 14.2 Types Ib, Ic, II

These subtypes collectively constitute the ‘core collapse supernovae’. They occur almost exclusively in the arms of spiral galaxies – strong circumstantial evidence that they are the end points of evolution of short-lived massive stars.

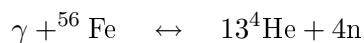
### 14.2.1 The death of a massive star

Although the composition of the outer layers of a star may influence the spectral appearance of its supernova explosion, the key physical processes take place in the stellar core.

As sequential burning processes exhaust their respective fuels in the core, it contracts, generating internal energy. In ‘normal’ evolutionary stages, this leads to the activation of the next fusion process; thermal energy increases and further contraction is opposed.

However, in the final evolutionary stages, the opposite happens; energy is *extracted*, pressure support is further removed, and gravitational contraction becomes gravitational collapse. There are two significant energy-extraction processes relevant to late-stage stellar evolution: photodisintegration, and inverse beta decay.

- (i) The contracting core eventually reaches temperatures sufficient to photodisintegrate iron nuclei (the helium-iron phase transition;  $T \sim 10^9\text{K}$ ):

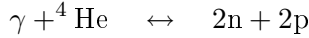


The disintegration requires the same energy as released in building the iron from helium in the first place,

$$Q = [13m(^4\text{He}) + 4m(\text{n}) - m(^{56}\text{Fe})]c^2 = 124.4 \text{ MeV}$$

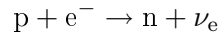
or  $2 \times 10^{14} \text{ J kg}^{-1}$ . About  $3/4$  of the iron is dissociated in this way if the core reaches  $\rho \simeq 10^{12} \text{ kg m}^{-3}$ ,  $T \simeq 10^{10}\text{K}$ .

Endothermic photodissociation of  $^4\text{He}$  can also occur at somewhat higher temperatures:



$$(5 \times 10^{14} \text{ J kg}^{-1}).$$

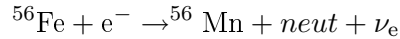
(ii) Electron capture by inverse  $\beta$  decay may also occur; schematically,



although in practice the protons are bound in nuclei:

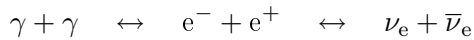


e.g.,



This neutronization occurs at high densities ( $\rho \simeq 10^{12}\text{--}10^{13} \text{ kg m}^{-3}$ ), and produces a copious neutrino flux (as well as a copious neutron flux, which feeds  $r$ -processing).

Neutrinos are also generated by pair production,



Remarkably, it is the neutrinos that carry off  $\sim 90\%$  of the energy released – the radiant and kinetic energies are minor perturbations.

The timescale associated with these processes is the dynamical free-fall timescale,

$$t_{\text{dyn}} = \sqrt{\frac{2r^3}{Gm(r)}} \simeq \sqrt{(G\rho^{-1})} \quad (12.2)$$

which is very short for such high densities – of order 1 ms. The velocities are correspondingly large (up to a quarter the speed of light!). The collapse is therefore indeed catastrophic, and is almost unimpeded until halted by neutron degeneracy; the core briefly achieves a density  $2\text{--}3 \times$

that of nuclear matter before rebounding to leave a neutron star. The rebound sends a shock wave through the overlying layers of the star, which is infalling on a much longer timescale; the shock reverses the infall resulting in an outwards explosion, which we see as the supernova.

The remnant is normally a neutron star, but just as there is a limit to mass of white dwarfs (supported by electron degeneracy pressure),  $\sim 1.4M_{\odot}$ , so there is a limit to the mass of neutron stars (supported by neutron degeneracy pressure),  $\sim 3M_{\odot}$ . If the remnant mass exceeds this limit, a black hole results.<sup>1</sup>

### 14.2.2 Light-curves

Type II SN are thought to arise from red supergiants (as has now been directly observed in several instances). The spectra of these SNe near maximum show roughly normal abundances (in particular, hydrogen is present), with velocities of  $\sim \pm 5000 \text{ km s}^{-1}$ , because we're seeing material from the near-normal outer layers of the progenitor.

The extended outer structure retains much of the heat deposited by the shock, and the initial light-curve in this case is dominated by release of this energy over several weeks.

Evidently, though, Types Ib and Ic, with their H-poor spectra, have lost most of their outer hydrogen envelopes, most probably as a result of strong stellar winds (or through binary interaction).<sup>2</sup> Type I SN (of all types) therefore originate in more compact structures, and their light-curves require an alternative source of heating – radioactive decay. The light-curve decay timescale in SN 1987A corresponds closely to the timescales for radioactive decay of  $^{56}\text{Co}$  to  $^{56}\text{Fe}$  (half-life 77d).<sup>3</sup>

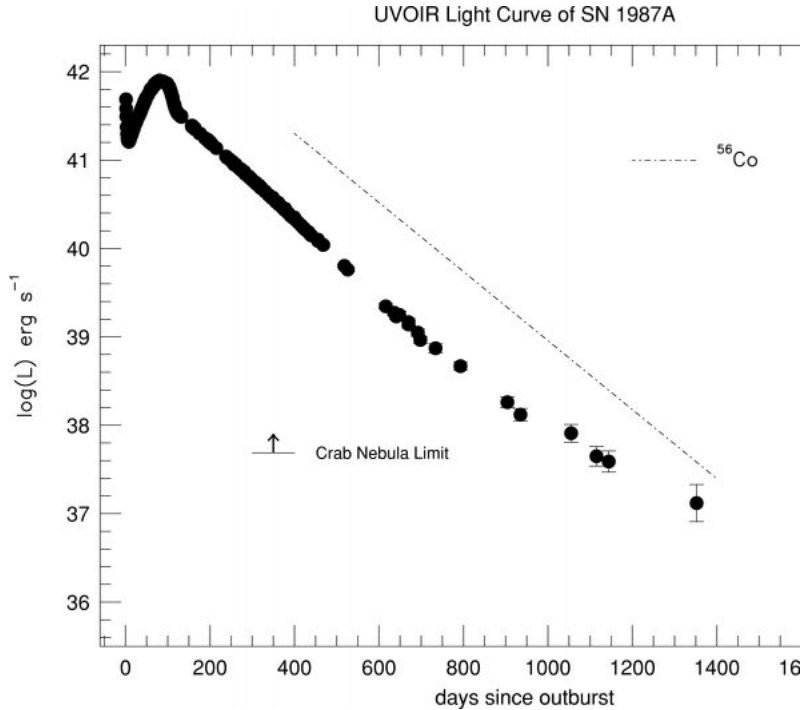
Maximum absolute visual magnitudes of core-collapse supernovae are typically  $-17$  to  $-18$ , with light-curves that are rather diverse, as a result of the differences in the structure of the body surrounding the collapsed core.

---

<sup>1</sup>Degenerate matter has sufficient density that the dominant contribution to the pressure results from the Pauli exclusion principle, arising because the constituent particles (fermions) are forbidden from occupying identical quantum states. Any attempt to force them close enough together that they are not clearly separated by position must place them in different energy levels. Therefore, reducing the volume requires forcing many of the particles into higher-energy quantum states. This requires additional compression force, and so is felt as a resisting pressure. The relevant fermions result in electron or neutron degeneracy pressure.

<sup>2</sup>Short gamma-ray bursts are generally believed to be associated with the collapse of Wolf-Rayet stars.

<sup>3</sup>The  $^{56}\text{Co}$  is in turn produced from the faster (6.1-d) decay of  $^{56}\text{Ni}$ . The late-time fading of 1987A, more than  $\sim 3$  yr after maximum, appears to correspond to decay of  $^{57}\text{Co}$ .



## 14.3 Type Ia SNe

### 14.3.1 Observational characteristics

The light-curves can reach  $M(V) \simeq -19$  ( $\sim 10^{10}L_{\odot}$ ) at maximum, the most luminous of the normal supernovae. They typically show a rather rapid initial decline (for  $\sim 30$ d after maximum), followed by an exponential decay (i.e., linear in magnitude),

$$L = L_0 \exp \{-t/\tau(\text{Ia})\}$$

with  $\tau(\text{Ia}) \simeq 77$ d (the  $^{56}\text{Co}$  decay timescale).

Velocities of up to  $20,000 \text{ km s}^{-1}$  are seen in the absorption- and emission-line spectra, with lines due to elements such as magnesium, silicon, sulfur, and calcium near maximum light.

Type Ia SNe occur in both spiral and, uniquely, elliptical galaxies. Because elliptical galaxies contain no massive stars, Ia SNe can't be core-collapse objects (see Section 14.2.1).

### 14.3.2 Interpretation

Type Ia SNe are believed to be the result of mass transfer onto a white dwarf (WD) in a binary system (or possibly through WD-WD mergers). Eventually the WD is pushed over the Chandrasekhar mass limit ( $1.4M_{\odot}$ ), electron degeneracy is overcome, and the object starts to

collapse; the conversion of gravitational energy to thermal energy drives the temperature to values where carbon burning can occur. The temperature increases, carbon burning accelerates – and a thermonuclear runaway occurs, throughout the star (generating the silicon observed in the spectrum).

Since these processes occur under essentially the same conditions irrespective of evolutionary history, all type Ia SNe are expected to be closely similar – a crucial aspect of their use as ‘standard candles’ in cosmological applications, where they are the only objects sufficiently luminous, and sufficiently ‘standard’, to be useful at large distances.

This standardization is observed to be the case in practice, although there are some systematic differences from object to object; e.g., some are a bit brighter than others, and the brighter events have slightly slower fades from maximum. This evidently relates to the details of the SN event – i.e., how the thermonuclear runaway progresses.

Two distinct routes have been identified for fusion processes to propagate. One is subsonic burning, or ‘deflagration’; the other is supersonic ‘detonation’. Current models suggest that carbon burning starts as a subsonic deflagration and moves to supersonic detonation; slightly different timescales for this process yield slightly different observational characteristics. The energy of the explosion is enough to disrupt completely the original object.

## 14.4 Pair-instability supernovae (for reference only)

If *extremely* massive stars exist ( $\gtrsim 130M_{\odot}$ ) core temperatures may become so great, before the fusion cascade is complete, that high-energy photons ( $\gamma$  rays) in the core annihilate, creating matter-antimatter pairs (mostly  $e^{-}/e^{+}$ ).

Once pair production starts to become the dominant mechanism for  $\gamma$ -ray capture, these photons’ mean free path starts to decrease; this leads to an increase in core temperature, further increasing the photon energy, in turn further decreasing the mean free path. This leads to a runaway instability, removing photons; and as the pressure support provided by the radiation is removed, outer layers fall inward, resulting in what is predicted to be an exceptionally bright supernova explosion.

In such a pair instability supernova (PISN), the creation and annihilation of positron/electron pairs causes the core to be so unstable that it cannot gravitationally collapse further; *everything* is ejected, leaving no remnant.

Stars which are rotating fast enough, or which do not have low metallicities, probably do not collapse in pair-instability supernovae due to other effects (e.g., the mass of high-metallicity stars is constrained by the Eddington limit).

No pair-production supernova has been identified with certainty, but the brightest supernova on record, SN 2006gy (in NGC 1260), is the best candidate. Studies indicate that perhaps  $\sim 40M_{\odot}$  of  $^{56}\text{Ni}$  were released – almost the entire mass of the star’s core regions.  $^{56}\text{Ni}$  decays to  $^{56}\text{Co}$  with a half-life of 6.1 d; in turn the cobalt decays with a half-life of 77 days.

# Appendix A

## SI units

### A.1 Base units

Astronomers have been rather bad at using the SI system; they prefer their own ‘custom’ units ( $M_{\odot}$ , pc, etc.), or adopt cgs units (centimetre, gram, second) in preference to mks units (metre, kilogram, second) from which the SI system derives. Nevertheless, students, in particular, really *should* strive to use SI, which (among other advantages) greatly simplifies treatments of electricity.<sup>1</sup>

The irreducible base units of the SI system [and their cgs counterparts, where different] are:

<i>Quantity</i>	<i>SI Unit</i>		<i>cgs equivalent</i>	
length	metre	m	[centimetre	cm = $10^{-2}$ m]
mass	kilogram	kg	[gram	g = $10^{-3}$ kg]
time	second	s		
electric current	ampere	A	[Biot	bi = $10^{-1}$ A]
amount of substance	mole	mol		
luminous intensity	candela	cd		
thermodynamic temp.	kelvin	K	[degree Celsius	$^{\circ}\text{C} = \text{K} - 273.15$ ]

<sup>1</sup>In SI, electric current is defined in terms of the directly measurable magnetic *force* it exerts, and charge is then defined as current multiplied with time.

In cgs ‘electrostatic units’, the unit of charge (or statcoulomb), is defined by the quantity of charge which gives a force constant of 1 in Coulomb’s law. That is, for two point charges, each with charge 1 statcoulomb, separated by 1 centimetre, the electrostatic force between them is one dyne. This also has the effect of making electric charge dimensionless (and not requiring a fundamental unit).

## A.2 Derived units

‘Derived quantities’ can be defined in terms of the seven base quantities. There are 20 derived quantities which are not dimensionless and which, for convenience, have named units; these are tabulated overleaf.

The units of angle and solid angle are, formally, simply the number 1 (being ratios of dimensionally identical quantities). Nonetheless, these two further derived quantities have named units, as the lack of units could easily be confusing. They are:

- radian (rad): the unit of angle is the angle subtended at the centre of a circle by an arc of the circumference equal in length to the radius of the circle (so there are  $2\pi$  radians in a circle).
- steradian (sr): the unit of solid angle is the solid angle subtended at the centre of a sphere of radius  $r$  by a portion of the surface of the sphere having an area  $r^2$  (so there are  $4\pi$  steradians on a sphere).

Many other derived quantities in more or less common use don’t have special names for their units; some are given in the tables which follow (in a few cases, these quantities do have named units in the cgs system). A number of other convenient units are not directly derived from the SI base units, but can nonetheless be expressed in terms of those units, and are recognized by the guardians of the SI system. Important examples for astrophysics include:

- The minute (m=60 s), hour (h = 3600 s), and day (d = 86 400 s).  
(The year is not an admitted unit, as it varies in length; for rough calculations it’s usually adequate to assume  $1 \text{ yr} \simeq 365.25 \text{ d}$ .)
- the degree ( $^\circ = 2\pi/360 \text{ rad}$ ), arcminute ( $' = 2\pi/21\,600 \text{ rad}$ ), and arcsecond ( $'' = 2\pi/1.296 \times 10^6 \text{ rad}$ )
- the atomic mass unit (amu =  $1.66053886 \times 10^{-27} \text{ kg}$ )
- the electron volt (eV =  $1.60217646 \times 10^{-19} \text{ J}$ )
- the ångström ( $\text{Å} = 10^{-10} \text{ m} = 0.1 \text{ nm}$ )
- the astronomical unit (AU =  $1.49598 \times 10^{11} \text{ m}$ ) and the parsec (pc =  $3.08568025 \times 10^{16} \text{ m}$ ).



<b>Unnamed Derived SI units</b>		
<i>Quantity</i>	<i>Units</i>	
area	$\text{m}^2$	$\text{m}^2$
volume	$\text{m}^3$	$\text{m}^3$
speed, velocity	$\text{m s}^{-1}$	$\text{m s}^{-1}$
acceleration	$\text{m s}^{-2}$	$\text{m s}^{-2}$
jerk	$\text{m s}^{-3}$	$\text{m s}^{-3}$
angular velocity	$\text{rad s}^{-1}$	$\text{s}^{-1}$
momentum, impulse	$\text{N s}$	$\text{kg m s}^{-1}$
angular momentum	$\text{N m s}$	$\text{kg m}^2 \text{s}^{-1}$
torque, moment of force	$\text{N m}$	$\text{kg m}^2 \text{s}^{-2}$
wavenumber	$\text{m}^{-1}$	$\text{m}^{-1}$
mass density	$\text{kg m}^{-3}$	$\text{kg m}^{-3}$
heat capacity, entropy	$\text{J K}^{-1}$	$\text{kg m}^2 \text{s}^{-2} \text{K}^{-1}$
specific heat capacity, specific entropy	$\text{J K}^{-1} \text{kg}^{-1}$	$\text{m}^2 \text{s}^{-2} \text{K}^{-1}$
specific energy	$\text{J kg}^{-1}$	$\text{m}^2 \text{s}^{-2}$
energy density	$\text{J m}^{-3}$	$\text{kg m}^{-1} \text{s}^{-2}$
surface tension	$\text{N m}^{-1} = \text{J m}^{-2}$	$\text{kg s}^{-2}$
heat flux density, irradiance	$\text{W m}^{-2}$	$\text{kg s}^{-3}$
thermal conductivity	$\text{W m}^{-1} \text{K}^{-1}$	$\text{kg m s}^{-3} \text{K}^{-1}$
diffusion coefficient	$\text{m}^2 \text{s}^{-1}$	$\text{m}^2 \text{s}^{-1}$
dynamic viscosity <sup>1</sup>	$\text{Pa s} = \text{N s m}^{-2}$	$\text{kg m}^{-1} \text{s}^{-1}$
kinematic viscosity <sup>2</sup>	$\text{m}^2 \text{s}^{-1}$	$\text{m}^2 \text{s}^{-1}$
electric charge density	$\text{C m}^{-3}$	$\text{m}^{-3} \text{A s}$
electric current density	$\text{A m}^{-2}$	$\text{A m}^{-2}$
conductivity	$\text{S m}^{-1}$	$\text{kg}^{-1} \text{m}^{-3} \text{s}^3 \text{A}^2$
permittivity	$\text{F m}^{-1}$	$\text{kg}^{-1} \text{m}^{-3} \text{s}^4 \text{A}^2$
permeability	$\text{H m}^{-1}$	$\text{kg m s}^{-2} \text{A}^{-2}$
electric field strength	$\text{V m}^{-1}$	$\text{kg m s}^{-3} \text{A}^{-1}$
magnetic field strength <sup>3</sup>	$\text{A m}^{-1}$	$\text{A m}^{-1}$
luminance <sup>4</sup>	$\text{cd m}^{-2}$	$\text{cd m}^{-2}$
cgs named units:		
<sup>1</sup> poise	$\text{P} = 0.1 \text{ Pa s}$	
<sup>2</sup> stokes	$\text{St} = 10^{-4} \text{ m}^2 \text{ s}^{-1}$	
<sup>3</sup> oersted	$\text{Oe} = \frac{1000}{4\pi} \text{ A m}^{-1}$	
<sup>4</sup> stilb	$\text{sb} = 10^4 \text{ cd m}^{-2}$	

### A.3 Prefixes

The SI system also specifies that names of multiples and submultiples of units are formed by means of the following prefixes:

<i>Multiplying Factor</i>	<i>Prefix</i>	<i>Symbol</i>	<i>Multiplying Factor</i>	<i>Prefix</i>	<i>Symbol</i>
10 <sup>24</sup>	yotta	Y	10 <sup>-1</sup>	deci	d
10 <sup>21</sup>	zetta	Z	10 <sup>-2</sup>	centi	c
10 <sup>18</sup>	exa	E	10 <sup>-3</sup>	milli	m
10 <sup>15</sup>	peta	P	10 <sup>-6</sup>	micro	μ
10 <sup>12</sup>	tera	T	10 <sup>-9</sup>	nano	n
10 <sup>9</sup>	giga	G	10 <sup>-12</sup>	pico	p
10 <sup>6</sup>	mega	M	10 <sup>-15</sup>	femto	f
10 <sup>3</sup>	kilo	k	10 <sup>-18</sup>	atto	a
10 <sup>2</sup>	hecto	h	10 <sup>-21</sup>	zepto	z
10 <sup>1</sup>	deca	da	10 <sup>-24</sup>	yocto	y

Multiple prefixes may not be used, even for the kilogram (unique among SI base units in having one of these prefixes as part of its name), for which the prefix names are used with the unit name ‘gram’, and the prefix symbols are used with the unit symbol ‘g’; e.g., 10<sup>-6</sup> kg = 1 mg (not 1 μkg).

With this exception, any SI prefix may be used with any SI unit (whether base or derived, including the degree Celsius and its symbol °C). Note that use of ‘micron’ for the μm persists very widely (almost universally!) in astrophysics, although the approved SI name is the micrometre.

According to SI rules, these prefixes strictly represent powers of 10, and should not be used to represent the powers of 2 commonly found in computing applications. Thus one kilobyte (1 kbyte) is 1000 bytes – and not 2<sup>10</sup> bytes = 1024 bytes. In an attempt to resolve this ambiguity, prefixes for binary multiples have been recommended by the International Electrotechnical Commission for use in information technology (though they’re achieving acceptance only very slowly):

Factor	Name	Symbol	Origin
2 <sup>10</sup>	kibi	Ki	‘kilobinary’, (2 <sup>10</sup> ) <sup>1</sup> kilo, (10 <sup>3</sup> ) <sup>1</sup>
2 <sup>20</sup>	mebi	Mi	‘megabinary’, (2 <sup>10</sup> ) <sup>2</sup> mega, (10 <sup>3</sup> ) <sup>2</sup>
2 <sup>30</sup>	gibi	Gi	‘gigabinary’, (2 <sup>10</sup> ) <sup>3</sup> giga, (10 <sup>3</sup> ) <sup>3</sup>
2 <sup>40</sup>	tebi	Ti	‘terabinary’, (2 <sup>10</sup> ) <sup>4</sup> tera, (10 <sup>3</sup> ) <sup>4</sup>
2 <sup>50</sup>	pebi	Pi	‘petabinary’, (2 <sup>10</sup> ) <sup>5</sup> peta, (10 <sup>3</sup> ) <sup>5</sup>
2 <sup>60</sup>	exbi	Ei	‘exabinary’, (2 <sup>10</sup> ) <sup>6</sup> exa, (10 <sup>3</sup> ) <sup>6</sup>

## A.4 Writing style

For those really interested in the details, here are some of the more important elements of recommended writing style for SI units:

- Symbols are written in upright Roman type ('m' for metres, 'l' for litres).
- Units are written without a capital (other than where the rules of punctuation require it), as are their corresponding symbols, except for symbols derived from the name of a person; thus "the symbol for the coulomb is 'C'". However, some American-speaking countries use 'L' for 'litre' (to avoid potential confusion with numeric '1').
- Names of units take plurals according to the usual rules of grammar; e.g., 20 kilograms, 40 henries. 'Hertz', 'lux', and 'siemens' have the same form in the singular and the plural. Symbols of units are *not* pluralised ('20 kg', not '20 kgs'), thereby avoiding confusion with the second ('s').
- A space should separate a number and its unit ('20 kg', not '20kg'). Exceptions are the symbols for degrees, arcminutes, and arcseconds ( $^{\circ}$ ,  $'$ ,  $''$ ), which should be contiguous with the number (e.g.,  $20^{\circ} 15'$ ).
- Symbols do not have an appended full stop (other than where the rules of punctuation require it; specifically, at the end of a sentence).
- Commas should not be used to break up long runs of digits, though spaces may be used (3.141 592 654, not 3.141,592,654).

# Appendix B

## Constants

### B.1 Physical constants

Speed of light	$c$	$2.99792458 \times 10^8 \text{ m s}^{-1}$
Universal gravitational constant	$G$	$6.67300 \times 10^{-11} \text{ m}^3 \text{ kg}^{-1} \text{ s}^{-2}$ (= N m <sup>2</sup> kg <sup>-2</sup> )
Planck's constant	$h$	$6.626068 \times 10^{-34} \text{ m}^2 \text{ kg s}^{-1}$ (=J s)
Boltzmann's constant	$k$	$1.3806503 \times 10^{-23} \text{ m}^2 \text{ kg s}^{-2} \text{ K}^{-1}$ (=J K <sup>-1</sup> )
Stefan-Boltzmann constant	$\sigma$	$5.67040 \times 10^{-8} \text{ W m}^{-2} \text{ K}^{-4}$
Radiation constant	$a = 4\sigma/c$	$7.55 \times 10^{-16} \text{ J m}^{-3} \text{ K}^{-4}$
Atomic mass unit	amu	$1.66053886 \times 10^{-27} \text{ kg}$
Hydrogen mass	$m(\text{H})$	1.00794 amu
Proton mass	$m_{\text{P}}$	$1.67262158 \times 10^{-27} \text{ kg}$
Electron mass	$m_{\text{e}}$	$9.10938188 \times 10^{-31} \text{ kg}$
Electron charge	$e$	$1.60217646 \times 10^{-19} \text{ C}$
	$\frac{\pi e^2}{m_{\text{e}} c}$	$2.654 \times 10^{-6} \text{ m}^2 \text{ s}^{-1}$

### B.2 Astronomical constants

Astronomical unit	AU	$1.49598 \times 10^{11} \text{ m}$
Parsec	pc	$3.08568025 \times 10^{16} \text{ m}$

#### B.2.1 Solar parameters

The 'solar constant' is the (very slightly variable) energy flux from the Sun measured at the mean distance of the Earth; numerically,

$$\text{solar constant, } C_{\odot} = 1366 \text{ J m}^{-2} \text{ s}^{-1}.$$

The mean Earth–Sun distance is

$$d_{\odot} \equiv 1 \text{ AU} = 1.496 \times 10^{11} \text{ m}$$

whence, since  $L_{\odot} = 4\pi d_{\odot}^2 C_{\odot}$ ,

$$L_{\odot} = 3.827 \times 10^{26} \text{ W}$$

This allows us to define the Sun's effective temperature, from  $L_{\odot} = 4\pi R_{\odot}^2 \sigma T_{\text{eff}}^4$ , using

$$R_{\odot} = 6.960 \times 10^8 \text{ m};$$

$$T_{\text{eff}}(\odot) = 5770 \text{ K}.$$

The solar mass is

$$M_{\odot} = 1.989 \times 10^{30} \text{ kg},$$

which follows from equating centrifugal and gravitational accelerations of the Earth in orbit,

$$\frac{M_{\oplus} v_{\oplus}^2}{R_{\oplus}} = \frac{GM_{\odot} M_{\oplus}}{d_{\odot}^2}$$

whence the mean density is

$$\begin{aligned} \bar{\rho} &= \frac{M_{\odot}}{4/3\pi R_{\odot}^3} \\ &= 1.4 \times 10^3 \text{ kg m}^{-3} \end{aligned}$$

Finally, the mean number density is

$$\bar{n} = \frac{\bar{\rho}}{\mu m(\text{H})} \simeq 1.4 \times 10^{30} \text{ m}^{-3}$$

(using mean molecular weight  $\mu \simeq 0.61$ ).